

The Belgian repository of fundamental atomic data and stellar spectra (BRASS)

II. Quality assessment of atomic data for unblended lines in FGK stars[★]

M. Laverick^{1,2}, A. Lobel², P. Royer¹, T. Merle³, C. Martayan⁴, P.A.M. van Hoof², M. Van der Swaelmen³, M. David⁵, H. Hensberge², and E. Thienpont⁶

¹ Instituut voor Sterrenkunde, KU Leuven, Celestijnenlaan 200D, box 2401, 3001 Leuven, Belgium

² Royal Observatory of Belgium, Ringlaan 3, B-1180 Brussels, Belgium

e-mail: mike.laverick@kuleuven.be

³ Institut d'Astronomie et d'Astrophysique, Université Libre de Bruxelles, Av. Franklin Roosevelt 50, CP 226, 1050 Brussels,

⁴ European Organisation for Astronomical Research in the Southern Hemisphere, Alonso de Córdova 3107, Vitacura, 19001 Casilla, Santiago de Chile, Chile Belgium

⁵ Onderzoeksgroep Toegepaste Wiskunde, Universiteit Antwerpen, Middelheimlaan 1, 2020 Antwerp, Belgium,

⁶ Vereniging voor Sterrenkunde, Kapellebaan 56, 2811 Leest, Belgium

Received June 4th, 2018; accepted February 5th, 2019

ABSTRACT

Context. Fundamental atomic transition parameters, such as oscillator strengths and rest wavelengths, play a key role in modelling and understanding the chemical composition of stars in the universe. Despite the significant work under way to produce these parameters for many astrophysically important ions, uncertainties in these parameters remain large and can limit the accuracy of chemical abundance determinations.

Aims. The Belgian repository of fundamental atomic data and stellar spectra (BRASS) aims to provide a large systematic and homogeneous quality assessment of the atomic data available for quantitative spectroscopy. BRASS shall compare synthetic spectra against extremely high quality observed spectra, at a resolution of ~ 85000 and signal-noise ratios of ~ 1000 , for around 20 bright BA FGK spectral type stars, in order to critically evaluate the atomic data available for over a thousand potentially useful spectral lines.

Methods. A large-scale homogeneous selection of atomic lines is performed by synthesising theoretical spectra of literature atomic lines, for FGK-type stars including the Sun, resulting in a selection of 1091 theoretically deep and unblended lines, in the wavelength range 4200-6800 Å, which may be suitable for quality assessment. Astrophysical $\log(gf)$ values are determined for the 1091 transitions using two commonly employed methods. The agreement of these $\log(gf)$ values are used to select well-behaving lines for quality assessment.

Results. 845 atomic lines were found to be suitable for quality assessment, of which 408 were found to be robust against systematic differences between analysis methods. Around $\sim 54\%$ of the quality-assessed lines were found to have at least one literature $\log(gf)$ value in agreement with our derived values, though the remaining values can disagree by as much as 0.5 dex. Only $\sim 38\%$ of Fe I lines were found to have sufficiently accurate $\log(gf)$ values, increasing to ~ 70 -75% for the remaining Fe-group lines.

Key words. Stars: solar-type - Line: profiles - Atomic data - Astronomical databases: miscellaneous

1. Introduction

Modern quantitative stellar spectroscopy routinely measures spectral line properties, such as elemental abundances, to a precision of 0.01 dex, however systematic errors often dominate derived spectral line properties resulting in actual errors that are typically an order of magnitude larger (Barklem 2016). The work of Lindegren & Feltzing (2013) shows that the uncertainties in elemental abundances are a limiting factor in discriminating stellar populations, and that small improvements in uncertainty can significantly reduce the number of stars required for galactic archaeology. Such improvements are important for current and upcoming large-scale galactic surveys such as Gaia (Gaia collaboration 2016), GALAH (De Silva et al. 2015), WEAVE (Dalton et al. 2012), and 4MOST (de Jong et al. 2012).

One of the main uncertainties in elemental abundances is the quality of the adopted atomic data used in spectral synthesis calculations (Bigot & Thevenin 2008). The Belgian repository of fundamental atomic data and stellar spectra (BRASS) aims to provide astronomers with quality information for the large amount of atomic data available for high-resolution optical spectroscopy, in an attempt to help reduce systematic input errors in quantitative spectroscopy from atomic data and line selection (Lobel et al. 2017). Previously, we retrieved and cross-matched a large quantity of atomic data from several major atomic databases such as the Vienna Atomic Line Database (VALD3; Ryabchikova et al. 2015), the National Institute of Standards and Technology Atomic Spectra Database (NIST ASD; Kramida et al. 2018), and providers within the Virtual Atomic and Molecular Data Centre (VAMDC; Dubernet et al. 2016), in preparation for quality assessment work (Lavrick et al. 2018; hereafter Paper 1). In this work the atomic

* Tables D.1, D.2, E.1, and F.1 are available in full, in electronic format via the CDS and at brass.sdf.org.

data of seemingly 'unblended' spectral lines are quality assessed against several benchmark dwarf stars, including the Sun, spanning late F-type to early K-type stars, for the spectral range 4200-6800 Å.¹ Unblended spectral lines for stars of ~G2V spectral type are identified in a homogeneous manner using both the observed benchmark spectra, and the theoretical input line list of Paper 1. Astrophysical oscillator strengths² are derived for these unblended lines, using two commonly utilised methods, to gauge the reliability of the spectral line for quantitative spectroscopy and to produce 'benchmark' $\log(gf)$ values for atomic data quality assessment. The literature $\log(gf)$ values are then compared against these benchmark $\log(gf)$ values to determine which literature values reliably reproduce the stellar spectra of cool dwarf stars, and thus whether the values can be recommended for spectroscopic modelling. This paper presents three main sets of results:

- a set of extremely high-quality stellar spectra, with signal-to-noise ratios of $S/N \sim 800$ -1200 and a resolution $R \sim 85000$, for six well-studied stars between 5000-6000 K
- an identification of unblended and reliable atomic lines in these stellar spectra, determined using theoretical input line lists and the behaviour of the observed spectra
- a set of benchmark $\log(gf)$ values for these unblended lines, including a quality assessment of the available atomic data $\log(gf)$ values per spectral line

Section 2 outlines the selection of the 5000-6000 K benchmark stars, the data reduction of the observed spectra, the details of the spectral synthesis calculations, and the stellar parameter determination of the benchmark stars. Section 3 covers the selection of theoretically unblended spectral lines and the measurement of their observed counterparts. Section 4 details the determination of astrophysical oscillator strengths for the selected lines, as well as their uncertainties. Finally, Section 5 explains how the derived oscillator strengths and uncertainties are used as benchmark values to quality-assess the available literature atomic data for the selected spectral lines, as well as the findings of our quality assessment for over 800 spectral lines.

2. Benchmark stars between 5000-6000 K

2.1. Selection and observations of benchmark stars

For the benchmark star selection the following criteria were imposed, the stars must:

- fall within the temperature range 5000-6000 K
- not belong to any known stellar variability classes
- not be chemically peculiar or metal-poor *i.e.* they must have roughly solar-like abundances
- have low $v \sin i$ -values so that spectral lines are narrow
- ideally be dwarf stars to avoid non-LTE effects due to extended atmospheres
- be brighter than 7th magnitude in V so that an extremely high signal-noise ratio spectrum of the object can be obtained

Using these criteria the following stars were chosen: ϵ Eri, 70 Oph A, 70 Vir, 51 Peg, 10 Tau, β Com, and the Sun. The benchmark spectra were obtained using the HERMES echelle

spectrograph mounted on the Mercator 1.2 m telescope at the Roche de los Muchachos Observatory, La Palma, Spain, which is able to observe the complete wavelength range 3800-9000 Å in a single exposure at a resolution of $R \sim 85000$ (Raskin et al. 2011). Each object was observed 10-50 times, depending on the V mag, in succession throughout a single night. Extra flat-fields were also taken during the night to avoid introducing systematic noise in the reduction process. The resultant exposures were reduced using the dedicated HERMES pipeline (release V6.0) and co-added to produce a single, stacked spectrum per object with S/N of ~800-1200. The Solar spectrum was obtained from Neckel & Labs (1984), taken using the NSO/KPNO Fourier Transform Spectrograph (FTS) with a spectral resolution of $R \sim 350000$ and a S/N of ~2500. The wavelength range in this work is limited to 4200-6800 Å to avoid heavily blended features in shorter wavelengths, and to avoid telluric contamination in the longer wavelengths.

2.2. Theoretical spectral modelling

The synthesis work is performed using the atomic line list detailed in Paper 1, and 1D hydrostatic, plane-parallel atmospheric models computed using the publicly available ATLAS9 code (Kurucz 1992). The models adopt the updated opacity distribution functions (ODFs) calculated by Castelli & Kurucz (2003), use the "mixing length" approximation detailed by Castelli et al. (1997) in conjunction with a mixing-length of $L/H_p = 1.25$, and with the ATLAS9 "approximate treatment of overshooting" turned off as recommended by Bonifacio et al. (2012). The model grid of Castelli et al. (1997), calculated with the updated ODFs, was used as a starting point to calculate a much finer grid of stellar models in order to derive stellar parameters for the benchmark spectra. The grid stellar parameters cover $4000 < T_{\text{eff}} < 15000$ K (step size of 50 K), $0.0 < \log g < 5.0$ dex (step size of 0.1 dex), $-5.0 < [\text{M}/\text{H}] < 1.0$ dex (step size of 0.2 dex), $0 < \zeta_{\mu} < 20 \text{ kms}^{-1}$ (step size of 0.5 kms^{-1}), and $0 < v \sin i < 300 \text{ kms}^{-1}$ (step size of 1 kms^{-1}).

The calculated models used the same mixing length and overshooting treatment as Castelli, but adopt the solar abundances of Grevesse et al. (2007) to be consistent with the transfer calculations. All synthetic spectra are computed in local thermal equilibrium (LTE), using the publicly-available radiative transfer code TurboSpectrum V12.1.1 (Alvarez & Plez 1998; Plez 2012). The synthetic spectra are computed using the solar abundances of Grevesse et al. (2007). We assume all benchmark stars to have the same elemental abundance distribution as the Sun, but scaled according to the metallicity of the given benchmark star. The spectra are rotationally broadened to the $v \sin i$ of the given star, and instrumentally broadened to the spectral resolution of HERMES (or the FTS for the solar spectrum). Finally, the SpectRes Python resampling tool was used when comparing synthetic and observed spectra (Carnall 2017). The choice of synthesis code and stellar models was governed by the goals of the project; constraining the atomic data of many lines, as homogeneously as possible, for stars of B-, A-, F-, G-, and K-spectral type. Section 4.3.2. provides a brief discussion of some of the uncertainties in the adopted modelling procedure.

2.3. Stellar parameter determination

For consistency the spectral parameters of the six benchmark stars observed by HERMES, initially outlined in Lobel et al. (2017), were determined as follows, taking account of the spec-

¹ Throughout this paper we use the term 'unblended' to refer to spectral lines that produce the majority of the flux absorption of their respective spectral feature, in the context of theoretical spectral calculations, as explained in Section 3.1.

² often written in terms of log weighted-oscillator strengths, or $\log(gf)$

Table 1. Stellar parameters of the FGK benchmark stars with effective temperatures in the range $5000 \leq T_{\text{eff}} \leq \sim 6000$ K. The associated stellar parameter errors are $T_{\text{eff}} \pm 50$ K, $\log g \pm 0.20$ dex, $[\text{M}/\text{H}] \pm 0.01$ dex, $\zeta_\mu \pm 0.10 \text{ km s}^{-1}$, and $v \sin i \pm 1.00 \text{ km s}^{-1}$.

Object	T_{eff} (K) ± 50	$\log g$ (dex) ± 0.20	$[\text{M}/\text{H}]$ (dex) ± 0.01	ζ_μ (km s^{-1}) ± 0.10	$v \sin i$ (km s^{-1}) ± 1.00
β Com	6010	4.35	0.06	1.14	5.70
10 Tau	5912	3.90	-0.11	1.27	5.25
51 Peg	5804	4.42	0.20	1.10	4.00
Sun	5777	4.44	0.00	1.10	2.50
70 Vir	5500	3.94	-0.11	1.05	3.60
70 Oph A	5354	4.60	0.07	0.96	3.15
ϵ Eri	5136	4.71	-0.03	0.90	3.40

tral modelling details discussed in Section 2.2. The stellar parameters are initially estimated using a limited number of diagnostic Balmer, Fe, and Mg absorption lines. The method then iterates over T_{eff} , $\log g$, $[\text{M}/\text{H}]$, and ζ_μ until the best fit is found to the detailed shapes of a more extensive set of ~ 30 diagnostic Fe I and Fe II photospheric lines. The fit method iterates until the best fit to the continuum-normalised Fe-line profiles has been accomplished using χ^2 minimization. The iterations over the ζ_μ proceed until the iron abundance value determined from the Fe I lines is in agreement with the iron abundance value determined from the Fe II lines. The iteration procedure assumes the ζ_μ stays constant with depth in the line formation regions of these medium-strong Fe lines. During each iteration, the spectrum is continuum-flux normalised using a semi-automatic template normalisation routine described in Appendix A.

The $v \sin i$ value, *i.e.* the convolution of the projected rotational velocity and macro-broadening, is also iterated in steps of 1 km s^{-1} while obtaining the best fit to the detailed Fe line profiles. The final stellar parameter errors are: $T_{\text{eff}} \pm 50$ K, $\log g \pm 0.20$ dex, $[\text{M}/\text{H}] \pm 0.01$ dex, $\zeta_\mu \pm 0.10 \text{ km s}^{-1}$, and $v \sin i \pm 1.00 \text{ km s}^{-1}$. The standard solar parameters of $T_{\text{eff}} = 5777$ K and $\log g = 4.44$ dex were adopted, with the remaining parameters determined in this work. The FTS solar spectrum normalisation is described by Neckel & Labs (1984). The stellar parameters of the benchmark stars are listed in Table 1, and are found to be in good agreement with other literature surveys deriving astrophysical parameters for these stellar objects (da Silva et al. 2015; Brewer et al. 2016).

3. Selection of unblended spectral lines

3.1. Quantification of theoretical line blending

We define the theoretical core blending, Ω_{core} , of a given line as follows:

$$\Omega_{\text{core}} = 1 - \frac{\int_{\lambda_0-x}^{\lambda_0+x} (1 - F(\lambda)^{\text{line}}_{\text{norm}}) d\lambda}{\int_{\lambda_0-x}^{\lambda_0+x} (1 - F(\lambda)^{\text{tot}}_{\text{norm}}) d\lambda} \quad (1)$$

where:

$$x = \frac{1}{2} \frac{W_\lambda^{\text{line}}}{d} \quad (2)$$

where W_λ^{line} is the equivalent width of the given line, d is the central depth of the line relative to the normalised continuum, λ_0 is the rest wavelength of the line, $F(\lambda)^{\text{line}}_{\text{norm}}$ is the normalised flux of the line, and $F(\lambda)^{\text{tot}}_{\text{norm}}$ is the normalised flux of the total

spectrum, including all other spectral features. A line with $d = 0$ does not appear in the spectrum, whereas a line with $d = 1$ absorbs all available flux at λ_0 . A line with $\Omega_{\text{core}} = 0$ (or 0%) is considered completely unblended in its core wavelength region $\lambda_0 - x$ to $\lambda_0 + x$, whereas a line with $\Omega_{\text{core}} \approx 1$ (or $\sim 100\%$) is completely blended with other spectral features.

The core blending, Ω_{core} , is calculated for all 82337 lines in the input atomic line list, for the spectra of the Sun and 51 Peg at the resolutions of R~350000 and R~85000 respectively. Fig. 1 shows the Ω_{core} as a percentage, plotted against the normalised central line depth, d , for the Sun and 51 Peg. Both the Sun and 51 Peg exhibit the same distributions: a substantial number of shallow, heavily-blended *background* lines, in addition to a number of relatively unblended lines. To reduce the impact of blending on the quality assessment (discussed later in Section 4.3.7) a cut-off of $\Omega_{\text{core}} \leq 10\%$ is imposed, marked by the blue vertical lines in Fig. 1. This cut-off was selected as a balance between Ω_{core} and the number of investigated lines, thus it encompasses the full peak in unblended lines for 51 Peg. An additional cut-off on central line depth $d \geq 0.02$ is imposed to help ensure that observed line profiles are actually measurable and less affected by any noise in the observed spectra.

Using these constraints 1515 atomic lines are retained for 51 Peg, and 1954 lines in the Sun. All 1515 lines are present in both 51 Peg and the Sun, the difference in quantity being attributed to the differing resolutions of the two spectra. Given that the majority of the benchmark spectra are taken with HERMES, the 1515 spectral lines were selected for measurements, and are henceforth described as 'unblended' lines. No limits have been placed on the investigated species, other than mandating that they must fall in the investigated wavelength range, and must be deep and relatively unblended according to the theoretical line list.

3.2. Measurement of observed line profiles

The 1515 unblended lines were automatically measured, in each of the seven observed benchmark spectra, using a single Gaussian profile fit to determine if the feature exists and to determine its equivalent widths, W_λ .

The Gaussian fit is optimised using Gauss-Newton non-linear regression, or a Nelder-Mead minimisation in the case of slow convergence, as described by Lobel et al. (2018). The best fit to the observed line flux is limited to the wavelength interval between the two local flux maxima either side of λ_0 that exceeding 2% of the normalised continuum flux level. A goodness-of-fit value of $\chi^2 \geq 0.95$, in addition to manual inspection, was used to filter out poorly-fitted, non-existent, heavily-blended, or telluric-contaminated features. After measurements 1091 spectral lines

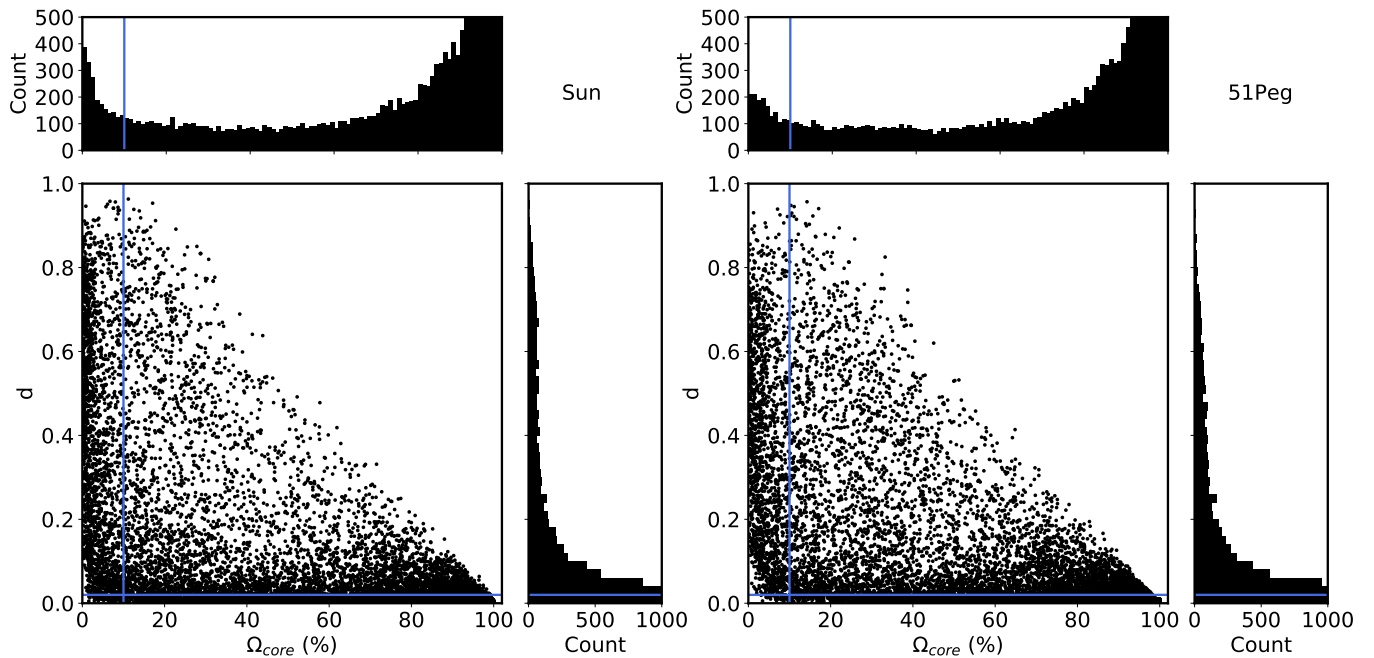


Fig. 1. Spectral line depth, d , plotted against theoretical core-blending, Ω_{core} , (defined in Eqn. 1 & 2) for all 82337 input atomic line list lines for the Sun (G2V) and 51 Peg (G2V). Solid blue lines show the selected cut-offs for the 5000–6000 K benchmark stars of $d \geq 0.02$ and $\Omega_{core} \leq 10\%$. Analysis of hotter benchmark stars will likely need different cut-offs, or potentially a different approach to treating blended spectral lines.

were found to be suitable for astrophysical $\log(gf)$ determination. A small number of these spectral lines cannot be assessed in all seven benchmark stars, due to poor fitting in only some of the profiles, however the line can still be investigated at the cost of increased statistical uncertainty, discussed in Section 4.3.8. Additionally, the adoption of a Gaussian fit, in place of a Voigt profile fit, is discussed in Section 4.3.5.

4. Determination of astrophysical oscillator strengths for selected lines

There are two commonly-employed methods to determine astrophysical $\log(gf)$ values: measuring a line equivalent width, W_λ , and converting it into a $\log(gf)$ value via the curve of growth (*e.g.* Sousa et al. 2007; Önehag et al. 2012; Andreasen et al. 2016), or by using detailed transfer calculations to vary a $\log(gf)$ value and determine a best-fitting value (*e.g.* Boeche & Grebel 2016; Tsantaki et al. 2018). Both these methods are subject to a number of assumptions, especially in their treatment of blended lines, that can lead to significant systematic differences in derived $\log(gf)$ value if not properly accounted for. As such, both the curve of growth and iterative modelling methods have been explored, with the following section detailing their implementation and associated uncertainties.

4.1. Determination of oscillator strengths using theoretical curves of growth

The measured W_λ value of a spectral line can be converted into a $\log(gf)$ value, on a star-by-star basis, by using the following curve of growth relationship:

$$\log\left(\frac{W_\lambda}{\lambda_0}\right) = \log(gf\lambda_0) + \log(A_{el}) - \frac{5040}{T_e}E_{low} + \log(C) \quad (3)$$

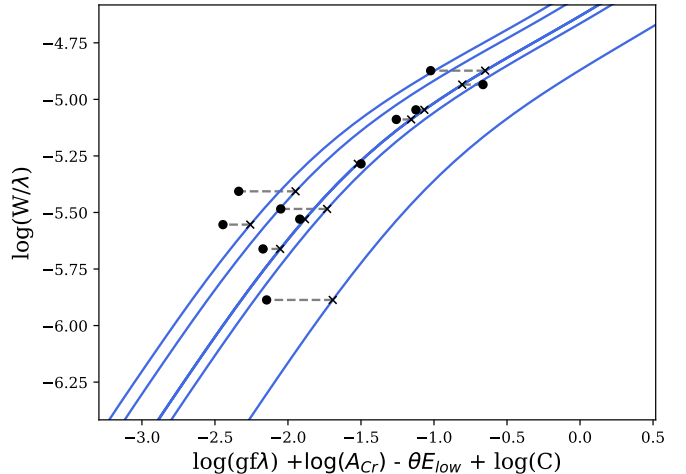


Fig. 2. Conversion of observed Cr II line equivalent width values into $\log(gf)$ values using theoretical curves of growth for a given star. Blue lines: theoretical curves of growth for different Cr II lines. Black circles: measured equivalent width values plotted using the $\log(gf)_{input}$ values, black crosses: measured equivalent width values plotted using derived $\log(gf)$ values *i.e.* the intersect of the equivalent width value with its respective curve of growth.

where W_λ is the equivalent width, λ_0 is the transition wavelength, A_{el} is the elemental abundance of the species, T_e is the excitation temperature, E_{low} is the transition lower energy level, and C contains the remaining terms such as the Saha population factor and the continuum opacity. Theoretical curves of growth are built by varying the $\log(gf)$ value of each of the 1091 selected lines over the range $-6.0 < \log(gf) < 4.0$ dex in steps of 0.1 dex, and then calculating the equivalent widths of the resultant line profiles. The curves are synthesised using the rest-wavelength and en-

ergy levels of the selected line, for each of the seven benchmark stars, resulting in a total of 7658 individual curves of growth. A high-order polynomial is fitted through each of the curves, with maximum fit deviation of $\Delta \log(gf) \ll 0.005$ dex. The measured W_λ values are converted into $\log(gf)$ values using their respective curve of growth per line, per star, as shown in Fig. 2. These individual $\log(gf)_{cog}$ values per star are averaged over the benchmark stars to produce a final mean $\overline{\log(gf)_{cog}}$ value and associated uncertainty, as discussed in Section 4.3.8.

4.2. Determination of wavelengths and oscillator strengths via iterative detailed modelling

Unlike the curve of growth line profiles, the grid spectra are computed using the line of interest and all other nearby lines present in the input atomic and molecular line lists. A grid of synthetic spectra is calculated for each selected line per benchmark star, in a wavelength window of ± 1 Å centred on the rest wavelength of the line. The grid method uses the rest-wavelength and the previously determined $\overline{\log(gf)_{cog}}$ values of the selected line as a central grid point, and covers the parameter ranges of $-0.05 < \lambda_{input} < +0.05$ Å (in steps of 0.01 Å) and $-0.5 < \log(gf) < +0.5$ dex (in steps of 0.05 dex). An example of the calculated grid line profiles is shown in Fig. 3 for the central and extrema wavelength grid values.

The observed benchmark spectra and calculated line profiles are used to calculate a corresponding grid of χ^2_{red} values, which are interpolated in steps of $\Delta\lambda = 0.005$ Å and $\Delta \log(gf) = 0.01$ dex using a bivariate cubic spline fit. The smallest χ^2_{red} value of the interpolated grid provides the final set of wavelength and $\log(gf)_{grid}$ values for the given line, for a given star, and confidence intervals at a 68.3% confidence limit are calculated for the pair of parameters to produce upper and lower error estimates on the parameters. These individual wavelengths, $\log(gf)_{grid}$ values, and errors per star can be combined to produce a final mean wavelength, mean $\overline{\log(gf)_{grid}}$ value, and errors for the line (see Section 4.3.8). Fig. 4 shows the χ^2_{red} grids calculated for the $\lambda 5682.2$ Ni I line in the several benchmark stars, in addition to the λ_{grid} and $\log(gf)_{grid}$ values corresponding to the χ^2 minimum per star, 68.3% confidence limit error bars, and the $\log(gf)_{grid}$ value of the line.

4.3. Uncertainties in the astrophysical oscillator strengths

4.3.1. Uncertainties due to S/N

Cayrel (1988) provides a formula for estimating the statistical uncertainty in measuring the W_λ of an observed profile using a Gaussian fit. Using Eqn. (7) of their work, the HERMES FWHM ~ 0.065 Å, a pixel size of $\delta\lambda \sim 0.026$ Å, and a S/N ~ 800 , a statistical uncertainty of ~ 0.08 mÅ is determined for the equivalent width measurements. This statistical uncertainty only yields differences in $\log(gf)$ values on the order of the 4th decimal place, and so is negligible compared to the other sources of uncertainty.

4.3.2. Uncertainties due to modelling assumptions

We do not attempt an exhaustive investigation into all aspects of spectral modelling, such as adopting different model atmospheres and transfer codes, however we have adopted stellar objects for which the modelling uncertainties should be mini-

mal. The plane-parallel atmospheric models of ATLAS9 were adopted, rather than the public MARCS models, as the MARCS model opacities do not contain enough ionised species to accurately model early-F stars and hotter (Plez 2011), which is required for future plans to extend the analysis to hotter stars and ionised lines. The benchmark star selection mandated dwarf-like objects so that the plane-parallel assumption of ATLAS9 is valid. In the context of cool stars, Gustafsson et al. (2008) show that the differences in temperature structures between ATLAS9 and MARCS are negligible for G-type dwarf stars of solar metallicity. Differences between ATLAS9, which uses ODFs, and ATLAS12, using opacity sampling, are shown to be extremely small when computed with the same chemical composition and line data (Plez 2011).

As shown in Lind et al. (2012), the magnitude of non-LTE effects on unsaturated, high-excitation Fe I lines for stars with stellar parameters of $5000 \leq T_{\text{eff}} \leq 6000$ K, $4.0 \leq \log g \leq 4.5$, and $[\text{M}/\text{H}] \approx [\text{M}/\text{H}]_{\odot}$ are between 0.00 - 0.02 dex at most, thus the majority of investigated lines should be free of non-LTE effects. We do expect that the adopted stellar model atmospheres will begin to suffer from shortcomings for the hottest A-type benchmark stars, and the resultant non-LTE effects will lead to systematic errors in astrophysical $\log(gf)$ values. It is hard to predict the exact magnitudes of non-LTE effects for individual spectral lines, but lines of lower excitation energies belonging to easily ionised species are more likely to exhibit non-LTE effects. As discussed in Section 5.2, we do not find any obvious evidence of non-LTE effects for the majority of our astrophysical $\overline{\log(gf)}$ values, except for transitions belonging to the lowest energy levels of $E_{low} \leq 0.25$ eV.

4.3.3. Uncertainties due to stellar parameters

Differences between the physical stellar parameters and the adopted stellar parameters will impact the derived $\log(gf)$ values, as any difference in number densities will be attributed to the derived $\log(gf)$ values. We also assume that the benchmark stars have the same elemental abundance distribution as the Sun, but scaled with metallicity. This means that any changes to the relative abundance ratios of an individual element, for a given benchmark star, will manifest as $\Delta \log(gf)$ values for all lines belonging to that element. Due to the highly-degenerate relationships between the stellar parameters, individual elemental abundances, and their dependence on the adopted atomic data, we do not propagate the stellar parameter errors into our $\log(gf)$ derivations or attempt to determine individual abundances. An accurate determination of these uncertainties warrants its own extensive investigation. Instead we adopt the position that the stellar parameters and metallicity-scaled solar abundance ratios are correct, and that using multiple benchmark stars in the $\overline{\log(gf)}$ derivations makes the final $\overline{\log(gf)}$ values less susceptible to an erroneous set of stellar parameters or changes in abundance ratios. The standard deviation associated with the $\overline{\log(gf)}$ value of a line will reflect the uncertainties of any of the sets of stellar parameters or abundance ratios.

4.3.4. Uncertainties due to normalisation

The benchmark spectra presented in this work are normalised using an automatic template normalisation in order to prevent the introduction of 'human factors' into the individual stellar spectra. The result should be a more consistent normalisation across the spectra, leading to a decrease in scatter, or random error, in

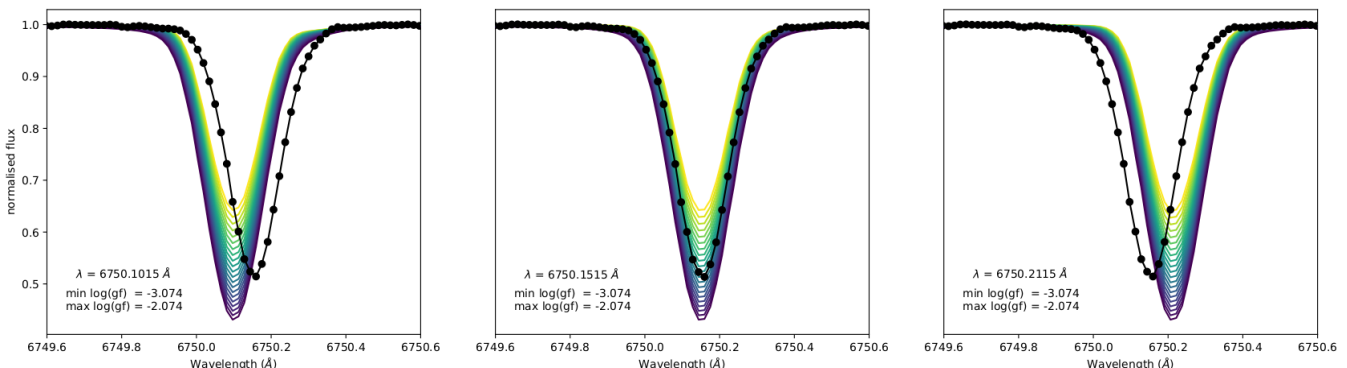


Fig. 3. An example of the iterative detailed modelling of the $\lambda 6750.2$ Fe I line in 51 Peg. The observed line profile is shown in black with solid markers, and the line profiles synthesised with varying input atomic parameters are shown in coloured lines (corresponding to different $\log(gf)$ values). The panels show three of the synthesised wavelength values: $\lambda_{\text{input}} - 0.05$ Å (left), λ_{input} (middle), and $\lambda_{\text{input}} + 0.05$ Å (right). Each panel shows the full $-0.5 \text{ dex} < \log(gf) < +0.5 \text{ dex}$ grid (in steps of 0.05 dex).

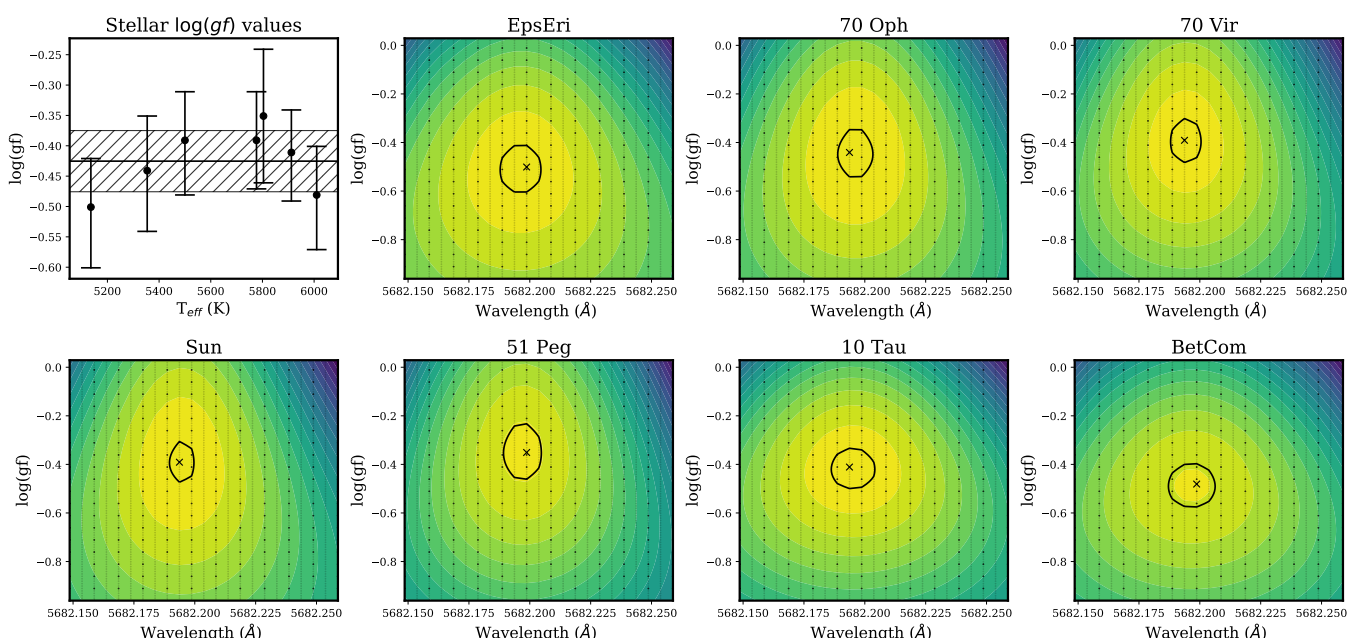


Fig. 4. $\log(gf)_{grid}$ values and χ^2_{red} distributions for the λ 5682.2 Ni I line. Top left panel: individual $\log(gf)_{grid}$ values per star, including 68.3% confidence-limit error bars, plotted against benchmark T_{eff} . The solid black line denotes the weighted $\overline{\log(gf)}_{grid}$ and the hatched region denotes the standard deviation estimation, discussed in Section 4.3.8. Remaining panels: χ^2_{red} distributions of the synthesised grid of λ and $\log(gf)$ values for the seven benchmark stars. Calculated grid points are denoted by black dots, the individual $\log(gf)_{grid}$ values are denoted by black crosses, and the 68.3% confidence-limits are denoted by black contours. Each plot has a normalised χ^2_{red} colour-scale, where yellow represents the χ^2_{red} minima, and dark blue represents the χ^2_{red} maximum.

the derived $\log(gf)$ values of a given line. To account for any deviations from unity in local continuum placement the Gaussian W_λ measurements are performed with a flat continuum offset term. In practice, this offset term allows the single Gaussian fit to mitigate the influence of nearby broad-winged lines. The iterative fitting does not attempt to measure any deviations in local continuum placement.

4.3.5. Impact of Gaussian profile for W_λ measurements

Spectral lines are often approximated as Gaussian profiles rather than Voigt profiles, however this assumption breaks down as

lines become saturated and the profile wing begin to grow. Fitting a line with a Gaussian profile will lead to an underestimation of the line W_λ as a function of increasing W_λ . This issue is discussed by [Luck \(2017\)](#), in addition to the difficulties of performing physically-accurate Voigt profile fits automatically for many lines.

In order to theoretically quantify this underestimation, Gaussian fits are performed on all synthetic line profiles of the curves of growth calculated in Section 4.1. Fig. 5 shows the difference in W_λ between the two profile shapes as a function of W_λ , computed for the 1091 lines in the Solar spectrum. The W_λ difference was calculated on a line-by-line, star-by-star basis and applied to

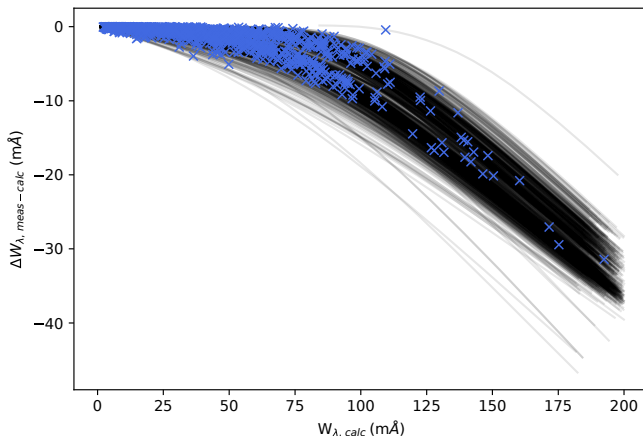


Fig. 5. Predicted ΔW_{λ} between Gaussian fits and transfer-calculation Voigt profiles plotted as a function of calculated W_{λ} shown for the 1091 investigated lines in the Sun (black lines). Blue crosses denote the proposed ΔW_{λ} corrections for the 1091 spectral lines.

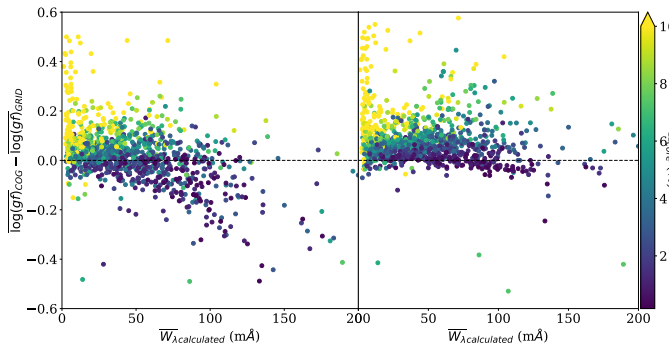


Fig. 6. Left: $\overline{\Delta \log(gf)_{\text{cog-grid}}}$ plotted against the calculated W_{λ} prior to the corrections to the Gaussian profiles. Right: as before but after corrections are applied on a line per line, star by star basis. The colour scale corresponds to the mean Ω_{core} (in percentage) of the line in question, recalculated using the new $\log(gf)_{\text{cog}}$ values. The stratification of the Ω_{core} is explained in Section 4.3.7.

each of the corresponding W_{λ} measurements discussed in Section 3.2. Fig. 6 shows the difference between the $\log(gf)_{\text{cog}}$ values, measured using a Gaussian profile fit, and $\log(gf)_{\text{grid}}$ values, calculated using the full radiative-transfer broadening, before and after the correction to the W_{λ} values. After correction there is a distinct improvement in the observed negative trend between $\Delta \log(gf)_{\text{cog-grid}}$ and W_{λ} , with the remaining positive scatter caused by differences in the treatment of theoretical blending between the two methods, as discussed in Section 4.3.7.

4.3.6. Uncertainties due to line blending in observed spectra

Observable blends, *i.e.* those that exhibit clear asymmetries or multiple peaks, are manually flagged and excluded on a line by line, star by star basis, to mitigate their impact on the $\log(gf)$ derivations. Hidden blends, *i.e.* those that do not cause measurable asymmetries or additional peaks in the line profile of interest, will cause an overestimation of the derived $\log(gf)$ value unless there is prior theoretical knowledge of this blend (see Section 4.3.7). If the two blending lines behave differently with tem-

perature then it is expected that the benchmark stars will produce systematic differences in the derived $\log(gf)$ value. As such, the standard deviation of the $\log(gf)$ values for a given line can be used as an indicator as to whether a line may be affected by hidden blends, and thus whether it is reliable to use as a single unblended line in our analysis and quality assessment for this paper.

4.3.7. Uncertainties due to theoretical line blending

The curve of growth approach assumes that a measured spectral feature is completely unblended, attributing the measured W_{λ} to a single spectral line, whereas the iterative modelling approach may contain some knowledge of potential blending components in the input line list. This difference will lead the curve of growth approach to overestimate the $\log(gf)_{\text{cog}}$ of the line of interest relative to the iterative modelling approach, assuming that the blending component is actually present in the observed spectrum.

Fig. 7 shows $\overline{\log(gf)_{\text{cog}}} - \overline{\log(gf)_{\text{grid}}}$ plotted against the theoretical W_{λ} of the Sun, for intervals of Ω_{core} that have been recalculated using the new $\log(gf)$ values. Fig. 8 shows the mean $\Delta \log(gf)_{\text{cog-grid}}$ plotted as a function of Ω_{core} , as well as the standard deviation of the $\log(gf)_{\text{cog-grid}}$ values and σ_{grid} values plotted as functions of Ω_{core} . The mean $\Delta \log(gf)$ is 0.00 dex when $\Omega_{\text{core}} \ll 1\%$, and increases steadily with Ω_{core} , confirming the systematic difference between the methods is due to theoretical blending. The standard deviation similarly increases with Ω_{core} , but levels out at roughly $\Omega_{\text{core}} \leq 5\%$ at a value of $1\sigma = \pm 0.04$ dex, which thus seems to represent the intrinsic scatter between the two methods. Properly correcting for this difference in methods is difficult as one must know how the background line presence would affect the single Gaussian fit, and rely on the assumption that the background line atomic data is accurate. Given that this problem verges into the territory of simultaneously quality assessing blended lines, we instead recommend using the intrinsic scatter value of 0.04 dex as a constraint on line selection, in order to reduce the impact of this systematic difference on the quality assessment results (see Section 5.1).

4.3.8. Final $\log(gf)$ values and uncertainties

The $\log(gf)_{\text{cog}}$ values are calculated by taking the mean of the n individually-derived stellar $\log(gf)_{\text{cog}}$ values, after individual corrections for the Gaussian approximation discussed in Section 4.3.5. The standard deviation of the $\log(gf)_{\text{cog}}$ values, σ_{cog} , are calculated as shown in Eqn. 4:

$$\sigma_{\text{cog}} = \sqrt{\frac{1}{n-1} \sum_{i=1}^n (\log(gf)_i - \overline{\log(gf)}_{\text{cog}})^2} \quad (4)$$

The $\log(gf)_{\text{grid}}$ values are calculated by using a weighted mean of the n individually-derived stellar $\log(gf)_{\text{grid}}$ values, shown by Eqn. 5, and the corresponding standard deviation estimations are shown by Eqn. 6 and Eqn. 7, where the weights per star are equal to the inverse square of the $\log(gf)_{\text{grid}}$ uncertainty estimates:

$$\overline{\log(gf)}_{\text{grid}} = \frac{\sum_{i=1}^n (\log(gf)_i / \sigma_i^2)}{\sum_{i=1}^n 1 / \sigma_i^2} \quad (5)$$

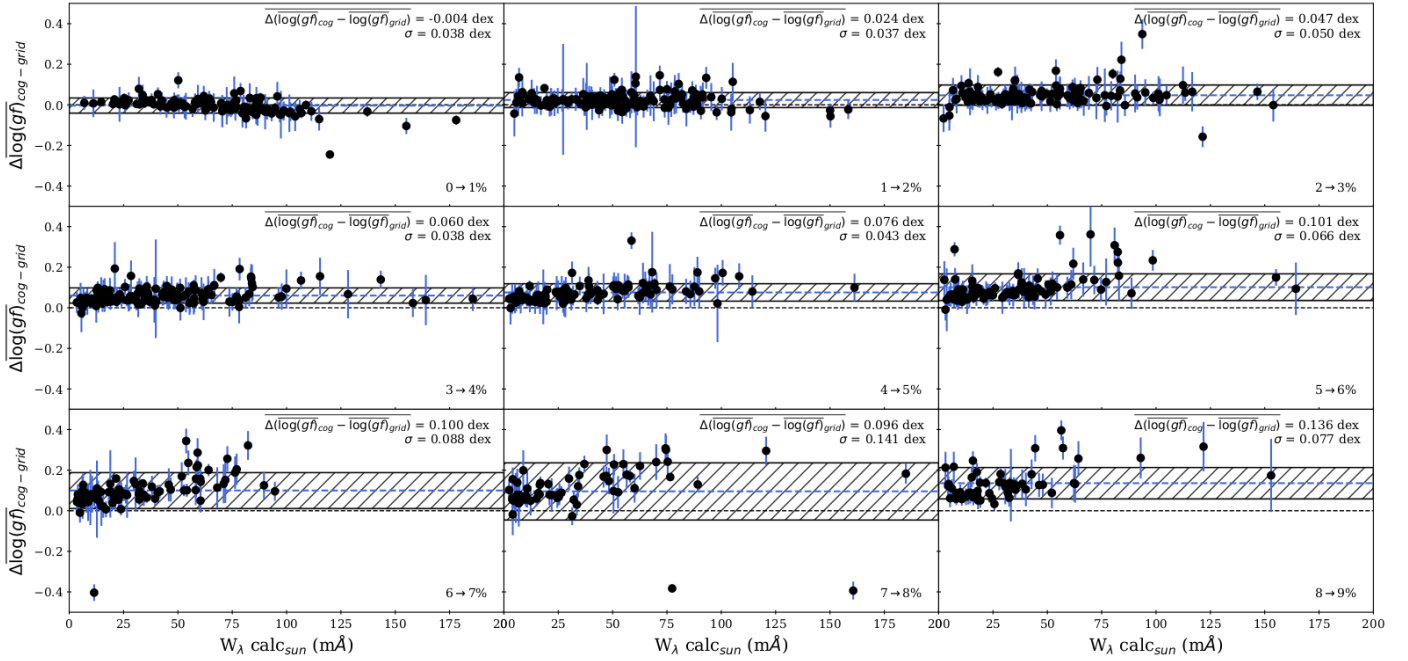


Fig. 7. $\Delta(\log(gf))_{\text{cog-grid}}$ plotted against theoretical W_λ values for the Sun, shown for different steps of Ω_{core} (left to right, top to bottom). The mean difference of the $\Delta(\log(gf))_{\text{cog-grid}}$ values is shown by the dashed blue lines, and the standard deviation is denoted by the hatched area. Fig. 8 shows the mean and standard deviation of the $\Delta(\log(gf))_{\text{cog-grid}}$ values plotted as a function of Ω_{core} .

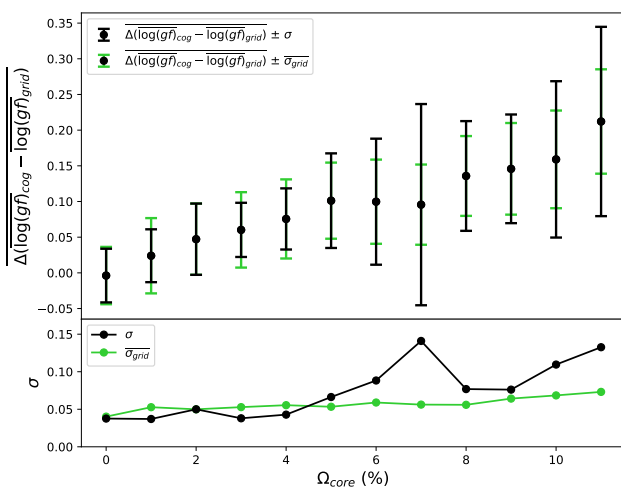


Fig. 8. Top panel: The mean $\Delta(\log(gf))_{\text{cog-grid}}$ values plotted against Ω_{core} . Black error bars show the standard deviation σ of the $\Delta(\log(gf))_{\text{cog-grid}}$ values, and green error bars show mean of the σ_{grid} values. Lower panel: the σ and $\bar{\sigma}_{\text{grid}}$ values plotted as a function of Ω_{core} . The mean of the $\Delta(\log(gf))_{\text{cog-grid}}$ values is shown to increase as Ω_{core} increases. The σ also increases with Ω_{core} , however the $\bar{\sigma}_{\text{grid}}$ exhibits a flatter trend. At $\Omega_{\text{core}} \leq 5\%$, σ is almost constant suggesting that the intrinsic scatter between the two methods is $\sigma = 0.04$ dex.

and:

$$\sigma_{\text{grid}} = \sqrt{\frac{\sum_{i=1}^n (\log(gf)_i - \overline{\log(gf)}_{\text{grid}})^2 / \sigma_i^2}{V_1 - (V_2/V_1)}} \quad (6)$$

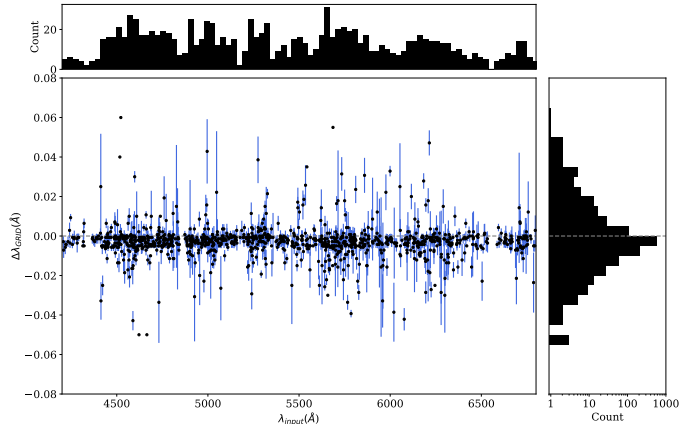


Fig. 9. $\Delta\lambda_{\text{grid-input}}$ versus λ_{input} for the 1091 investigated lines. 1σ error bars are shown in blue. A slight negative offset is present, however this is within the uncertainty in the HERMES spectrograph wavelength calibration. A small fraction of transitions have wavelength offsets that are attributed to inaccuracies in the atomic data.

where V_1 and V_2 are defined as follows:

$$V_1 = \sum_{i=1}^n 1/\sigma_i^2 \quad V_2 = \sum_{i=1}^n (1/\sigma_i^2)^2 \quad (7)$$

In the case that all the weights are equal Eqn. 6 and Eqn. 7 simplify to take the same form as the standard deviation shown in Eqn 4.

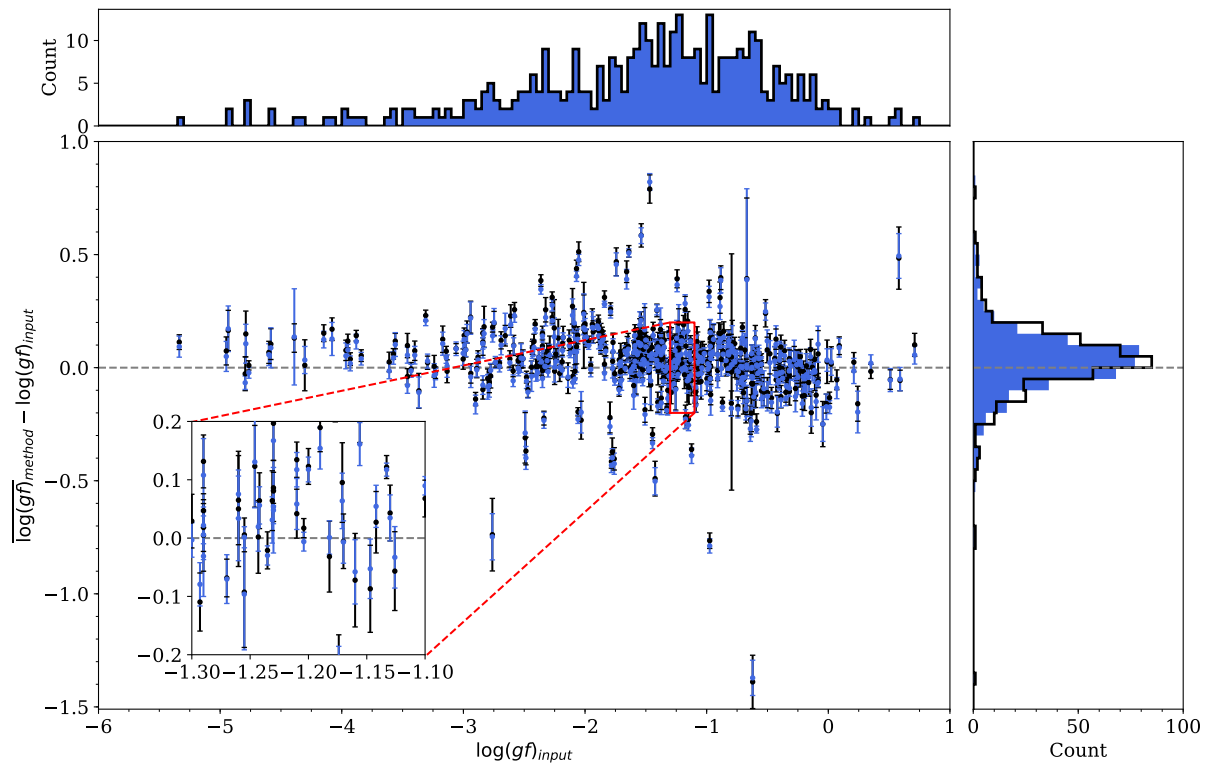


Fig. 10. $\overline{\Delta \log(gf)}_{\text{grid}-\text{input}}$ (in blue) and $\overline{\Delta \log(gf)}_{\text{cog}-\text{input}}$ (in black) plotted against $\log(gf)_{\text{input}}$ for the 408 analysis-independent lines discussed in Section 5.1. There are no clear trends in either the $\overline{\Delta \log(gf)}_{\text{grid}-\text{input}}$ values or $\overline{\Delta \log(gf)}_{\text{cog}-\text{input}}$ values with respect to $\log(gf)_{\text{input}}$, however there are a significant number of transitions for which both methods, which agree within 0.04 dex of each other, find sizeable offsets compared to the $\log(gf)_{\text{input}}$. Some transitions even show differences between $\log(gf)_{\text{input}}$ and our $\log(gf)$ values of ± 0.50 dex or more. The zoomed subplot shows transitions that have significantly smaller differences between the derived and input $\log(gf)$ values, however a number of them still do not agree within the derived uncertainties.

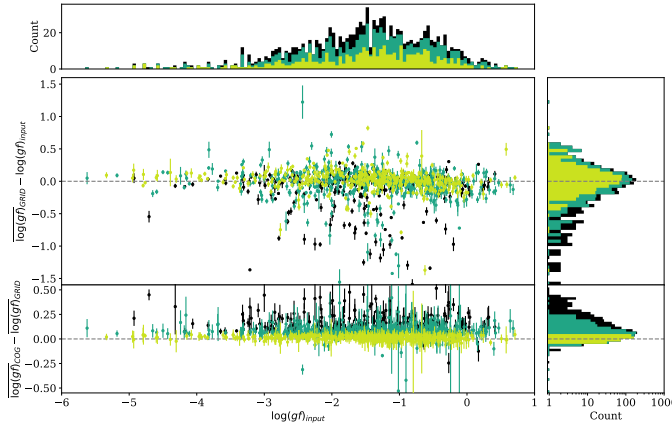


Fig. 11. $\overline{\Delta \log(gf)}_{\text{grid}-\text{input}}$ versus $\log(gf)_{\text{input}}$ for the 1091 investigated lines. Bottom panel: as above but for $\overline{\Delta \log(gf)}_{\text{cog}-\text{grid}}$. The 408 analysis-independent lines are shown in light-green, the remainder of the 845 quality-assessable lines are shown in dark green, and the remainder of the 1091 investigated lines are shown in black. There are no obvious trends in either $\overline{\Delta \log(gf)}_{\text{grid}-\text{input}}$ nor $\overline{\Delta \log(gf)}_{\text{cog}-\text{grid}}$ with respect to $\log(gf)_{\text{input}}$, except for a number of transitions where both methods, agreeing within error of each other, find significant upward revisions of the $\log(gf)_{\text{input}}$ values as $\Delta \log(gf) = 1.5$ dex.

5. Quality assessment and discussion

5.1. Selection of quality-assessable lines

A line is considered quality-assessable if both the curve of growth and iterative methods derive $\log(gf)$ values with overlapping errors, otherwise the line is deemed too difficult to accurately work with, be it due to measuring, modelling, or blending issues. An additional constraint, requiring the $\overline{\Delta \log(gf)}$ of the two methods to be ≤ 0.04 dex, can be imposed to increase the likelihood that the selected lines are free of systematic differences in analysis methods due to theoretical blending. Lines that fulfil this criterion are referred to as *analysis-independent* lines. As an example of the quality-assessable line selection, appendix Fig. B.1, Fig. B.2, and Fig. B.3 show the synthesised line profiles belonging to the $\overline{\log(gf)}_{\text{cog}}$ and $\overline{\log(gf)}_{\text{grid}}$ values, plotted against the observed line profile, for a non quality-assessable line (Fig. B.1), a quality-assessable line (Fig. B.2), and an analysis-independent spectral line (Fig. B.3), for the several benchmark stars. The quality of the observed data is sufficiently high enough that even lines as weak as central line depth $d \approx 0.02$ can be reliably quality-assessed.

5.2. Distributions of derived λ and $\log(gf)$ values

Fig. 9 shows the $\overline{\Delta \lambda}_{\text{grid}-\text{input}}$ plotted against λ_{input} for the 1091 investigated lines. For most lines there is excellent agreement between the literature wavelengths and those derived via the iterative modelling. A small fraction of transitions do have signif-

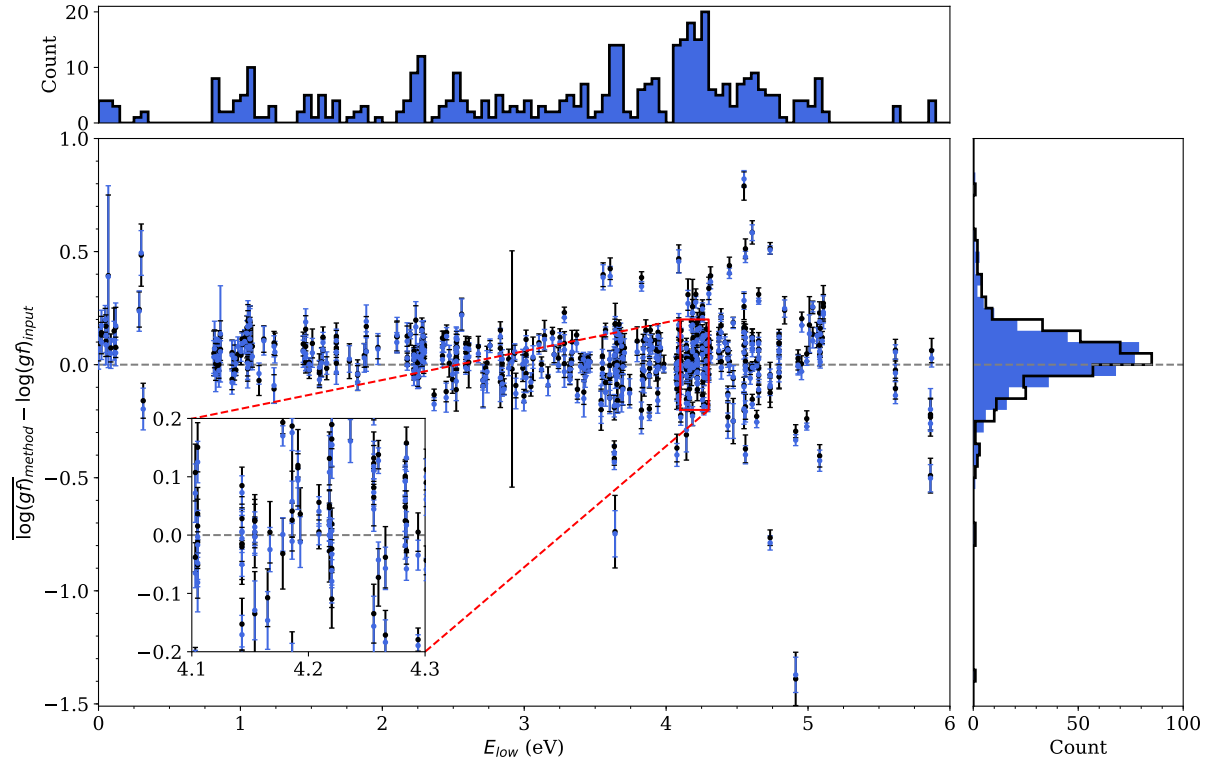


Fig. 12. As in Fig. 10, but plotted as a function of E_{low} . There is a slight upward inflection of $\log(gf)$ values at excitation energies of $E_{low} \leq 0.25$ eV which is possibly a symptom of non-LTE effects in these low-level transitions. Between $3.5 \leq E_{low} \leq 5.0$ eV we find an increase in scatter of $\log(gf)$ values, often belonging to higher excitation Fe I transitions. The zoomed subplot shows that a significant number of analysis-independent transitions have multiplets in common, and that the $\log(gf)$ values of these multiplets can show significant scatter.

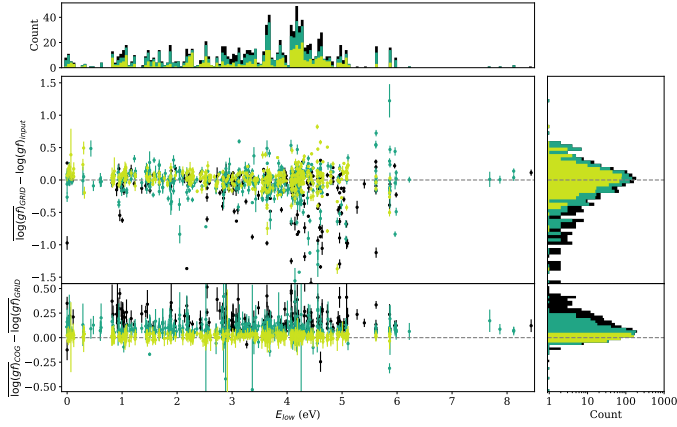


Fig. 13. As in Fig. 11, but plotted as a function of E_{low} . The large downward revisions pertain to Fe I transitions originating from higher excitation energies. The upward trend towards $E_{low} = 0$ eV is still visible, however to a lesser degree than the distribution of solely the analysis-independent lines.

ificant offsets of up to $|\Delta\lambda| \leq 0.06$ Å, which are caused by inaccuracies in the atomic data. There is a slight negative offset in $\Delta\bar{\lambda}_{grid-input}$, however this is well within the uncertainties of the HERMES spectrograph wavelength calibration.

Fig. 10 shows the $\Delta\log(gf)_{grid-input}$ and $\Delta\log(gf)_{cog-input}$ plotted against $\log(gf)_{input}$ for the 408 analysis-independent lines. We find that for a number of transitions both methods show significant revisions of the $\log(gf)_{input}$ values as large as ± 0.50 dex or more. We do not find any obvious trends between

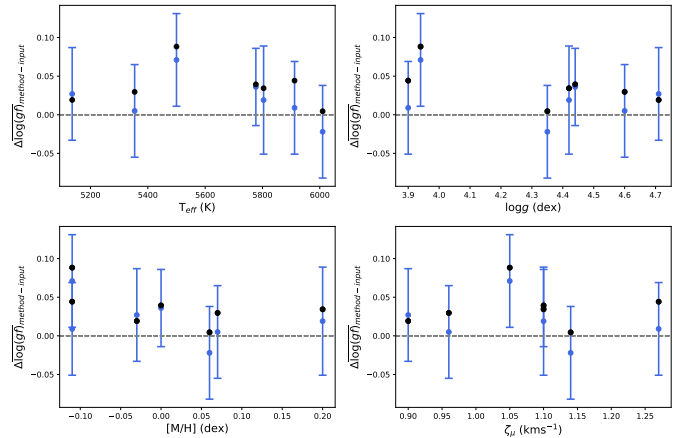


Fig. 14. The median of the 408 analysis-independent $\Delta\log(gf)_{method-input}$ values, for both the curve of growth (black circles) and iterative modelling (blue circles) methods, are plotted against the stellar parameters of the seven benchmark stars. The median of the σ_{grid} values are denoted by the blue error bars. The overestimation of the $\log(gf)_{cog}$ relative to the $\log(gf)_{grid}$ values can be seen. Apart from V I, we do not find any clear trends with respect to the stellar parameters for any of the 14 remaining species in the analysis-independent subset of lines.

the two methods $\log(gf)$ values and the $\log(gf)_{input}$ values, nor is there a correlation between the uncertainties and either a) the $\Delta\log(gf)_{method-input}$ values or b) the $\log(gf)_{input}$ values. Fig. 11 shows the $\Delta\log(gf)_{grid-input}$ plotted against $\log(gf)_{input}$ for the

1091 investigated lines, in addition to the $\overline{\log(gf)}_{\text{cog-grid}}$ plotted against $\overline{\log(gf)}_{\text{input}}$. Both the 845 quality-assessable lines, and the 1091 investigated lines, contain a number of transitions for which we find a significant downward $\log(gf)$ revision of up to 1.50 dex.

Fig. 12 shows the $\Delta\overline{\log(gf)}_{\text{grid-input}}$ and $\Delta\overline{\log(gf)}_{\text{cog-input}}$ plotted against $\overline{\log(gf)}_{\text{input}}$ for the 408 analysis-independent lines. We find an increase in scatter of the derived $\log(gf)$ values for higher excitation transitions. This increase in scatter is uncorrelated with the uncertainties of the derived $\log(gf)$ values, and is emphasised even more by the quality-assessable lines shown in Fig. 13. We also find a positive offset for transitions belonging to the lowest excitation energies. This is possibly due to non-LTE effects in a small number of lines belonging to either the lowest terms of easily ionised species, or resonant lines of other species. Fig. 13 shows the $\Delta\overline{\log(gf)}_{\text{grid-input}}$ plotted against E_{low} for the 1091 investigated lines. The increase in scatter of $\Delta\overline{\log(gf)}_{\text{grid-input}}$ with increasing E_{low} is present for the species Fe I and Si I, with the vast majority of the $\log(gf)_{\text{input}}$ values originating from the theoretical Kurucz 2007 line lists (Kurucz 1999–2014). The likely cause for this apparent relationship is transitions with a high degree of atomic configuration mixing, for which $\log(gf)$ values are difficult to calculate.

Fig. 14 shows the median of the 408 analysis-independent $\Delta\overline{\log(gf)}_{\text{method-input}}$ values, for both the curve of growth and iterative modelling methods, plotted against the benchmark stellar parameters. There is a small offset between the curve of growth and iterative modelling methods which is caused by the different treatments of line blending. There is no clear trend between the median $\Delta\overline{\log(gf)}_{\text{method-input}}$ values and any of the stellar parameters, with the median $\Delta\overline{\log(gf)}_{\text{grid-input}}$ values centred around ~ 0.00 dex, suggesting that the analysis is not subject to significant systematic modelling issues with respect to the stellar parameters. The exception to this is V I, which shows a negative trend with respect to increasing effective temperature. The cause of this is not clear, and could be linked to a number of possibilities: hyperfine splitting - which can easily be seen in the profile shapes of the $\lambda 4379.2$ and $\lambda 4594.1$ V I lines (see Appendix Table F.1 hyperlinks for interactive line plots), non-LTE effects - as V I is an easily ionised species and several of the V I lines originate from low-lying energy levels, or even differences in the [V/Fe] ratio between the different benchmark stars. Given that the same trend appears in multiple V I lines we believe the trend is less likely to be caused by line blending issues.

5.3. Discussion of quality assessment results

Of the 1091 atomic lines investigated, 845 are found to be quality-assessable and 408 of them are found to be analysis-independent lines. The ionic distribution of these lines is listed in Table 2. Approximately half of the investigated and quality-assessable lines belong to Fe I, and another $\sim 10\%$ of the lines belong to singly-ionised species. The literature atomic data belonging to a quality-assessable line is considered in agreement with our work, and therefore we can be recommend the value for use, if it agrees within error of the derived $\overline{\log(gf)}_{\text{grid}}$ and σ_{grid} values. We do not make use of any literature errors as these are only available in a handful of the retrieved databases. The $\overline{\log(gf)}_{\text{grid}}$ value is adopted as the benchmark value as in almost all cases it produces better χ^2_{red} values than the $\overline{\log(gf)}_{\text{cog}}$ value. In addition the $\overline{\log(gf)}_{\text{cog}}$ value relies upon theoretical corrections to the adopted line profile shape when measuring W_λ values. Of the

Table 2. Elemental and ionic distribution of the investigated, quality-assessable, and analysis-independent lines. In brackets are the number of lines having atomic data within σ_{grid} of the $\overline{\log(gf)}_{\text{grid}}$ values. It is worth noting that isotopic and hyperfine lines did not receive special treatment throughout the analysis, which may have lead to their under-representation in the line sets.

Species	number of investigated lines	quality assessable	analysis independent
C I	1	1 (1)	-
Na I	3	3 (1)	2 (0)
Mg I	5	5 (2)	2 (0)
Al I	2	2 (0)	1 (0)
Si I	56	42 (19)	14 (7)
Si II	2	2 (2)	-
S I	1	1 (1)	-
Ca I	21	21 (13)	10 (7)
Ca II	1	-	-
Sc I	1	1 (1)	-
Sc II	19	17 (12)	3 (2)
Ti I	90	80 (60)	47 (32)
Ti II	36	28 (21)	10 (9)
V I	15	14 (12)	6 (4)
V II	1	1 (1)	-
Cr I	82	61 (45)	36 (25)
Cr II	12	7 (3)	3 (1)
Mn I	13	9 (7)	1 (1)
Fe I	543	401 (145)	231 (92)
Fe II	30	15 (11)	4 (4)
Co I	15	9 (6)	-
Ni I	126	112 (86)	38 (30)
Zn I	2	2 (0)	-
Sr I	1	1 (0)	-
Y II	9	8 (5)	-
Ba II	1	-	-
La II	2	1 (1)	-
Ce II	1	1 (0)	-
Total:	1091	845 (455)	408 (214)

845 quality-assessable lines, 455 lines are found to have literature atomic data in agreement with the $\overline{\log(gf)}_{\text{grid}}$ values, corresponding to $\sim 54\%$ of the quality-assessable lines. This fraction is also representative of the analysis-independent lines, where 214 lines have sufficiently accurate atomic data. The majority of Fe-group species (Sc II, Ti I-II, V I, Cr I, Mn I, Fe II, Co I, Ni I) have a reasonable number of lines with accurate atomic data, typically 70–75% of lines, however the Fe I lines only have $\sim 38\%$ of lines with accurate atomic data.

Table F.1 provides the detailed break down of the 1091 investigated lines; literature wavelengths and E_{low} values, the derived $\overline{\lambda}_{\text{grid}}$, $\overline{\log(gf)}_{\text{cog}}$, $\overline{\log(gf)}_{\text{grid}}$, whether a line is quality-assessable and analysis-independent, the available literature data for the line, and which atomic data accurately reproduce the line. In an effort to help ascertain the quality of the $\log(gf)$ value of a given spectral line, interested readers can find interactive online plots of all 1091 investigated spectral lines, for all 7 benchmark spectra, as hyperlinks in the appendix Table F.1. The hyperlinks display all cross-matched atomic data for the line in question, including additional information such as level configurations and terms, in addition to interactive plots of the observed line profiles and synthetic line profiles using all $\log(gf)$ values derived

here and found in the literature, and their respective equivalent widths per $\log(gf)$ value, per star.

To better visualise the quality assessment process, appendix Fig. C.1, Fig. C.2, and Fig. C.3 show the observed lines profiles of three transitions in the seven benchmark spectra, including synthetic line profiles calculated using the $\log(gf)_{grid}$ and available literature values. The three transitions show examples of the three quality assessment outcomes: an example for which all available literature is within error of the $\log(gf)_{grid}$ value (Fig. C.1); an example for which only some of the available literature values are within error of the $\log(gf)_{grid}$ value (Fig. C.2); and an example for which none of the available literature is within error of the derived $\log(gf)_{grid}$ value (Fig. C.3). It is clear that the $\log(gf)_{grid}$ values reproduce the several line profiles extremely well, and that in some cases the available literature data is insufficient to reproduce the observed line profiles.

It is worth mentioning important limitations of this work. The astrophysical $\log(gf)$ values derived in this work have been determined using the solar abundances of Grevesse et al. (2007), and any updates to these elemental abundances would require a correction to the $\log(gf)$ values of lines belonging to updated species. Fortunately, the majority of the lines investigated here would only require directly-inverse corrections, *i.e.* if an abundance is revised by $\Delta[X/H] = 0.01$ dex, then all lines of element X will require a simple update of $\Delta \log(gf) = -0.01$ dex. This means that the astrophysical $\log(gf)$ values should remain useful, especially in the context of differential abundance analysis, for years to come.

Blended lines, even accurately known ones, have been avoided here due to the complexity of simultaneously quality assessing multiple components. Hyperfine and isotopically split lines have not received any special treatment throughout this analysis. In the case of isotopic lines, of which the components are often represented as individual entries in a line list, there is a clear under-representation of s-process elements in the investigated lines due to the fact that the Ω_{core} treats the multiple components as individual lines, and thus are considered heavily blended features. The hyperfine splitting of lines has not been addressed here, as while hyperfine splitting information is becoming more abundant in the literature it was not included in the investigated atomic databases at the time of retrieval³. Unlike the s-process elements, lines that require hyperfine splitting may be present in the quality assessment results, though inaccuracies in their derived $\log(gf)$ values depend heavily on the observed profile shape. Isotopic and hyperfine lines may benefit from an additional dedicated investigation, where the methods described in this paper are expanded to account for the multiple components of such transitions.

6. Summary

In this work we present a homogeneous quality assessment of the literature atomic data available for unblended spectral lines, in the wavelength range 4200–6800 Å, present in seven benchmark stars that span the effective temperature range 5000–6000 K. The work presented here was performed for multiple benchmark stars to help make the analysis more robust against any erroneous stellar parameter derivations, and also to investigate whether spectral lines are subject to different degrees of blending that would

otherwise be unnoticed when analysing a single star. Apart from T_{eff} , the stars are chosen to have similar stellar parameters to minimise any systematic modelling differences between objects. The objects were also chosen to minimise the impact of potential non-LTE effects which could systematically affect the derived $\log(gf)$ values. No clear correlations were found between the derived $\log(gf)$ values and the stellar parameters. The high-quality benchmark spectra were obtained using the Mercator-HERMES spectrograph, each with a resolution of $R \sim 85000$ and $S/N \sim 1000$. The spectra are available, in both normalised and unnormalised format, at brass.sdf.org.

Of the 82337 atomic transitions found in the literature for this wavelength range, 1091 were found to be theoretically deep, unblended, and having observable line profiles that can be fitted accurately with a single Gaussian profile. Given the high S/N ratios and high resolution of our benchmark spectra not all of our investigated lines can be utilised in other spectroscopic works, however the quality assessment results and $\log(gf)$ values themselves are valid at all spectral resolutions and S/N ratios. In addition, this work provides quality information for many lines previously unused in spectroscopic analysis.

Astrophysical $\log(gf)$ values were derived for each of the 1091 transitions using two commonly employed methods: equivalent width and spectral synthesis fitting methods. Care was taken to address, minimise, and remove as many potential systematic errors as possible from the derived $\log(gf)$ values, as well as producing representative error bars. Agreement between the two derived $\log(gf)$ values was used as a criterion to select a subset of 845 well-behaving lines which could be reliably quality-assessed. An additional constraint, mandating that the $\log(gf)$ values of the two methods are within 0.04 dex of each other, was imposed to produce a further subset of 408 spectral lines which are free of systematic differences caused by the adopted analysis methods.

A key conclusion of this work is that the treatment of blending lines is vital when aiming to reduce systematic errors and uncertainty from quantitative spectroscopy. Careful comparison between the curve of growth and detailed modelling methods revealed that even small background lines, contributing as little as 5% of the total equivalent width of a spectral feature, can lead to systematic offsets of ~ 0.10 dex or more between the two methods.

The available atomic data for these 845 spectral lines were compared against the $\log(gf)_{grid}$ values to determine whether the literature values were in agreement with the presented work, as discussed in Section 5.3. It was found that $\sim 54\%$ of the quality-assessed lines have at least one literature $\log(gf)$ value in agreement with our work. For Fe I this value is $\sim 38\%$ and for the remaining Fe-group elements the value is around 70–75% on average.

We provide recommendations, where possible, on which literature atomic data will produce sufficiently accurate spectroscopic results, and where the literature is insufficient, in some cases over 0.5 dex from our values, we suggest to use the astrophysical $\log(gf)$ values derived in this work. While the quality assessment presented here is limited to the atomic data compiled in Paper 1, the astrophysical $\log(gf)$ values and errors can easily be used to quality assess other literature $\log(gf)$ values, allowing astronomers and atomic physicists to evaluate the quality of newly produced atomic data. All results of the presented investigation are available in the Appendix, as well as in digital format via the CDS and at brass.sdf.org.

³ We note that in the time since our atomic data retrievals, VALD3 has expanded their database so that they can now provide HFS data for a large number of atomic species (Pakhomov et al. 2017)

Acknowledgements. We thank the atomic data producers and providers for their invaluable work towards improving the accuracy of stellar spectroscopy and the ease at which vast quantities of data can be retrieved. We also thank the referee for their useful comments and feedback towards the manuscript. The research for the present results has been subsidised by the Belgian Federal Science policy Office under contract No. BR/143/A2/BRASS. T.M and M.V.d.S are supported by a grant from the Fondation ULB. This work has made use of the VALD database, operated at Uppsala University, the Institute of Astronomy RAS in Moscow, and the University of Vienna. This work is based on observations made with the Mercator Telescope, operated on the island of La Palma by the Flemish Community, at the Spanish Observatorio del Roque de los Muchachos of the Instituto de Astrofísica de Canarias. This work is also based on observations obtained with the HERMES spectrograph, which is supported by the Research Foundation - Flanders (FWO), Belgium, the Research Council of KU Leuven, Belgium, the Fonds National de la Recherche Scientifique (F.R.S.-FNRS), Belgium, the Royal Observatory of Belgium, the Observatoire de Genève, Switzerland and the Thüringer Landessternwarte Tautenburg, Germany.

References

- Alvarez, R., Plez, B. 1998, A&A, 330, 1109-1119
- Andreasen D. T., Sousa S. G., Delgado Mena E., et al. 2016, A&A, 585, A143
- Bard, A., Kock, A., Kock, M. 1991, A&A, 248, 315-322
- Bard, A., Kock, M. 1994, A&A, 282, 1014-1020
- Barklem, P. 2016, A&ARv, 24, 9B
- Baschek, B., Garz, T., Holweger, H., Richter, J. 1970, A&A, 4, 229
- Biémont, E., Quinet, P., Zeippen, C. J. 1993, A&AS, 102, 435
- Biémont, E., Blagoev, K., Engstrom, L., et al. 2011, MNRAS, 414, 3350-3359
- Bigot, L., Thevenin, F. 2008, J. Phys. Conf. Ser., 130, 012001
- Bizzarri, A., Huber, M. C. E., Noels, A., et al. 1993, A&A, 273, 707
- Blackwell, D. E., Ibbetson, P. A., Petford, A. D., Shallis, M. J. 1979a, MNRAS, 186, 633
- Blackwell, D. E., Petford, A. D., Shallis, M. J. 1979b, MNRAS 186, 657
- Blackwell, D. E., Petford, A. D., Shallis, M. J., Simmons, G. J. 1980a, MNRAS 191, 445
- Blackwell, D. E., Shallis, M. J., Simmons, G. J. 1980b, A&A, 81, 340-343
- Blackwell, D. E., Petford, A. D., Shallis, M. J., Simmons, G. J. 1982a, MNRAS 199, 43
- Blackwell, D. E., Menon, S. L. R., Petford, A. D., Shallis, M. J. 1982b, MNRAS, 201, 611-617
- Blackwell, D. E., Menon, S. L. R., Petford, A. D. 1983 MNRAS 204, 883-890
- Blackwell, D. E., Menon, S. L. R., Petford, A. D. 1984, MNRAS, 207, 533
- Blackwell, D. E., Booth, A. J., Menon, S. L. R., Petford, A. D. 1986a, MNRAS, 220, 289-302
- Blackwell, D. E., Booth, A. J., Haddock, D. J., Petford, A. D., Leggett, S. K. 1986b, MNRAS 220, 549
- Blackwell-Whitehead, R. J., Lundberg, H., Nave, G., et al. 2006, MNRAS, 373, 1603
- Boeche, C., Grebel, E. K. 2016, A&A, 587, A2
- Bonifacio, P., Caffau, E., Ludwig, H. G., Steffen, M. 2012, IAU Symp. 282, 213-220
- Booth, A. J., Blackwell, D. E., Petford, A. D., Shallis, M. J. 1984, MNRAS 208, 147
- Brewer, J. M., Fischer, D. A., Valenti, J. A., Piskunov, N. 2016, ApJS, 225, 32B
- Bridges J. M., Kornblith, R. L. 1974, ApJ, 192, 793
- Butler, K., Mendoza, C., Zeippen C.J. 1993, J. Phys. B 26, 4409
- Carnall, A. C. 2017, arXiv:1705.05165
- Castelli, F., Gratton, R. G., Kurucz, R. L. 1997, A&A, 318, 841-869
- Castelli, F., Kurucz, R. L. 2003, IAU Symp. 210, Modelling of Stellar Atmospheres, ASP-210
- Cayrel, R. 1988, IAU Symp. 132, The Impact of Very High S/N Spectroscopy on Stellar Physics, 34
- Chang, T. N., Tang, X. 1990, JQSRT, 43, 207
- Corliss, C. H., Bozman, W. R. 1962, NBS Monograph, Experimental transition probabilities for spectral lines of seventy elements; derived from the NBS Tables of spectral-line intensities (US Government Printing Office), 53
- Cunto, W., Mendoza, C., Ochsenbein, F., Zeippen, C. J. 1993, A&A, 275, L5
- Dalton, G., Trager S. C., Abrams, D. C. et al. 2012, SPIE, 8446, 84460P
- Danzmann, K., Kock, M. 1980, J. Phys. B 13, 2051-2059
- Davidson, M. D., Snoek, L. C., Volten, H., Donszelmann, A. 1992, A&A, 255, 457-458
- De Silva, G.M., Freeman, K.C., Bland-Hawthorn, J. et al. 2015, MNRAS, 499, 2604
- Den Hartog, E. A., Lawler, J. E., Sobeck, J. S., Sneden, C., Cowan, J. J. 2011, ApJS, 194, 35
- Den Hartog, E. A., Ruffoni, M. P., Lawler, J. E., et al. 2014, ApJ, 215, 2
- Doerr, A., & Kock, M., 1985, JQSRT, 33, 307-318
- Dubernet, M. L., Antony, B. K., Ba, Y. A. et al. 2016, J. phys. B: At. Mol. Opt. Phys., 49, 074003
- Froese Fischer, C., The MCHF/MCDHF Collection (non-orthogonal B-spline CI calculations), downloaded on May 6, 2002.
- Froese Fischer, C., Tachiev, G. 2012, The MCHF/MCDHF Collection, Version 2
- Fuhr, J. R., Martin, G. A., Wiese, W. L. 1988, J. Phys. Chem. Ref., Data 17, Suppl. 4
- Fuhr, J. R., Wiese, W. L. 1998, CRC Handbook of Chemistry and Physics, 79th Edition, 10-88-10-146, (NIST compilation)
- Gaia Collaboration, et al. 2016, A&A, 595, A1
- Garz, T. 1973, A&A, 26, 471
- Garz, T. & Kock, M. 1969, A&A, 2, 274
- Grevesse, N., Blackwell, D.E., Petford, A.D. 1989, A&A, 208, 157
- Grevesse, N., Asplund, M., Sauval, A. J. 2007, Space Science Reviews, 130, 105
- Gustafsson, B., Edvardsson, B., Eriksson, K., et al. 2008, A&A, 486, 951-970
- Hannaford, F., Lowe, R. M., Grevesse, N., et al. 1982, ApJ, 261, 736-746
- Hibbert, A., Biémont, E., Godefroid, M., Vaeck, N. 1993, A&AS, 99, 179
- Holys, A., & Fuhr, J. R. 1980, A&A, 90, 14-17
- Hummer, D. G., Berrington, K. A., Eissner, W., et al. 1993, A&A, 279, 298-309
- de Jong, R. S., Bellido-Tirado, O., Chiappini, C. et al. 2012, SPIE, 8446, 84460T
- Kelleher, D. E., Podobedova, L. I. 2008, J. Phys. Chem. Ref. Data 37, 1285-1501
- King, R. B. 1947, Astrophys. J. 105, 376-389
- Kostyk, R. I. 1981, Astrometriya Astrofiz. 45, 3-9 (Russ.)
- Kostyk, R. I. 1982, Sov. Astron.-AJ 26, 422-426
- Kostyk, R. I. 1982, Astrometriya Astrofiz. 46, 58
- Kostyk, R. I., & Orlova, T. V. 1983, Astrometriya Astrofiz. 49, 39-41 (Russ.)
- Kramida, A., Ralchenko, Y., Reader, J., & NIST ASD Team 2018. NIST Atomic Spectra Database (version 5.6.1) [Online]. Available: <http://physics.nist.gov/asd>

- Kroll, S., Kock, M. 1987, A&A Suppl. Ser., 67, 225
 Kuhne, M., Danzmann, K., Kock, M. 1978, A&A, 64, 111-113
 Kurucz, R. L. 1992, Rev. Mexicana AyA, 23, 45
 Kurucz, R. L., 1999-2014, Robert L. Kurucz On-Line Database of Observed and Predicted Atomic Transitions <http://kurucz.harvard.edu/atoms/>
 Kurucz R. L., Peytremann E., 1975, SAO Special Report, 362, 1
 Landi, E., et al. 2013, ApJS, 763, 86
 Laverick, M., Lobel, A., Merle, T. et al. 2018, A&A, 612, A60
 Lawler, J. E., Bonvallet, G., Sneden, C. 2001a, ApJ, 556, 452
 Lawler, J. E., Sneden, C., Cowan, J. J., Ivans, I. I., Den Hartog, E. A. 2009, ApJ Suppl. Ser., 182, 51
 Lawler, J. E., Guzman, A., Wood, M. P., Sneden, C., Cowan, J. J. 2013, ApJS, 205, 11
 Lawler, J. E., Wood, M. P., Den Hartog, E. A., et al. 2014, ApJS, 215, 2
 Lawler, J. E., Dakin, J. T. 1989, JOSAB, 6, 8
 Lennard, W. N., Whaling, W., Scalo, J. M., Testerman, L. 1975, ApJ, 197, 517
 Lind, K., Bergemann, M., Asplund, M. 2012, MNRAS, 427, 50-60
 Lindegren, L., Feltzing, S. 2013, A&A, 533, A94
 Lobel, A. 2008, J. J. Phys. Conf. Ser. 130, 012015
 Lobel, A., Royer, P., Martayan, C. et al. 2017, Can. J. Phys. 2017, 95(9), 833-839
 Lobel, A., Royer, P., Martayan, C. et al. 2018, Workshop on Astrophysical Opacities 2017, ASPC, 515, 255
 Lotrian, J., Cariou, J., Johannin-Gilles, A. 1975, JQSRT, 15, 815-821
 Luck, R. E. 2017, AJ, 153, 21
 Martin, G., Fuhr, J., Wiese, W. 1988, J. Phys. Chem. Ref. Data Suppl., 17, 3
 May, M., Richter, J., Wichelmann, J. 1974, A&A, Suppl. Ser. 18, 405
 Melendez, J., Barbuy, B. 2009, A&A, 497, 2
 Mendoza, C., Eissner, W., Le Dourneuf, M., Zeippen, C. J. 1995, TOPBASE (Opacity Project), downloaded on July 28, 1995.
 Miles, B. M., Wiese, W. L. 1969, Atomic Data, 1, 1
 Moity, J. 1983, A&A, Suppl. Ser. 52, 37-62
 Morton, D. C. 2003, ApJ, Suppl. Ser. 149, 205-238; Erratum: 151, 403 (2004)
 Nahar, S. N. 1993, Phys. Scr, 48, 297
 Nahar, S. N., Pradhan, A. K. 1993, J. Phys. B 26, 1109-1127
 Neckel, H., Labs, D. 1984, Solar Phys., 90, 205
 Nicholls, R. W. 1964, Ann. Geophys. 20(2), 144-181
 Nitz, D. E., Wickliffe, M. E., Lawler, J. E. 1998, ApJ Suppl. Ser., 117, 1
 O'Brian, T. R., Wickliffe, M. E., Lawler, J. E., et al. 1991, JOSAB, 8, 1185-1201
 O'Brian, T. R., Lawler, J. E. 1991, Phys. Rev. A 44, 7134
 Önehag, A., Heiter, U., Gustafsson, B., et al. 2012, A&A, 542, A33
 Ostrovskii, Yu. I., Penkin, N. P. 1958, Opt. Spektrosk. 5(4), 345-353 (Russ.)
 Pakhomov, Y., Piskunov, N., Ryabchikova, T. 2017, ASP Conference Series, Vol. 510, 518
 Parkinson, W. H., Reeves, E. M., Tomkins, F. S. 1976, Royal Society of London Proceedings Series A, 351, 569-579
 Pickering, J. C., Thorne, A. P., Perez, R. 2001, Astrophys. ApJ Suppl. Ser., 132, 2; Erratum: 2002, 138, 247-248
 Pinnington, E. H., Ji, Q., Guo, B., et al. 1993, Can. J. Phys., 71, 47
 Pitts, R. E., Newson, G. H. 1986, JQSRT, 35, 383
 Plez, B. 2011, J. Phys. Conf. Ser. 328 012005
 Plez, B. 2012, Astrophysics Source Code Library, record ascl:1205.004
 Raassen, A., Uylings, P. 1998a, A&A, 340, 300-304
 Raassen, A., Uylings, P. 1998b, J. Phys. B 31, 3137-3146
 Ralchenko Y., Kramida A., Reader J., NIST ASD Team 2010, NIST Atomic Spectra Database (ver. 4.0.0), [Online].
 Raskin, G., Van Winckel, H., Hensberge, H. et al. 2011, A&A, 526, A69
 Roberts, J. R., Andersen, T., Sorensen, G. 1973, ApJ, 181, 567-586
 Ruffoni, M. P., Den Hartog, E. A., Lawler, J. E., et al. 2014, MNRAS, 441, 3127-3136
 Ryabchikova, T. A., Hill, G. M., Landstreet, J. D., Piskunov, N., & Sigut, T. A. A. 1994, MNRAS, 267, 697
 Ryabchikova, T. A., Piskunov, N. E., Stempels, H. C., et al. 1999, Physics Scripta Volume T, 83, 162-173
 Ryabchikova, T., Piskunov, N., Kurucz, R. et al. 2015, PhysS., 90, 5
 Saraph, H., Storey, P. 2012, publication in preparation, available online at <http://cdsweb.u-strasbg.fr/topbase/topbase.html>
 Schnabel, R., Schultz-Johanning, M., Kock, M. 2004, A&A, 414, 1169-1176
 Sigut, T. A. A., Landstreet, J. D. 1990, MNRAS, 247, 611
 da Silva, R., Milone, A., Rocha-Pinto, H. 2015, A&A, 580, A24
 Sitnova, T. M., Mashonkina, L. I., Ryabchikova, T. A. 2016, MNRAS, 461, 1
 Smith, G. 1988, JPhB, 21, 16
 Smith, G., O'Neill J. A. 1975, A&A, 38, 1
 Smith, G., Raggett, D. S. J. 1981, JPhB, 14, 21
 Sobeck, J. S., Lawler, J. S., Sneden, C. 2007, ApJ, 667, 2
 Sousa, S. G., Santos, N. C., Israeli, G., Mayor, M., Monteiro, M. J. 2007, A&A, 469, 783
 Tachiev, G., Froese Fischer, C., The MCHF/MCDHF Collection (energy-adjusted MCHF calculations), downloaded on Dec. 10, 2003.
 Tozzi, G. P., Brunner, A. J., Huber, M. C. E. 1985, MNRAS 217, 423
 Tsantaki, M., Andreasen, D. T., Teixeira, G. D. C., et al. 2018, MNRAS, 473, 4
 Warner, B. 1968, MNRAS, 140, 53
 Wickliffe, M. E., Lawler, J. E., 1997, ApJS, 110, 163
 Wiese, W. L., Smith, M. W., Miles, B. M. 1969, NSRDS-NBS 22, 268 (U.S. Government Printing Office)
 Wiese W.L., Martin G.A. 1990, NSRDS-NBS 68 (U.S. Government Printing Office)
 Whaling, W., Scalo, J. M., Testerman, L. 1977, ApJ 212, 581-590
 Whaling, W., Hannaford, P., Lowe, R. M., Biémont, E., Grevesse, N. 1985, A&A 153, 109-115
 Wood, M. P., Lawler, J. E., Sneden, C., Cowan, J. J. 2013, ApJS, 208, 27
 Wood, M. P., Lawler, J. E., Sneden, C., Cowan, J. J. 2014, ApJS, 211, 2
 Wujec, T., Weniger, S. 1981, JQSRT, 25, 167-182
 Zatsarinny, O. & Bartschat, K. 2006, JPhB, 39, 2861

Appendix A: Automatic normalisation of the observed benchmark spectra

The observed benchmark spectra are continuum flux normalised using a semi-automatic spectral-template normalisation procedure. It searches for a series of wavelength points over sufficiently continuous flux regions close to the stellar continuum level in the theoretical spectra between 4000 Å and 6800 Å. The selected wavelength regions are then used as continuum anchor points for a polynomial fit to normalise the observed spectrum. We opt to use an automatic template normalisation procedure to remove the 'human-factor' from the spectrum normalisation, leading to repeatable and consistent global continuum flux normalisations. The final results are scrutinised to ensure they behave as expected. There are no obvious issues in the continuum placement of the automatically normalised spectra (see Section 4.3.4 for discussion on the $\log(gf)$ uncertainties due to normalisation).

Appendix B: Line profile comparisons with the curve of growth and iterative modelling methods

Fig. B.1, Fig. B.2, and Fig. B.3 show the synthesised line profiles of the $\log(gf)_{grid}$ and $\log(gf)_{cog}$ values, including line profile error bars, alongside the observed line profiles in the seven observed benchmark stars. Fig. B.1 shows an example where the $\log(gf)_{grid}$ and $\log(gf)_{cog}$ values do not agree within error of each other, and thus the spectral line is not suitable for quality assessment. Fig. B.2 shows an example where the $\log(gf)_{grid}$ and $\log(gf)_{cog}$ values do agree within error of each other, making the line suitable for quality assessment. Fig. B.2 shows a quality assessable line where the $\log(gf)_{grid}$ and $\log(gf)_{cog}$ values agree within 0.04 dex of each other, indicating the line is free of systematic issues due to the treatment of line blending by the two methods.

Appendix C: Line profile comparisons with the cross-matched literature data

Fig. C.1, Fig. C.2, and Fig. C.3 show the synthesised line profiles of the $\log(gf)_{grid}$ values, including line profile error bars, alongside the observed line profiles in the seven observed benchmark stars. In addition the figures show synthetic line profiles corresponding to the available literature $\log(gf)$ values of the given transition. All three examples show a analysis-independent line. Fig. C.1 shows an example where all literature $\log(gf)$ values agree within error of the $\log(gf)_{grid}$ value. Fig. C.2 shows an example where only one of the literature $\log(gf)$ values agrees within error of the $\log(gf)_{grid}$ value. Finally Fig. C.3 shows an example where none of the literature $\log(gf)$ values agree within error of the $\log(gf)_{grid}$ value.

Appendix D: Tables of individual $\log(gf)_{cog}$ and $\log(gf)_{grid}$ values per benchmark star for the 1091 investigated lines

The individual $\log(gf)_{cog}$, $\log(gf)_{grid}$, and σ_{grid} values per benchmark star are available, for each of the 1091 investigated lines, in digital format via the CDS and at brass.sdf.org. Table D.1 shows an example of the available individual $\log(gf)_{cog}$ values per benchmark star. Table D.2 shows the same but for the

individual $\log(gf)_{grid}$ values, which have the additional σ_{grid} values corresponding to the 68.3% confidence intervals discussed in Section 4.2.

Appendix E: Tables of W_λ values per benchmark star for the 1091 investigated lines

The measured W_λ values, ΔW_λ corrections (as discussed in Section 4.3.5), and calculated W_λ values for the $\log(gf)_{grid}$ values, $\log(gf)_{cog}$ values, and available literature $\log(gf)$ values are available, for each of the benchmark stars, in digital format via the CDS and at brass.sdf.org. Table E.1 shows an example of the W_λ values associated with the benchmark star ϵ Eri for the 1091 investigated spectral lines. Similar tables are available for each of the benchmark stars.

Appendix F: Table of quality assessment information for the 1091 investigated lines

Table F.1 presents both the line selection and quality assessment results for the full 1091 spectral lines investigated in this work. The table is available in digital format via the CDS and at brass.sdf.org.

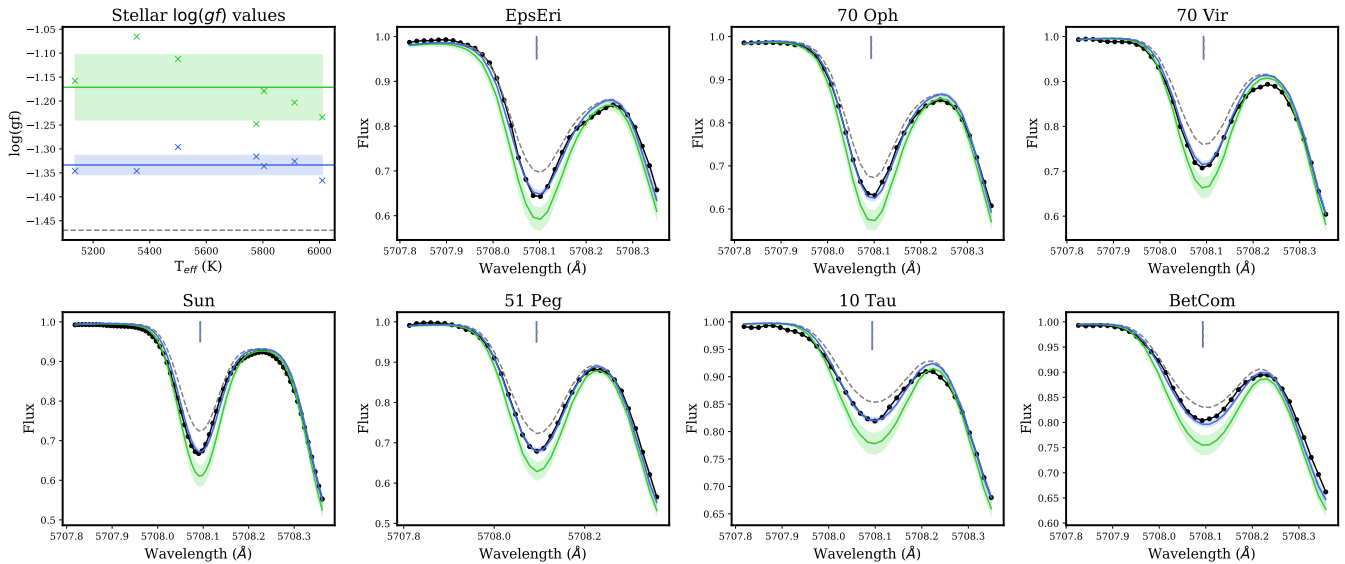


Fig. B.1. The eight panels show the $\log(gf)$ determinations for the $\lambda 5708.1$ Fe I line, which is deemed to be unsuitable for quality assessment due to the disagreement between the $\log(gf)_{\text{cog}}$ and $\log(gf)_{\text{grid}}$ values. Observed line profiles are shown in black dots, line profiles calculated using the $\log(gf)_{\text{input}}$ values are shown in dashed gray, line profiles calculated using the $\log(gf)_{\text{cog}}$ values are shown in green, line profiles calculated using the $\log(gf)_{\text{grid}}$ values are shown in blue, and errors are shown as green and blue shaded areas respectively. Vertical blue and dashed gray lines denote the $\bar{\lambda}_{\text{grid}}$ and λ_{input} values respectively. The disagreement in this case is likely caused by the presence of a nearby spectral line affecting the single Gaussian fit of the curve of growth method.

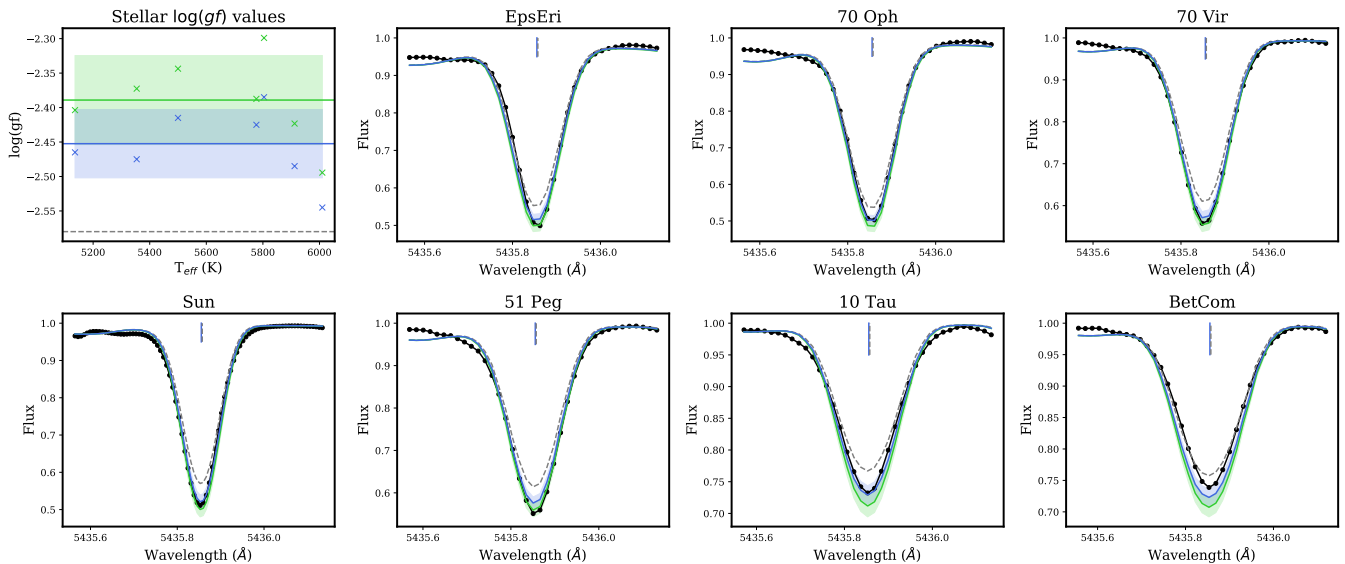


Fig. B.2. The eight panels show the $\log(gf)$ determinations for the $\lambda 5435.8$ Ni I line which is deemed to be quality-assessable. Observed line profiles are shown in black dots, line profiles calculated using the $\log(gf)_{\text{input}}$ values are shown in dashed gray, line profiles calculated using the $\log(gf)_{\text{cog}}$ values are shown in green, line profiles calculated using the $\log(gf)_{\text{grid}}$ values are shown in blue, and errors are shown as green and blue shaded areas respectively. Vertical blue and dashed gray lines denote the $\bar{\lambda}_{\text{grid}}$ and λ_{input} values respectively.

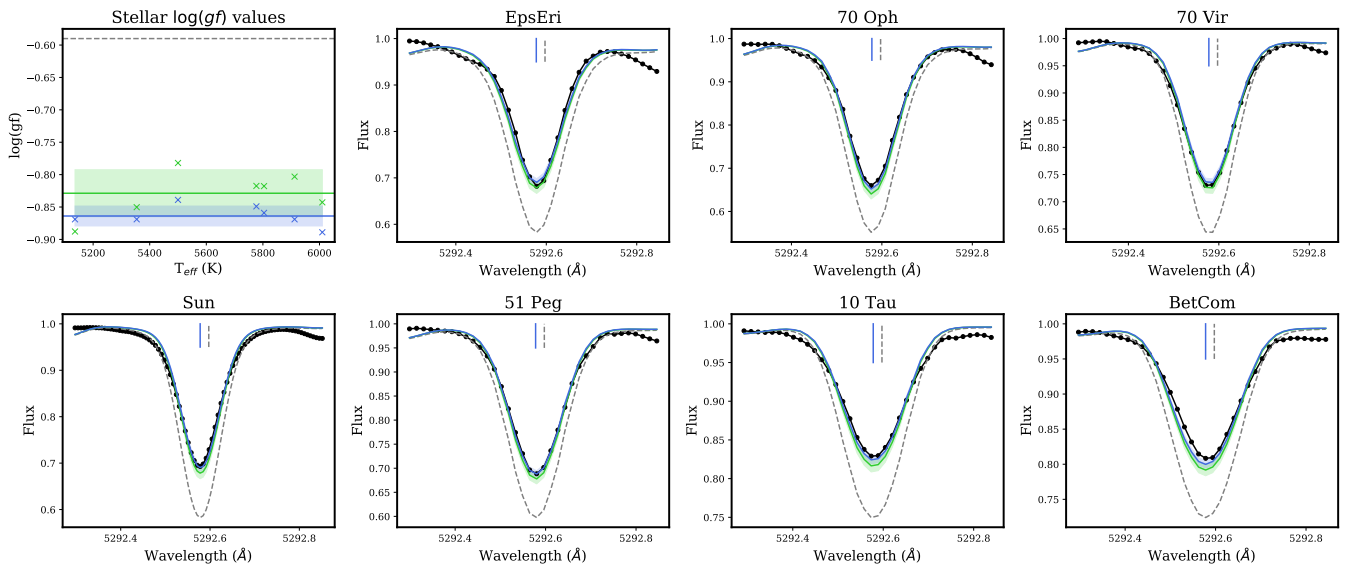


Fig. B.3. The eight panel show the $\log(gf)$ determinations for the $\lambda 5292.6$ Fe I line deemed suitable for quality assessment and deemed to be robust against adopted analysis method. Observed line profiles are shown in black dots, line profiles calculated using the $\log(gf)_{\text{input}}$ values are shown in dashed gray, line profiles calculated using the $\log(gf)_{\text{cog}}$ values are shown in green, line profiles calculated using the $\log(gf)_{\text{grid}}$ values are shown in blue, and errors are shown as green and blue shaded areas respectively. Vertical blue and dashed gray lines denote the $\bar{\lambda}_{\text{grid}}$ and λ_{input} values respectively. This line also shows a measurable $\Delta\lambda$ correction of ~ 0.02 Å to the input wavelength.

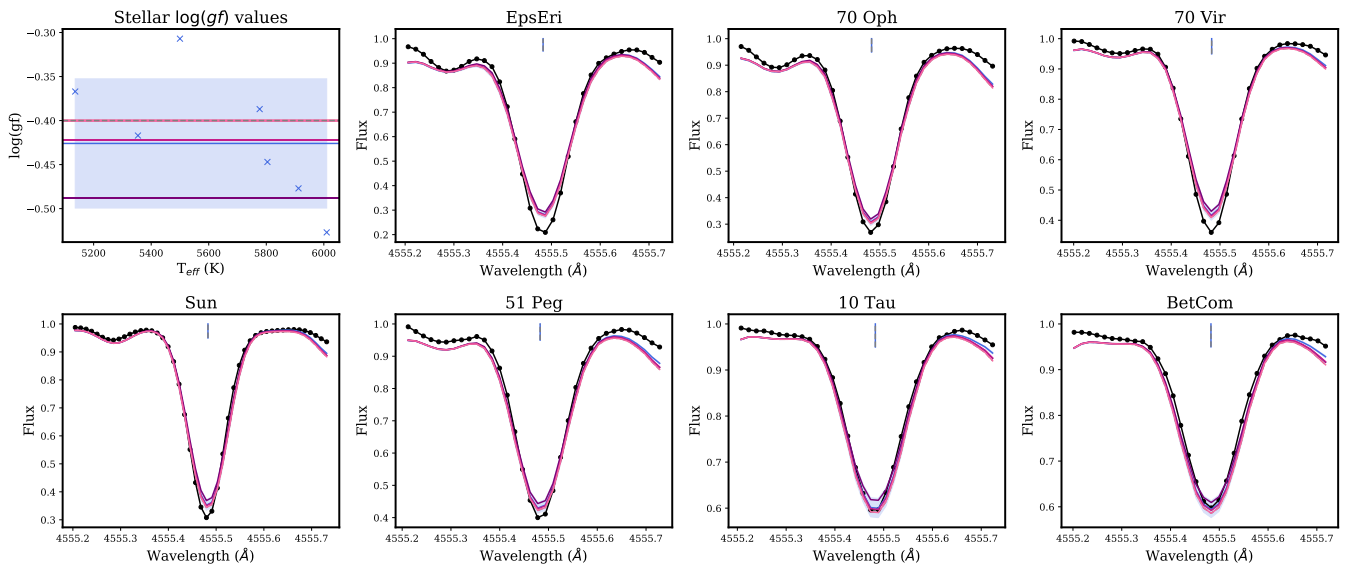


Fig. C.1. The eight panels show the quality assessment for the $\lambda 4555.5$ Ti I line. The style follows that of Fig. B.1-B.3, minus the $\log(gf)_{\text{cog}}$ line profiles, and with several additional line profiles corresponding to the available literature $\log(gf)$ values of the transition. In this case all literature $\log(gf)$ values are within error of the $\log(gf)_{\text{grid}}$ value and can be recommended for use.

Table D.1. An excerpt of the individual $\log(gf)_{\text{cog}}$ values derived per benchmark star for each of the 1091 investigated lines. The full table is available in digital format via the CDS and at brass.sdf.org.

Line number	$\log(gf)_{\text{cog}}$						
	ϵ Eri	70 Oph A	70 Vir	Sun	51 Peg	10 Tau	β Com
1	-1.72	-1.66	-1.41	-1.47	-1.54	-1.46	-1.49
2	-1.22	-1.19	-0.96	-0.99	-1.06	-0.91	-0.96
3	-0.76	-0.71	-0.50	-0.50	-0.60	-0.41	-0.51
...

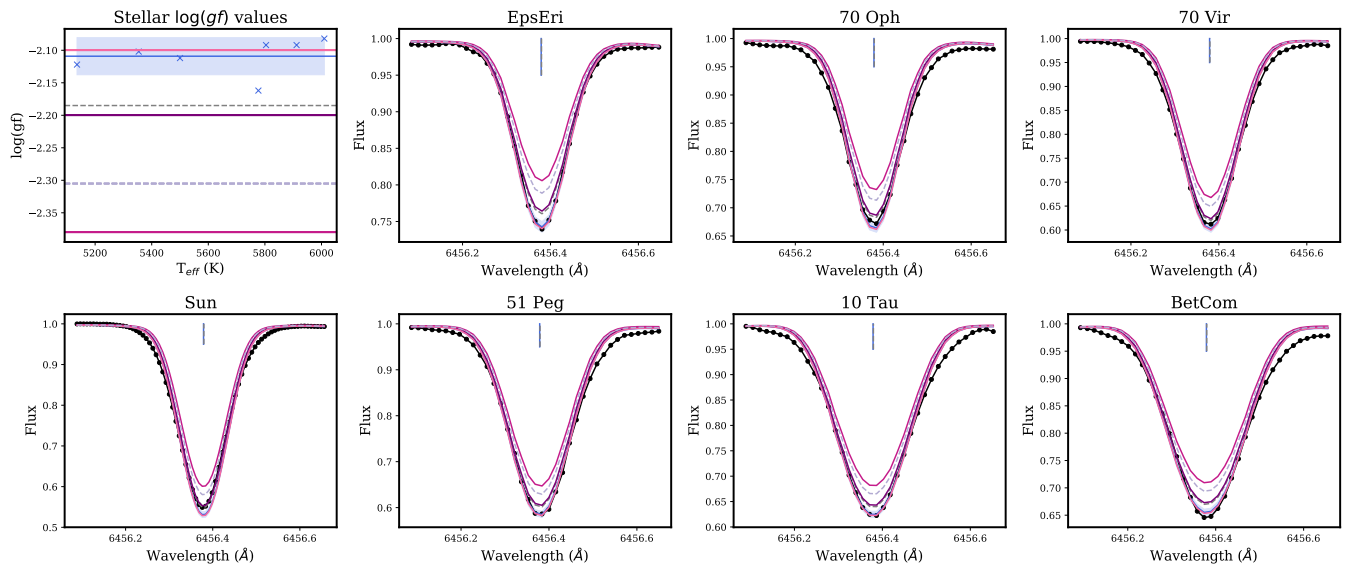


Fig. C.2. The eight panels show the quality assessment for the $\lambda 6456.4$ Fe II line. The style follows that of Fig. B.1-B.3, minus the $\log(gf)_{\text{cog}}$ line profiles, and with several additional line profiles corresponding to the available literature $\log(gf)$ values of the transition. In this case only one literature $\log(gf)$ value is within error of the $\log(gf)_{\text{grid}}$ value, and thus only this value is recommended for use.

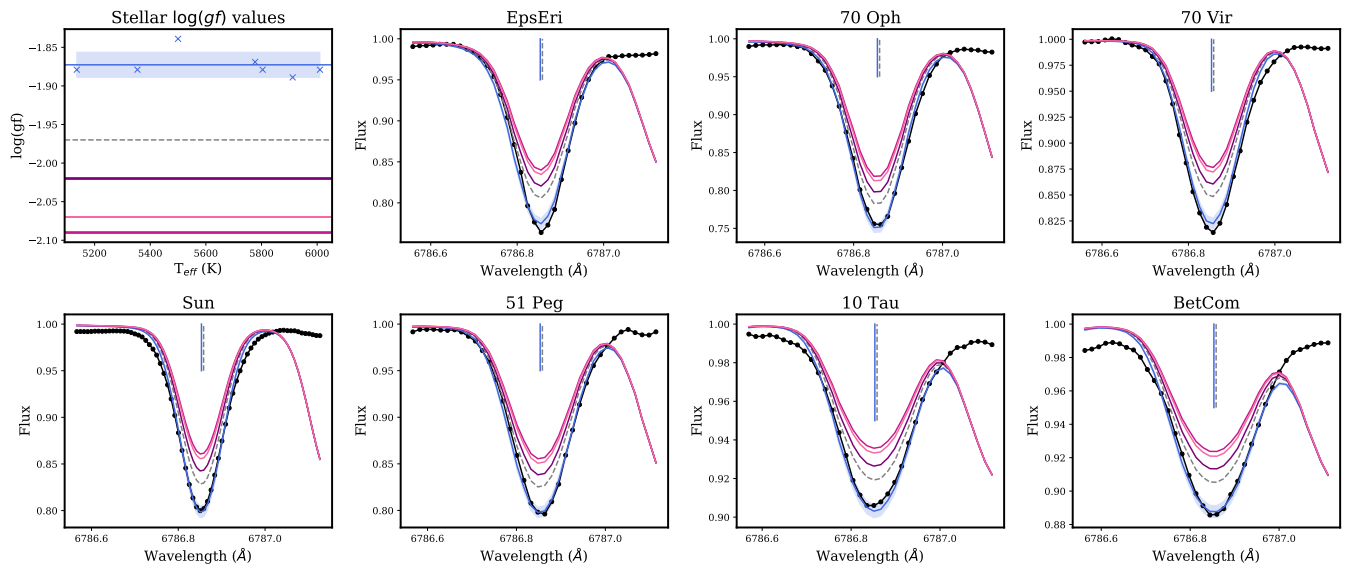


Fig. C.3. The eight panels show the quality assessment for the $\lambda 6786.8$ Fe I line. The style follows that of Fig. B.1-B.3, minus the $\log(gf)_{\text{cog}}$ line profiles, and with several additional line profiles corresponding to the available literature $\log(gf)$ values of the transition. In this case none of the literature $\log(gf)$ values can accurately reproduce the observed profile, with $\Delta \log(gf)$ values ranging between 0.1-0.25 dex, thus we would propose our $\log(gf)_{\text{grid}}$ as a more accurate alternative.

Table D.2. An excerpt of the individual $\log(gf)_{\text{grid}}$ values, and corresponding σ_{grid} values, derived per benchmark star for each of the 1091 investigated lines. The full table is available in digital format via the CDS and at brass.sdf.org.

Line number #	$\log(gf)_{\text{grid}}$							
	ϵ Eri	70 Oph A	70 Vir	Sun	51 Peg	10 Tau	β Com	
1	-1.77 ± 0.30	-1.72 ± 0.30	-1.44 ± 0.16	-1.44 ± 0.14	-1.56 ± 0.23	-1.53 ± 0.17	-1.55 ± 0.22	
2	-1.40 ± 0.22	-1.26 ± 0.22	-0.93 ± 0.14	-0.93 ± 0.12	-1.00 ± 0.14	-0.93 ± 0.10	-0.97 ± 0.11	
3	-1.06 ± 0.13	-1.00 ± 0.16	-0.71 ± 0.17	-0.59 ± 0.14	-0.73 ± 0.17	-0.60 ± 0.16	-0.68 ± 0.17	
...

Table E.1. An excerpt of the individual various W_λ values available for ϵ Eri for each of the 1091 investigated lines. The table provides the observed W_λ values measured using a single Gaussian fit, $\Delta W_{\lambda \text{ corr}}$ values used to correct the measured values Gaussian profile assumption (as described in Section 4.3.5), as well as calculated $W_{\lambda \text{ calc}}$ values for the $\overline{\log(gf)}_{\text{grid}}$ values, $\overline{\log(gf)}_{\text{cog}}$ values, and available literature $\log(gf)$ values: ^{a)} Paper 1 input list ^{b)} NIST ^{c)} SpectroWeb ^{d)} VALD3 ^{e)} Spectr-W³ ^{f)} CHIANTI ^{g)} TIPbase ^{h)} TOPbase. Similar tables are available for the remaining benchmark stars. The full tables are available in digital format via the CDS and at brass.sdf.org.

Line number #	$W_{\lambda \text{ meas}}$ (mÅ)	$\Delta W_{\lambda \text{ corr}}$ (mÅ)	$W_{\lambda \text{ calc}}$ (mÅ)									
			grid	cog	a)	b)	c)	d)	e)	f)	g)	h)
1	92.8	+5.3	113.5	112.1	118.4	-	118.4	-	-	-	60.6	-
2	119.2	+13.8	166.6	158.9	117.9	-	-	-	-	-	-	-
3	175.8	+27.5	200.7	248.4	272.1	-	263.9	-	341.0	-	-	-
...

Table F.1. Table of results for the 1091 investigated lines in FGK stars, belonging to 28 different ionic species. Lines are listed in elemental and ionic order (from lightest to heaviest, beginning with the neutral species of each element). Each transition shows: ¹⁾ the corresponding line number, #, of the transition used to identify the 1091 investigated lines in the various digital tables belonging to this work ²⁾ the input wavelength ³⁾ the derived $\bar{\lambda}_{grid}$ including 1 σ error ⁴⁾ the lower energy E_{low} of the transition ⁵⁾ the $\overline{\log(gf)}_{cog}$ and $\overline{\log(gf)}_{grid}$ values derived in this work including 1 σ errors ⁶⁾ whether a transition is considered quality-assessable (QA) and independent of adopted analysis methods (analysis-independent, or AI) ⁷⁾ the available literature $\log(gf)$ values for a transition taken from Paper 1 including references, where the following columns represent the database of origin for the given literature value: ⁸⁾ Paper 1 input list ^{b)} NIST ^{c)} SpectroWeb ^{d)} VALD3 ^{e)} Spectr-W^{3,f)} CHIANTI ^{g)} TIPbase ^{h)} TOPbase ⁱ⁾ which literature references, if any, reproduce the $\overline{\log(gf)}_{grid}$ values within the σ_{grid} errors and can thus be recommended for use. If a line cannot be quality-assessed then the 'recommended literature' column will display an 'X', and if the line can be quality-assessed but has no recommended literature values it displays a '-' . Each line number, #, is hyperlinked to a corresponding web-page where interested readers can find interactive line profile plots of all the $\log(gf)$ values in each benchmark star (in a similar manner to Fig. B.1 and Fig. C.1). Additional atomic information, such as configurations, terms, J-values, and equivalent widths, can be found via these links, or via brass.sdf.org.

#	Wavelength (\AA) Input	E_{low} (eV) $\Delta\lambda_{grid}$	$\log(gf)$ this work		Flags		Literature $\log(gf)$ values				Recommended literature	
			cog	grid	QA?	AI?	a)	b)	c)	d)	e)	
409	5052.144	0.002 \pm 0.006	7.685	-1.12 \pm 0.11	-1.29 \pm 0.12	✓	X	-1.30 ¹	-1.30 ²	-1.30 ³	-1.27 ⁴	-
358	4982.814	0.004 \pm 0.002	2.104	-0.76 \pm 0.08	-0.86 \pm 0.11	✓	X	-0.92 ⁶	-	-0.96 ²	-	-
901	6154.225	-0.006 \pm 0.002	2.102	-1.42 \pm 0.06	-1.45 \pm 0.04	✓	✓	-1.55 ⁶	-1.55 ⁷	-1.56 ²	-1.55 ³	-
905	6160.747	-0.004 \pm 0.002	2.104	-1.12 \pm 0.07	-1.12 \pm 0.08	✓	✓	-1.25 ⁶	-1.25 ⁷	-1.26 ²	-1.25 ³	-
125	4571.096	-0.008 \pm 0.003	0.000	-5.46 \pm 0.09	-5.57 \pm 0.09	✓	X	-5.62 ³	-5.62 ⁸	-5.62 ³	-5.62 ³	-
227	4730.029	0.001 \pm 0.003	4.346	-2.17 \pm 0.10	-2.23 \pm 0.08	✓	X	-2.35 ³	-2.35 ⁹	-2.32 ²	-2.35 ³	-
760	5785.313	-0.039 \pm 0.002	5.108	-1.83 \pm 0.07	-1.77 \pm 0.06	✓	X	-2.11 ¹⁰	-	-1.71 ²	-2.11 ¹⁰	-
978	6318.717	-0.011 \pm 0.009	5.108	-1.83 \pm 0.08	-1.87 \pm 0.07	✓	✓	-2.10 ¹¹	-2.10 ¹¹	-	-2.10 ³	-
979	6319.237	-0.003 \pm 0.011	5.108	-2.07 \pm 0.05	-2.10 \pm 0.04	✓	✓	-2.32 ¹¹	-2.32 ¹¹	-	-2.32 ³	-
1056	6696.023	-0.006 \pm 0.002	3.143	-1.40 \pm 0.08	-1.45 \pm 0.07	✓	X	-1.57 ¹²	-1.57 ¹²	-2.85 ²	-1.35 ¹³	-1.04 ⁴
1057	6698.673	-0.007 \pm 0.003	3.143	-1.74 \pm 0.07	-1.76 \pm 0.04	✓	✓	-1.87 ¹²	-1.87 ¹²	-2.65 ²	-1.65 ¹³	-1.64 ⁴
340	4947.607	-0.009 \pm 0.002	5.082	-2.16 \pm 0.05	-2.18 \pm 0.05	✓	✓	-1.76 ¹⁴	-	-2.20 ²	-1.76 ¹⁴	-2.29 ⁴
415	5070.950	-0.026 \pm 0.016	5.082	-2.81 \pm 0.22	-3.22 \pm 0.10	X	X	-2.25 ¹⁴	-	-4.00 ²	-2.25 ¹⁴	-
571	5421.168	-0.007 \pm 0.004	5.619	-1.21 \pm 0.06	-1.28 \pm 0.05	✓	X	-2.01 ¹⁴	-	-1.35 ²	-2.01 ¹⁴	-
594	5488.983	-0.015 \pm 0.003	5.614	-1.68 \pm 0.06	-1.75 \pm 0.06	✓	X	-2.30 ¹⁴	-	-1.90 ²	-2.31 ¹⁴	-
610	5517.533	0.000 \pm 0.003	5.082	-2.38 \pm 0.05	-2.42 \pm 0.05	✓	✓	-2.61 ¹⁴	-	-2.61 ²	-2.61 ¹⁴	-
647	5622.220	0.014 \pm 0.009	4.930	-2.87 \pm 0.07	-3.07 \pm 0.06	X	X	-2.61 ¹⁴	-1.64 ¹⁵	-3.06 ²	-2.61 ¹⁴	-1.64 ⁴
665	5645.613	-0.013 \pm 0.004	4.930	-1.98 \pm 0.03	-2.06 \pm 0.05	✓	X	-2.04 ¹⁶	-1.63 ¹⁵	-2.14 ²	-2.14 ¹⁷	-
675	5654.919	0.001 \pm 0.006	5.614	-1.52 \pm 0.04	-1.60 \pm 0.03	X	X	-1.89 ¹⁴	-	-1.73 ²	-1.89 ¹⁴	-
683	5665.555	-0.016 \pm 0.002	4.920	-1.91 \pm 0.04	-2.06 \pm 0.05	X	X	-1.94 ¹⁶	-2.04 ¹⁷	-2.04 ²	-2.04 ¹⁷	-
684	5666.677	0.001 \pm 0.002	5.616	-1.50 \pm 0.05	-1.60 \pm 0.04	X	X	-1.80 ¹⁴	-	-1.65 ²	-1.80 ¹⁴	-
693	5684.484	-0.005 \pm 0.001	4.954	-1.55 \pm 0.04	-1.58 \pm 0.04	✓	✓	-1.55 ¹⁶	-1.42 ¹⁵	-1.65 ²	-1.65 ¹⁷	-1.78 ⁵
697	5690.425	-0.006 \pm 0.002	4.930	-1.74 \pm 0.04	-1.78 \pm 0.04	✓	✓	-1.77 ¹⁶	-1.87 ¹⁷	-1.87 ²	-1.76 ⁴	-1.95 ⁵
704	5701.104	-0.007 \pm 0.003	4.930	-1.94 \pm 0.03	-1.96 \pm 0.03	✓	✓	-1.95 ¹⁶	-2.05 ¹⁷	-2.05 ²	-2.05 ¹⁷	-1.82 ⁵
711	5708.400	-0.009 \pm 0.002	4.954	-1.29 \pm 0.05	-1.37 \pm 0.04	✓	X	-1.37 ¹⁶	-1.47 ¹⁷	-1.47 ²	-1.47 ⁴	-1.25 ⁵
735	5747.667	-0.003 \pm 0.003	5.614	-1.30 \pm 0.05	-1.40 \pm 0.05	✓	X	-1.54 ¹⁴	-	-1.48 ²	-1.54 ¹⁴	-

Table F.1. $\langle Q_A \rangle$ Quality-assessable (A^1) Analysis-independent line $^{(a)}$ Paper 1 input list $^{(b)}$ NIST $^{(c)}$ VALD3 $^{(d)}$ SpectroWeb $^{(e)}$ CHIANTI $^{(f)}$ TIPbase $^{(g)}$ TOPbase

#	Wavelength (Å) Input	E_{low} (eV) $\Delta\lambda_{grid}$	$\log(gf)$ cog	$\log(gf)$ this work grid	Flags QA? AI?	a)	b)	c)	d)	e)	f)	g)	h)	Recommended literature	
741	5753.623	0.011 ± 0.003	5.616	-1.15 ± 0.04	-1.22 ± 0.04	✓	X	-1.75 ± 14	-	-1.33 ± 2	-1.75 ± 14	-	-	-	
751	5772.146	-0.008 ± 0.004	5.082	-1.57 ± 0.05	-1.59 ± 0.04	✓	✓	-1.65 ± 16	-1.75 ± 17	-1.75 ± 2	-1.75 ± 17	-2.22 ± 4	-	-1.54 ± 5	
764	5793.073	-0.008 ± 0.003	4.930	-1.85 ± 0.05	-1.93 ± 0.05	✓	X	-1.96 ± 16	-2.02 ± 18	-2.06 ± 2	-2.06 ± 17	-2.06 ± 17	-	-2.01 ± 5	
768	5797.856	-0.002 ± 0.005	4.954	-1.80 ± 0.03	-1.88 ± 0.04	X	X	-1.95 ± 16	-2.05 ± 17	-2.05 ± 2	-2.05 ± 17	-	-	-1.74 ± 5	
777	5810.768	0.024 ± 0.007	5.863	-1.91 ± 0.08	-1.93 ± 0.06	✓	✓	-1.42 ± 14	-	-	-1.42 ± 14	-	-	-	
799	5859.201	0.031 ± 0.009	4.954	-2.89 ± 0.11	-3.30 ± 0.08	X	X	-2.41 ± 14	-2.50 ± 18	-3.10 ± 2	-2.41 ± 14	-	-	-2.49 ± 5	
829	5948.541	-0.007 ± 0.003	5.082	-1.09 ± 0.05	-1.10 ± 0.04	✓	✓	-1.13 ± 16	-1.23 ± 17	-1.23 ± 2	-1.23 ± 17	-1.01 ± 4	-	-1.00 ± 5	
830	5950.092	-0.016 ± 0.035	5.863	-2.26 ± 0.08	-2.23 ± 0.09	✓	✓	-2.03 ± 14	-	-3.82 ± 2	-2.03 ± 14	-	-	-	
853	6022.229	-0.004 ± 0.018	5.863	-2.12 ± 0.10	-2.35 ± 0.10	X	X	-1.97 ± 14	-	-4.03 ± 2	-1.97 ± 14	-	-	X	
864	6076.925	-0.042 ± 0.006	5.964	-1.47 ± 0.06	-1.57 ± 0.06	✓	X	-2.01 ± 14	-	-	-2.01 ± 14	-	-	-2.54 ± 5	
872	6091.919	-0.007 ± 0.006	5.871	-1.18 ± 0.06	-1.23 ± 0.04	✓	X	-1.47 ± 14	-	-1.40 ± 2	-1.46 ± 14	-	-	-	
883	6112.928	-0.007 ± 0.004	5.616	-1.99 ± 0.05	-2.13 ± 0.05	X	X	-1.96 ± 14	-	-1.75 ± 2	-1.96 ± 14	-	-	X	
885	6125.021	-0.006 ± 0.002	5.614	-1.44 ± 0.04	-1.49 ± 0.05	✓	X	-1.46 ± 14	-	-1.53 ± 2	-1.47 ± 14	-	-	2, 14	
889	6131.573	-0.008 ± 0.003	5.616	-1.57 ± 0.03	-1.65 ± 0.04	X	X	-1.56 ± 14	-	-1.70 ± 2	-1.56 ± 14	-	-	X	
890	6131.852	-0.001 ± 0.004	5.616	-1.56 ± 0.04	-1.63 ± 0.04	✓	X	-1.62 ± 14	-	-1.74 ± 2	-1.62 ± 14	-	-	14	
891	6133.212	-0.011 ± 0.017	5.863	-2.22 ± 0.09	-2.32 ± 0.07	✓	X	-2.11 ± 14	-	-4.55 ± 2	-2.11 ± 14	-	-	-	
895	6142.483	0.001 ± 0.002	5.619	-1.39 ± 0.04	-1.45 ± 0.05	X	X	-1.29 ± 14	-	-1.52 ± 2	-1.30 ± 14	-	-	-	
896	6145.016	-0.004 ± 0.002	5.616	-1.33 ± 0.05	-1.35 ± 0.04	✓	✓	-1.31 ± 14	-	-1.42 ± 2	-1.31 ± 14	-	-	14	
900	6152.292	0.007 ± 0.007	5.964	-2.12 ± 0.06	-2.19 ± 0.04	✓	X	-1.36 ± 14	-	-2.12 ± 2	-1.36 ± 14	-	-	-1.48 ± 5	
902	6155.134	0.005 ± 0.004	5.619	-0.68 ± 0.08	-0.73 ± 0.06	X	X	-0.75 ± 14	-	-0.80 ± 2	-0.76 ± 14	-	-	14	
923	6194.416	-0.013 ± 0.006	5.871	-1.53 ± 0.05	-1.61 ± 0.06	✓	✓	X	-2.08 ± 14	-	-1.90 ± 2	-2.08 ± 14	-	-	-
924	6194.884	-0.029 ± 0.006	5.871	-2.27 ± 0.25	-2.35 ± 0.27	✓	✓	X	-2.19 ± 14	-	-2.40 ± 2	-2.19 ± 14	-	-	2, 14
925	6195.433	0.016 ± 0.003	5.871	-1.52 ± 0.06	-1.59 ± 0.06	✓	X	-1.49 ± 14	-	-1.80 ± 2	-1.57 ± 14	-	-	14	
930	6208.541	0.018 ± 0.006	5.984	-1.88 ± 0.08	-1.96 ± 0.06	X	X	-1.47 ± 14	-	-2.68 ± 2	-1.47 ± 14	-	-	-	
934	6220.211	0.004 ± 0.009	5.863	-1.69 ± 0.04	-1.75 ± 0.04	✓	X	-2.05 ± 14	-	-1.83 ± 2	-2.04 ± 14	-	-	-1.41 ± 5	
943	6237.319	0.001 ± 0.003	5.614	-0.97 ± 0.07	-1.03 ± 0.06	✓	X	-0.98 ± 14	-	-2.33 ± 2	-0.97 ± 14	-	-	14	
947	6243.815	-0.003 ± 0.003	5.616	-1.18 ± 0.05	-1.19 ± 0.03	✓	✓	-1.24 ± 14	-	-1.77 ± 2	-1.24 ± 14	-	-	-	
948	6244.466	0.001 ± 0.002	5.616	-1.20 ± 0.05	-1.23 ± 0.04	✓	✓	-1.09 ± 14	-	-1.69 ± 2	-1.09 ± 14	-	-	-	
963	6279.343	-0.029 ± 0.017	5.863	-1.52 ± 0.05	-1.21 ± 0.26	X	X	-2.43 ± 14	-	-2.01 ± 2	-2.43 ± 14	-	-	-	
970	6299.599	-0.030 ± 0.019	5.984	-1.04 ± 0.03	-1.10 ± 0.10	X	X	-1.12 ± 19	-	-1.50 ± 2	-1.66 ± 14	-	-	-1.12 ± 5	
973	6308.825	-0.014 ± 0.007	5.863	-2.02 ± 0.07	-2.06 ± 0.03	✓	✓	-1.79 ± 14	-	-2.95 ± 2	-1.79 ± 14	-	-	-	
986	6331.956	-0.005 ± 0.004	5.082	-2.36 ± 0.07	-2.50 ± 0.05	X	X	-1.82 ± 14	-3.74 ± 13	-2.80 ± 2	-1.82 ± 14	-	-	-2.71 ± 5	
1001	6394.235	-0.012 ± 0.008	5.871	-1.83 ± 0.14	-2.02 ± 0.06	✓	X	-1.84 ± 14	-	-1.84 ± 14	-	-	-	-	
1004	6408.671	-0.009 ± 0.005	5.984	-1.66 ± 0.06	-1.78 ± 0.04	X	X	-1.55 ± 14	-	-3.09 ± 2	-1.55 ± 14	-	-	-	
1006	6414.980	-0.001 ± 0.004	5.871	-0.97 ± 0.05	-1.01 ± 0.04	✓	✓	-1.03 ± 14	-	-1.05 ± 2	-1.04 ± 14	-	-	2, 14	
1013	6452.296	-0.004 ± 0.016	5.619	-2.22 ± 0.04	-2.55 ± 0.08	X	X	-1.43 ± 14	-	-2.48 ± 2	-1.43 ± 14	-	-	X	
1029	6527.202	-0.003 ± 0.005	5.871	-1.05 ± 0.03	-1.14 ± 0.03	X	X	-1.08 ± 14	-	-1.16 ± 2	-1.07 ± 14	-	-	X	
1045	6635.687	-0.001 ± 0.004	5.863	-1.73 ± 0.05	-1.78 ± 0.04	X	X	-1.65 ± 14	-	-1.93 ± 2	-1.65 ± 14	-	-	-	

Table F.1. ^(*a*) Quality-assessable (*AI*) Analysis-independent line ^(*a*) Paper 1 input list ^(*b*) NIST ^(*c*) Paper 1 input list ^(*d*) VALD3 ^(*e*) SpectroWeb ^(*f*) CHIANTI ^(*g*) TIPbase ^(*h*) TOPbase

#	Wavelength (Å) Input	E_{low} (eV) $\Delta\lambda_{grid}$	$\log(gf)$ cog grid	Flags this work	Flags QA? AI?	a)	b)	c)	d)	e)	f)	g)	h)	Recommended literature
1069	6721.848	-0.009 ±0.004	5.863	-1.02 ±0.04	-1.07 ±0.04	✓	X	-1.06 ¹⁹	-0.94 ¹³	-	-1.53 ¹⁴	-	-	19
1078	6741.628	0.000 ±0.009	5.984	-1.47 ±0.09	-1.54 ±0.04	✓	X	-1.65 ¹⁶	-	-3.25 ²	-1.75 ¹⁷	-	-	-
1091	6795.788	0.003 ±0.008	5.964	-1.75 ±0.06	-1.86 ±0.10	✓	X	-1.82 ¹⁴	-	-1.98 ²	-1.82 ¹⁴	-	-	14
990	6347.109	-0.017 ±0.004	8.121	0.37 ±0.04	0.31 ±0.04	✓	X	0.17 ¹⁶	-	0.35 ²	-	0.53 ⁴	0.18 ²⁰	-
997	6371.371	-0.016 ±0.003	8.121	0.07 ±0.04	-0.01 ±0.05	✓	X	-0.04 ¹⁶	-	-0.20 ²	-	-0.08 ⁴	-0.12 ²⁰	-
1085	6757.150	0.012 ±0.016	7.870	-0.15 ±0.05	-0.23 ±0.06	✓	X	-0.24 ²¹	-	-0.31 ²	-0.24 ²²	-	-	21,22
15	4283.011	-0.004 ±0.005	1.886	-0.38 ±0.12	-0.50 ±0.17	✓	X	-0.14 ¹⁴	-0.22 ¹³	-0.04 ²	-0.14 ¹⁴	-0.00 ⁴	-	-0.12 ⁵
20	4318.652	0.002 ±0.004	1.899	-0.42 ±0.09	-0.47 ±0.14	✓	X	-0.14 ¹⁴	-0.21 ¹³	-0.21 ²	-0.14 ¹⁴	-	-	-0.12 ⁵
40	4425.437	-0.005 ±0.001	1.879	-0.42 ±0.09	-0.50 ±0.07	✓	X	-0.36 ²³	-0.36 ²⁴	-0.36 ²	-0.36 ²³	-	-	-0.57 ⁵
87	4512.268	-0.014 ±0.005	2.526	-1.85 ±0.05	-1.91 ±0.08	✓	X	-1.90 ²⁵	-	-1.89 ²	-1.90 ²⁵	-	-	-0.14 ⁵
99	4526.928	-0.008 ±0.003	2.709	-0.60 ±0.06	-0.68 ±0.08	✓	X	-0.55 ²⁵	-	-0.51 ²	-0.55 ²⁵	-0.64 ⁴	-	4
131	4578.551	-0.001 ±0.002	2.521	-0.81 ±0.09	-0.77 ±0.09	✓	✓	-0.70 ²⁵	-0.56 ¹³	-0.56 ²	-0.70 ²⁵	-0.34 ⁴	-	-0.34 ⁵
206	4685.268	-0.010 ±0.001	2.933	-0.81 ±0.06	-0.87 ±0.04	✓	✓	-0.88 ²⁶	-0.88 ¹³	-0.88 ²	-0.88 ²⁶	-0.66 ⁴	-	-0.47 ⁵
497	5260.387	-0.006 ±0.002	2.521	-1.68 ±0.03	-1.70 ±0.05	✓	✓	-1.72 ²⁵	-1.90 ²⁷	-1.72 ²	-1.72 ²⁵	-	-	-2.02 ⁵
500	5265.556	-0.011 ±0.002	2.523	-0.65 ±1.28	-0.83 ±0.01	✓	X	-0.11 ²⁵	-0.26 ²⁷	-0.11 ²	-0.11 ²⁵	-0.48 ⁴	-	-0.37 ⁵
550	5349.465	-0.005 ±0.001	2.709	-0.50 ±0.11	-0.44 ±0.09	✓	X	-0.31 ²⁵	-	-0.28 ²	-0.31 ²⁵	-	-	-0.73 ⁵
631	5581.965	0.004 ±0.002	2.523	-0.48 ±0.05	-0.53 ±0.04	✓	X	-0.56 ²⁵	-0.71 ²⁷	-0.56 ²	-0.56 ²⁵	-0.56 ⁴	-	-0.57 ⁵
636	5590.114	-0.004 ±0.002	2.521	-0.55 ±0.05	-0.51 ±0.04	✓	✓	-0.57 ²⁵	-0.71 ²⁷	-0.57 ²	-0.57 ²⁵	-0.49 ⁴	-	-0.58 ⁵
804	5867.562	-0.009 ±0.002	2.933	-1.52 ±0.04	-1.51 ±0.03	✓	✓	-1.57 ²⁶	-	-1.60 ²	-1.57 ²⁶	-	-	-2.40 ⁵
906	6161.297	-0.009 ±0.002	2.523	-1.16 ±0.04	-1.23 ±0.04	✓	X	-1.27 ²⁵	-1.03 ²⁷	-1.27 ²⁵	-1.27 ²⁵	-1.03 ⁴	-	-2.5
907	6163.755	-0.010 ±0.001	2.521	-1.14 ±0.05	-1.23 ±0.04	✓	X	-1.29 ²⁵	-1.02 ²⁷	-1.30 ²	-1.29 ²⁵	-1.02 ⁴	-	-
909	6166.439	-0.009 ±0.002	2.521	-1.11 ±0.05	-1.09 ±0.04	✓	✓	-1.14 ²⁵	-0.90 ²⁷	-1.16 ²	-1.14 ²⁵	-1.38 ⁴	-	-
910	6169.042	-0.009 ±0.002	2.523	-0.75 ±0.06	-0.72 ±0.04	✓	✓	-0.80 ²⁵	-0.54 ²⁷	-0.80 ²	-0.80 ²⁵	-0.76 ⁴	-	4
1012	6449.808	0.000 ±0.001	2.521	-0.42 ±0.06	-0.38 ±0.05	✓	✓	-0.50 ²⁵	-0.55 ¹³	-0.50 ²	-0.50 ²⁵	-0.33 ⁴	-	4
1014	6455.598	-0.001 ±0.002	2.523	-1.27 ±0.04	-1.28 ±0.04	✓	✓	-1.29 ²⁵	-1.36 ¹³	-1.35 ²	-1.34 ²⁶	-	-	25
1018	6471.662	-0.005 ±0.001	2.526	-0.61 ±0.05	-0.57 ±0.04	✓	✓	-0.69 ²⁵	-0.59 ²⁷	-0.68 ²	-0.69 ²⁵	-0.59 ⁴	-	4,27
1024	6499.650	-0.006 ±0.002	2.523	-0.72 ±0.05	-0.70 ±0.04	✓	✓	-0.82 ²⁵	-0.59 ²⁷	-0.65 ²	-0.82 ²⁵	-0.59 ⁴	-	-
1016	6456.875	0.002 ±0.010	8.438	0.65 ±0.06	0.52 ±0.05	✓	X	0.41 ²⁸	-	-0.28 ²	-	-	-	X
238	4743.830	-0.008 ±0.006	1.448	0.34 ±0.06	0.28 ±0.07	✓	X	0.42 ²⁹	0.42 ²⁹	0.24 ²	0.42 ²⁹	-	-	2
9	4246.822	0.009 ±0.002	0.315	0.08 ±0.08	0.05 ±0.09	✓	✓	0.24 ²⁹	0.24 ²⁹	-	0.24 ²⁹	0.31 ⁴	-	-
18	4314.083	-0.005 ±0.001	0.618	0.08 ±0.15	-0.12 ±0.08	✓	X	-0.10 ²⁹	-0.10 ²⁹	-0.10 ²	-0.10 ²⁹	-0.21 ⁴	-	-

Table F.1. $\langle Q_A \rangle$ Quality-assessable (A^I) Analysis-independent line $a)$ Paper 1 input list $b)$ NIST $c)$ SpectroWeb $d)$ VALD3 $e)$ Spectr-W 3 $f)$ CHIANTI $g)$ TIPbase $h)$ TOPbase

#	Wavelength (Å) Input	E_{low} (eV) $\Delta\lambda_{grid}$	$\log(gf)$ cog grid	$\log(gf)$ this work grid	Flags QA? AI?	Flags a) b)	Flags c) d)	Flags e) f)	Flags g) h)	Recommended literature
21	4320.732	0.006 ±0.002	0.605	-0.21 ±0.11	-0.28 ±0.08	✓ X	-0.25 29	-0.10 2	-0.25 29	- - - - -
30	4400.389	0.000 ±0.001	0.605	-0.45 ±0.09	-0.52 ±0.09	✓ X	-0.54 29	-0.48 2	-0.54 29	- - - - -
37	4420.669	-0.006 ±0.003	0.618	-2.19 ±0.06	-2.30 ±0.08	✓ X	-2.27 29	-2.15 2	-2.27 29	- - - - -
198	4670.407	-0.012 ±0.003	1.357	-0.46 ±0.09	-0.71 ±0.08	✓ X	-0.58 29	-0.52 2	-0.58 29	-0.24 4
397	5031.021	-0.007 ±0.003	1.357	-0.35 ±0.05	-0.44 ±0.07	✓ X	-0.40 29	-0.40 2	-0.40 29	-0.48 4
481	5239.813	0.004 ±0.002	1.455	-0.65 ±0.08	-0.75 ±0.06	✓ X	-0.76 29	-0.77 2	-0.77 29	-0.29 4
552	5357.199	-0.001 ±0.012	1.507	-2.03 ±0.11	-2.15 ±0.09	✓ X	-2.11 29	-2.14 2	-2.11 29	- - - - -
614	5526.790	0.019 ±0.002	1.768	0.04 ±0.08	0.05 ±0.06	✓ ✓	0.02 29	0.02 29	0.02 29	0.02 4
659	5641.001	-0.026 ±0.002	1.500	-0.87 ±0.09	-1.01 ±0.06	✓ X	-1.13 29	-0.99 2	-1.13 29	- - - - -
677	5657.896	-0.030 ±0.001	1.507	-0.40 ±0.09	-0.52 ±0.06	✓ X	-0.60 29	-0.60 29	-0.60 29	-0.51 4
685	5667.149	-0.017 ±0.003	1.500	-1.07 ±0.07	-1.16 ±0.06	✓ X	-1.31 29	-1.19 2	-1.31 29	- - - - -
686	5669.042	-0.012 ±0.004	1.500	-1.04 ±0.07	-1.13 ±0.05	✓ X	-1.20 29	-1.20 29	-1.20 29	- - - - -
692	5684.202	-0.015 ±0.001	1.507	-0.98 ±0.06	-1.02 ±0.06	✓ ✓	-1.07 29	-1.00 2	-1.07 29	- - - - -
949	6245.637	-0.025 ±0.001	1.507	-1.07 ±0.06	-1.13 ±0.07	✓ X	-1.02 14	- -	-1.03 2	-1.02 14
964	6279.753	-0.011 ±0.024	1.500	-1.15 ±0.02	-0.98 ±0.17	✓ X	-1.25 14	- -	-1.26 2	-1.25 14
971	6300.698	-0.021 ±0.004	1.507	-1.93 ±0.07	-2.06 ±0.05	✓ X	-1.90 14	- -	-1.89 2	-1.90 14
980	6320.851	-0.014 ±0.002	1.500	-1.85 ±0.06	-1.90 ±0.05	✓ X	-1.82 14	- -	-1.82 2	-1.82 14
14	4281.367	-0.001 ±0.002	0.813	-1.21 ±0.10	-1.23 ±0.07	✓ ✓	-1.26 30	-1.36 31	-1.26 30	- - - - -
16	4287.403	-0.001 ±0.002	0.836	-0.24 ±0.09	-0.37 ±0.08	✓ X	-0.37 30	-0.44 31	-0.44 2	-0.37 30
50	4449.142	0.001 ±0.002	1.887	0.56 ±0.05	0.45 ±0.06	✓ X	0.47 30	-	0.43 2	0.47 30
53	4450.894	-0.003 ±0.003	1.879	0.54 ±0.11	0.32 ±0.07	✓ X	0.32 30	0.41 32	0.24 2	0.32 30
57	4453.699	-0.001 ±0.002	1.873	0.19 ±0.07	0.10 ±0.07	✓ X	0.10 30	-0.01 32	0.11 2	0.10 30
88	4512.734	-0.002 ±0.003	0.836	-0.37 ±0.06	-0.37 ±0.08	✓ ✓	-0.40 30	-	-0.41 2	-0.40 30
92	4518.022	-0.001 ±0.002	0.826	-0.25 ±0.07	-0.29 ±0.08	✓ ✓	-0.25 30	-0.32 31	-0.25 2	-0.25 30
96	4522.797	0.000 ±0.003	0.818	0.06 ±0.17	-0.31 ±0.07	✓ X	-0.27 30	-0.39 32	-0.27 2	-0.27 30
101	4534.776	-0.001 ±0.002	0.836	0.33 ±0.03	0.37 ±0.04	✓ ✓	0.35 30	0.28 31	0.38 2	0.35 30
110	4548.764	-0.001 ±0.002	0.826	-0.25 ±0.07	-0.25 ±0.09	✓ ✓	-0.28 30	-0.35 31	-0.27 2	-0.28 30
113	4555.483	0.000 ±0.001	0.848	-0.40 ±0.06	-0.43 ±0.07	✓ ✓	-0.40 30	-0.49 31	-0.42 2	-0.40 30
119	4562.628	-0.007 ±0.004	0.021	-2.51 ±0.05	-2.48 ±0.07	✓ ✓	-2.66 33	-2.59 34	-2.54 2	-2.66 33
179	4639.363	-0.006 ±0.002	1.739	0.10 ±0.07	-0.05 ±0.06	✓ X	-0.05 30	-	-0.02 2	-0.05 30
180	4639.939	-0.002 ±0.003	1.734	-0.12 ±0.06	-0.17 ±0.07	✓ X	-0.16 30	-0.19 35	-0.19 2	-0.16 30
182	4645.188	-0.006 ±0.002	1.734	-0.40 ±0.07	-0.49 ±0.07	✓ X	-0.51 30	-0.56 35	-0.48 2	-0.51 30
186	4656.468	-0.001 ±0.002	0.000	-1.09 ±0.06	-1.20 ±0.09	✓ X	-1.29 36	-	-1.34 2	-1.29 36
204	4681.909	-0.001 ±0.002	0.048	-0.87 ±0.06	-0.95 ±0.08	✓ X	-1.03 36	-	-1.13 2	-1.03 36
229	4731.164	-0.034 ±0.021	2.175	-0.30 ±0.04	-0.33 ±0.08	✓ X	-0.43 30	-	-0.60 2	-0.43 30
237	4742.789	-0.001 ±0.003	2.236	0.23 ±0.04	0.20 ±0.06	✓ ✓	0.21 30	0.21 37	0.21 2	0.21 30
248	4758.118	-0.001 ±0.002	2.249	0.46 ±0.04	0.46 ±0.05	✓ ✓	0.51 30	0.42 35	0.42 2	0.51 30
249	4759.270	-0.005 ±0.001	2.256	0.53 ±0.05	0.54 ±0.05	✓ ✓	0.59 30	0.51 35	0.51 2	0.59 30

Table F.1. $\langle g \rangle A$) Quality-assessable (A) Analysis-independent line $a)$ Paper 1 input list $b)$ NIST $c)$ SpectroWeb $d)$ VALD3 $e)$ CHIANTI $f)$ TIPbase $g)$ TOPbase

#	Wavelength (Å) Input	E_{low} (eV) $\Delta\lambda_{grid}$	$\log(gf)$ cog	$\log(gf)$ this work grid	Flags QA? AI?	Flags a) b)	Flags c) d)	Flags e) f)	Flags g) h)	Recommended literature
286	4820.409	-0.001 ±0.002	1.503	-0.26 ±0.08	-0.36 ±0.07	✓ X	-0.38 30	-	-0.44 2	-0.38 30
294	4840.874	-0.007 ±0.003	0.900	-0.34 ±0.08	-0.58 ±0.10	✗ X	-0.43 30	-	-0.51 2	-0.43 30
299	4885.079	-0.002 ±0.003	1.887	0.64 ±0.09	0.45 ±0.10	✓ X	0.41 30	0.36 35	0.41 30	-
308	4899.909	-0.004 ±0.002	1.879	0.43 ±0.11	0.22 ±0.06	✗ X	0.31 30	-	0.35 2	0.31 30
322	4913.613	0.000 ±0.001	1.873	0.25 ±0.07	0.19 ±0.06	✓ X	0.22 30	0.16 35	0.16 2	0.22 30
324	4915.229	-0.003 ±0.003	1.887	-0.85 ±0.07	-0.85 ±0.09	✓ X	-0.91 30	-1.02 35	-0.94 2	-0.91 30
330	4926.148	-0.003 ±0.003	0.818	-2.02 ±0.08	-2.02 ±0.12	✓ X	-2.09 30	-2.17 38	-2.27 2	-2.09 30
346	4964.720	-0.006 ±0.003	1.969	-0.74 ±0.05	-0.75 ±0.07	✓ X	-0.82 39	-0.82 40	-0.99 2	-0.82 40
355	4978.188	-0.023 ±0.006	1.969	0.05 ±0.08	-0.12 ±0.06	✗ X	-0.30 14	-	-0.45 2	-0.30 14
371	4997.097	-0.004 ±0.002	0.000	-1.98 ±0.08	-2.00 ±0.09	✓ X	-2.07 30	-	-2.12 2	-2.07 30
379	5009.645	-0.003 ±0.003	0.021	-2.06 ±0.11	-2.12 ±0.09	✓ X	-2.20 30	-	-2.26 2	-2.20 30
384	5016.161	-0.002 ±0.003	0.848	-0.42 ±0.09	-0.46 ±0.10	✓ X	-0.48 30	-	-0.51 2	-0.48 30
386	5020.026	-0.003 ±0.003	0.836	-0.07 ±0.09	-0.31 ±0.07	✗ X	-0.33 30	-0.41 31	-0.35 2	-0.33 30
390	5024.844	0.001 ±0.002	0.818	-0.37 ±0.07	-0.54 ±0.10	✓ X	-0.53 30	-0.60 31	-0.60 2	-0.53 30
393	5025.570	-0.014 ±0.002	2.041	0.46 ±0.07	0.38 ±0.08	✓ X	0.25 40	0.25 40	0.07 2	0.25 40
400	5036.464	-0.007 ±0.004	1.443	0.33 ±0.11	0.27 ±0.14	✗ X	0.14 30	0.13 35	0.13 2	0.14 30
401	5038.398	-0.012 ±0.003	1.430	0.20 ±0.06	-0.07 ±0.07	✗ X	0.02 30	0.01 35	0.01 2	0.02 30
402	5039.957	-0.001 ±0.002	0.021	-1.00 ±0.06	-1.05 ±0.07	✗ X	-1.08 30	-	-1.13 2	-1.08 30
404	5043.584	-0.008 ±0.004	0.836	-1.47 ±0.05	-1.55 ±0.06	✗ X	-1.59 30	-	-1.73 2	-1.59 30
413	5064.653	-0.005 ±0.001	0.048	-0.71 ±0.09	-0.93 ±0.09	✗ X	-0.94 30	-	-0.99 2	-0.94 30
436	5113.440	-0.001 ±0.002	1.443	-0.66 ±0.08	-0.72 ±0.07	✗ X	-0.70 30	-0.78 35	-0.78 2	-0.70 30
449	5147.478	-0.003 ±0.003	0.000	-1.81 ±0.11	-1.91 ±0.09	✗ X	-1.94 30	-	-2.01 2	-1.94 30
452	5152.184	-0.001 ±0.002	0.021	-1.85 ±0.11	-1.92 ±0.09	✗ X	-1.95 30	-	-1.95 2	-1.95 30
459	5192.969	-0.001 ±0.002	0.021	-0.83 ±0.11	-0.94 ±0.09	✗ X	-0.95 30	-	-0.85 2	-0.95 30
464	5210.384	-0.001 ±0.002	0.048	-0.64 ±0.18	-0.84 ±0.08	✓ X	-0.82 30	-	-0.73 2	-0.82 30
467	5219.702	-0.004 ±0.002	0.021	-2.09 ±0.08	-2.12 ±0.08	✓ X	-2.22 30	-	-2.29 2	-2.22 30
473	5223.620	-0.015 ±0.008	2.092	-0.34 ±0.05	-0.40 ±0.05	✓ X	-0.49 40	-	-0.49 2	-0.49 40
489	5247.290	-0.006 ±0.002	2.103	-0.60 ±0.08	-0.66 ±0.07	✓ X	-0.64 40	-0.64 40	-0.86 2	-0.64 40
496	5259.972	-0.001 ±0.006	2.738	-0.17 ±0.07	-0.21 ±0.09	✓ X	-0.18 33	-0.18 37	-0.32 2	-0.18 33
518	5295.776	0.003 ±0.006	1.067	-1.48 ±0.05	-1.51 ±0.07	✓ X	-1.59 30	-1.63 38	-1.63 2	-1.59 30
551	5351.068	-0.014 ±0.007	2.778	0.11 ±0.04	0.04 ±0.03	✓ X	-0.07 14	0.01 37	-0.21 2	0.01 33
580	5460.499	-0.025 ±0.020	0.048	-2.55 ±0.05	-2.55 ±0.06	✓ X	-2.75 41	-2.74 34	-2.80 2	-2.80 33
586	5471.192	0.001 ±0.002	1.443	-1.36 ±0.06	-1.36 ±0.07	✓ X	-1.42 30	-1.39 37	-1.40 2	-1.42 30
590	5474.223	0.000 ±0.003	1.460	-1.15 ±0.05	-1.18 ±0.07	✓ X	-1.23 30	-1.23 37	-1.23 32	-1.23 30
595	5490.148	-0.001 ±0.002	1.460	-0.83 ±0.05	-0.81 ±0.06	✓ X	-0.84 30	-0.93 35	-0.93 2	-0.84 30
604	5503.895	-0.006 ±0.002	2.578	0.05 ±0.04	-0.03 ±0.06	✓ X	-0.05 30	0.03 37	0.02 2	-0.05 30
606	5514.343	0.000 ±0.003	1.430	-0.41 ±0.09	-0.53 ±0.06	✓ X	-0.66 30	-	-0.55 2	-0.66 30
607	5514.533	-0.002 ±0.003	1.443	-0.33 ±0.10	-0.41 ±0.06	✓ X	-0.50 30	-	-0.41 2	-0.50 30
668	5648.565	-0.004 ±0.002	2.495	-0.23 ±0.06	-0.20 ±0.07	✓ X	-0.16 14	-0.25 37	-0.27 2	-0.26 33

Table F.1. $\langle Q_A \rangle$ Quality-assessable (A^I) Analysis-independent line $a)$ Paper 1 input list $b)$ NIST $c)$ SpectroWeb $d)$ VALD3 $e)$ CHIANTI $f)$ TIPbase $g)$ TOPbase

#	Wavelength (Å) Input	E_{low} (eV) $\Delta\lambda_{grid}$	$\log(gf)$ cog	$\log(gf)$ this work grid	Flags QA? AI?	a)	b)	c)	d)	e)	f)	g)	h)	Recommended literature
680	5662.150	-0.005 \pm 0.001	2.318	0.02 \pm 0.04	-0.04 \pm 0.06	✓	✗	0.01 40	-	-0.18 2	0.01 40	-	-	40
690	5679.916	-0.006 \pm 0.002	2.472	-0.56 \pm 0.06	-0.53 \pm 0.05	✓	✓	-0.57 33	-0.57 37	-0.62 2	-0.57 33	-	-	33, 37
696	5689.460	-0.001 \pm 0.003	2.297	-0.29 \pm 0.05	-0.31 \pm 0.05	✓	✓	-0.36 40	-0.36 40	-0.36 2	-0.36 40	-	-	2, 40
706	5702.660	-0.001 \pm 0.007	2.292	-0.56 \pm 0.06	-0.58 \pm 0.06	✓	✓	-0.59 40	-0.60 40	-0.78 2	-0.59 40	-	-	40
715	5713.880	0.018 \pm 0.025	2.289	-0.82 \pm 0.07	-0.82 \pm 0.07	✓	✓	-0.94 14	-	-1.07 2	-0.94 14	-	-	-
717	5716.450	-0.008 \pm 0.003	2.297	-0.63 \pm 0.05	-0.66 \pm 0.06	✓	✓	-0.72 40	-0.72 40	-0.91 2	-0.72 40	-	-	40
730	5739.469	-0.001 \pm 0.002	2.249	-0.60 \pm 0.06	-0.57 \pm 0.06	✓	✓	-0.61 30	-0.60 37	-0.75 2	-0.61 30	-	-	30, 37
748	5766.359	-0.034 \pm 0.004	3.294	0.51 \pm 0.03	0.43 \pm 0.05	✓	✗	0.29 14	-	0.25 2	0.29 14	-	-	-
771	5804.259	0.001 \pm 0.003	3.337	0.81 \pm 0.05	0.77 \pm 0.04	✓	✓	0.71 33	-	0.71 2	0.71 33	-	-	-
803	5866.451	-0.002 \pm 0.003	1.067	-0.68 \pm 0.10	-0.71 \pm 0.10	✓	✓	-0.79 30	-0.84 31	-0.84 2	-0.79 30	-0.63 4	-	4, 30
811	5880.270	0.000 \pm 0.004	1.053	-1.81 \pm 0.04	-1.83 \pm 0.05	✓	✓	-2.00 30	-	-2.00 2	-2.00 30	-	-	-
814	5899.294	0.004 \pm 0.010	1.053	-0.92 \pm 0.08	-0.98 \pm 0.09	✗	✗	-1.10 30	-1.15 31	-1.19 2	-1.10 30	-0.87 4	-	-
816	5903.315	0.009 \pm 0.021	1.067	-1.90 \pm 0.07	-1.89 \pm 0.06	✓	✓	-2.09 41	-	-2.19 2	-2.15 33	-	-	-
819	5922.110	-0.001 \pm 0.005	1.046	-1.30 \pm 0.05	-1.30 \pm 0.07	✓	✓	-1.38 30	-1.47 38	-1.50 2	-1.38 30	-	-	-
825	5937.809	-0.004 \pm 0.006	1.067	-1.75 \pm 0.07	-1.76 \pm 0.07	✓	✓	-1.94 30	-1.89 42	-1.89 2	-1.94 30	-	-	-
827	5941.752	-0.003 \pm 0.012	1.053	-1.36 \pm 0.11	-1.34 \pm 0.12	✓	✓	-1.51 30	-1.52 43	-1.65 2	-1.51 30	-	-	-
832	5953.160	-0.009 \pm 0.004	1.887	-0.15 \pm 0.05	-0.20 \pm 0.05	✗	✗	-0.27 39	-0.33 35	-0.33 2	-0.33 33	-	-	-
837	5965.828	-0.007 \pm 0.004	1.879	-0.29 \pm 0.04	-0.36 \pm 0.08	✗	✗	-0.35 39	-0.41 35	-0.47 2	-0.41 33	-	-	33, 35, 39
840	5978.541	-0.001 \pm 0.002	1.873	-0.40 \pm 0.05	-0.41 \pm 0.06	✗	✗	-0.44 39	-0.50 35	-0.56 2	-0.50 33	-	-	39
863	6064.626	-0.002 \pm 0.003	1.046	-1.72 \pm 0.05	-1.75 \pm 0.06	✓	✓	-1.89 41	-1.94 38	-1.94 2	-1.94 33	-	-	-
871	6091.171	-0.001 \pm 0.003	2.267	-0.28 \pm 0.04	-0.29 \pm 0.06	✓	✓	-0.32 30	-0.42 35	-0.39 2	-0.32 30	-	-	30
873	6092.792	-0.009 \pm 0.014	1.887	-1.21 \pm 0.04	-1.19 \pm 0.07	✓	✓	-1.38 30	-1.38 35	-1.59 2	-1.38 30	-	-	-
879	6098.658	-0.004 \pm 0.002	3.062	0.02 \pm 0.10	0.02 \pm 0.05	✓	✓	-0.01 14	-0.01 37	-0.20 2	-0.01 33	-	-	14, 33, 37
886	6126.216	-0.001 \pm 0.002	1.067	-1.26 \pm 0.05	-1.25 \pm 0.05	✓	✓	-1.37 41	-1.42 38	-1.27 2	-1.43 33	-	-	2
935	6220.474	-0.007 \pm 0.009	2.677	-0.07 \pm 0.05	-0.10 \pm 0.04	✓	✓	-0.15 14	-0.14 37	-0.25 2	-0.14 33	-	-	33, 37
953	6258.102	-0.001 \pm 0.002	1.443	-0.30 \pm 0.05	-0.33 \pm 0.05	✓	✓	-0.39 30	-0.35 35	-0.34 2	-0.39 30	-0.21 4	-	2, 35
954	6258.707	-0.001 \pm 0.004	1.460	0.10 \pm 0.15	-0.24 \pm 0.06	✗	✗	-0.28 30	-0.24 44	-0.09 2	-0.28 30	-	-	X
956	6261.099	-0.002 \pm 0.003	1.430	-0.34 \pm 0.08	-0.39 \pm 0.08	✗	✗	-0.53 30	-0.48 35	-0.45 2	-0.53 30	-	-	2
975	6312.236	-0.002 \pm 0.003	1.460	-1.39 \pm 0.06	-1.36 \pm 0.06	✗	✗	-1.55 30	-1.55 35	-1.55 2	-1.55 30	-	-	-
1079	6745.544	-0.005 \pm 0.014	2.236	-1.03 \pm 0.06	-1.06 \pm 0.11	✓	✓	-1.23 30	-	-1.75 2	-1.23 30	-	-	-
Ti II														
19	4316.794	-0.003 \pm 0.003	2.048	-1.35 \pm 0.07	-1.47 \pm 0.06	✓	✗	-1.62 45	-1.58 46	-1.58 2	-1.62 45	-	-	-
22	4320.950	-0.005 \pm 0.001	1.165	-1.53 \pm 0.08	-1.72 \pm 0.08	✗	✗	-1.88 45	-1.80 46	-1.69 2	-1.88 45	-	-	X
29	4395.839	-0.001 \pm 0.002	1.243	-1.82 \pm 0.06	-1.87 \pm 0.07	✗	✗	-1.93 45	-1.93 46	-1.65 2	-1.93 45	-	-	45, 46
31	4409.518	-0.001 \pm 0.002	1.231	-2.40 \pm 0.04	-2.46 \pm 0.05	✗	✗	-2.53 45	-2.37 46	-2.55 2	-2.53 45	-	-	-
36	4417.714	-0.001 \pm 0.002	1.165	-1.03 \pm 0.07	-1.10 \pm 0.07	✗	✗	-1.19 46	-1.43 47	-1.19 2	-1.19 46	-	-	-
52	4450.482	-0.001 \pm 0.002	1.084	-1.44 \pm 0.09	-1.48 \pm 0.06	✓	✓	-1.52 45	-1.52 46	-1.52 2	-1.52 45	-	-	2, 45, 46
62	4468.493	-0.001 \pm 0.002	1.131	-0.70 \pm 0.07	-0.67 \pm 0.05	✓	✓	-0.63 45	-0.62 48	-0.27 2	-0.63 45	-	-	45, 48

Table F.1. (g) Quality-assessable (h) Analysis-independent line ^{a)} Paper 1 input list ^{b)} NIST ^{c)} SpectroWeb ^{d)} VALD3 ^{e)} CHIANTI ^{f)} TIPbase ^{g)} TOPbase

#	Wavelength (Å) Input	E_{low} (eV) $\Delta\lambda_{grid}$	$\log(gf)$ cog grid	$\log(gf)$ this work grid	Flags QA? AI?	a)	b)	c)	d)	e)	f)	g)	h)	Recommended literature
64	4470.853	-0.006 ±0.002	1.165	-1.92 ±0.06	-2.01 ±0.05	✓ X	-2.02 ±0.46	-2.28 ±7	-2.02 ±2	-2.02 ±46	-	-	-	2, 46
69	4488.324	-0.001 ±0.002	3.124	-0.28 ±0.04	-0.44 ±0.06	X X	-0.50 ±45	-0.51 ±46	-0.50 ±2	-0.50 ±45	-	-	-	X
76	4493.522	-0.001 ±0.002	1.080	-2.70 ±0.05	-2.76 ±0.05	✓ X	-2.78 ±45	-2.74 ±49	-2.77 ±2	-2.78 ±45	-	-	-	2, 45, 49
93	4518.332	-0.001 ±0.002	1.080	-2.21 ±0.13	-2.47 ±0.07	X X	-2.56 ±45	-	-2.56 ±2	-2.56 ±45	-	-	-	X
100	4533.960	0.000 ±0.001	1.237	-0.64 ±0.06	-0.62 ±0.08	✓ X	-0.53 ±46	-0.77 ±47	-0.61 ±2	-0.53 ±46	-	-	-	2
108	4545.133	-0.003 ±0.003	1.131	-2.22 ±0.07	-2.35 ±0.06	✓ X	-2.45 ±45	-	-2.29 ±2	-2.45 ±45	-	-	-	2
120	4563.757	-0.005 ±0.001	1.221	-0.61 ±0.04	-0.75 ±0.04	X X	-0.69 ±46	-0.96 ±47	-0.80 ±2	-0.69 ±46	-	-	-	X
123	4568.314	0.010 ±0.004	1.224	-2.62 ±0.08	-2.70 ±0.06	✓ X	-3.03 ±50	-	-2.75 ±2	-3.03 ±50	-	-	-	2
126	4571.971	0.000 ±0.001	1.572	-0.30 ±0.06	-0.30 ±0.06	✓ ✓	-0.31 ±45	-0.32 ±46	-0.21 ±2	-0.31 ±45	-	-	-	45, 46
136	4583.409	-0.004 ±0.002	1.165	-2.73 ±0.06	-2.73 ±0.06	✓ ✓	-2.84 ±45	-2.72 ±49	-2.68 ±2	-2.84 ±45	-	-	-	2, 49
142	4589.958	-0.015 ±0.001	1.237	-1.47 ±0.09	-1.57 ±0.06	✓ X	-1.62 ±50	-1.78 ±47	-1.67 ±2	-1.62 ±50	-	-	-	50
162	4609.265	0.010 ±0.013	1.180	-3.12 ±0.07	-3.21 ±0.07	✓ X	-3.32 ±45	-3.26 ±49	-3.37 ±2	-3.32 ±45	-	-	-	49
188	4657.201	-0.005 ±0.001	1.243	-2.20 ±0.05	-2.23 ±0.05	✓ ✓	-2.29 ±45	-2.15 ±49	-2.24 ±2	-2.29 ±45	-	-	-	2
219	4708.663	-0.004 ±0.002	1.237	-2.25 ±0.05	-2.27 ±0.05	✓ ✓	-2.35 ±45	-2.34 ±46	-2.21 ±2	-2.35 ±45	-	-	-	-
222	4719.511	-0.007 ±0.003	1.243	-3.10 ±0.05	-3.18 ±0.06	✓ X	-3.32 ±45	-	-3.32 ±45	-	-	-	-	-
251	4762.778	0.001 ±0.003	1.084	-2.71 ±0.06	-2.84 ±0.06	X X	-2.89 ±45	-2.74 ±46	-2.87 ±2	-2.89 ±45	-	-	-	X
253	4764.525	-0.002 ±0.003	1.237	-2.52 ±0.06	-2.60 ±0.06	✓ X	-2.69 ±45	-	-2.77 ±2	-2.69 ±45	-	-	-	-
259	4779.985	-0.009 ±0.002	2.048	-1.14 ±0.04	-1.23 ±0.07	✓ X	-1.25 ±14	-1.37 ±47	-1.37 ±2	-1.26 ±50	-	-	-	14, 50
271	4798.531	-0.001 ±0.002	1.080	-2.51 ±0.05	-2.57 ±0.05	✓ X	-2.66 ±45	-2.68 ±46	-2.62 ±2	-2.66 ±45	-	-	-	2
318	4911.194	-0.003 ±0.003	3.124	-0.39 ±0.06	-0.49 ±0.04	✓ X	-0.64 ±45	-0.61 ±46	-0.53 ±2	-0.64 ±45	-	-	-	2
440	5129.156	-0.001 ±0.002	1.892	-0.92 ±0.09	-1.20 ±0.06	X X	-1.34 ±45	-1.24 ±46	-1.25 ±2	-1.34 ±45	-	-	-	X
458	5185.902	0.003 ±0.005	1.893	-1.04 ±0.20	-1.40 ±0.06	X X	-1.41 ±45	-1.49 ±46	-1.35 ±2	-1.41 ±45	-	-	-	X
465	5211.530	-0.001 ±0.004	2.590	-1.36 ±0.05	-1.38 ±0.04	✓ X	-1.41 ±45	-1.17 ±46	-1.36 ±2	-1.41 ±45	-	-	-	2, 45
546	5336.786	-0.001 ±0.002	1.582	-1.54 ±0.06	-1.53 ±0.04	✓ ✓	-1.60 ±45	-	-1.50 ±2	-1.60 ±45	-	-	-	2
555	5381.022	-0.006 ±0.002	1.566	-1.78 ±0.05	-1.89 ±0.04	X X	-1.97 ±45	-	-1.85 ±2	-1.97 ±45	-	-	-	X
570	5418.768	-0.003 ±0.003	1.582	-2.01 ±0.05	-2.03 ±0.05	✓ X	-2.13 ±45	-	-2.00 ±2	-2.13 ±45	-	-	-	2
596	5490.693	-0.001 ±0.002	1.566	-2.61 ±0.05	-2.66 ±0.04	✓ X	-2.43 ±46	-	-2.65 ±2	-2.66 ±44	-	-	-	2, 14
598	5492.862	0.017 ±0.003	1.582	-2.91 ±0.08	-3.00 ±0.04	✓ X	-3.31 ±51	-	-2.96 ±2	-3.31 ±51	-	-	-	2
932	6214.600	0.047 ±0.006	2.048	-2.64 ±0.23	-2.87 ±0.14	✓ X	-2.03 ±51	-	-3.05 ±2	-2.03 ±51	-	-	-	-
								V ₁						
26	4379.230	-0.003 ±0.003	0.301	1.06 ±0.14	1.07 ±0.10	✓ ✓	0.58 ±33	0.58 ±52	0.60 ±2	0.58 ±53	-	-	-	-
43	4437.834	-0.005 ±0.001	0.287	-0.54 ±0.22	-0.67 ±0.22	✓ ✓	-0.66 ±33	-0.66 ±52	-0.74 ±2	-	-	-	-	2, 33, 52
55	4452.006	-0.006 ±0.002	1.868	0.77 ±0.12	0.58 ±0.12	✓ X	0.64 ±33	0.64 ±54	0.58 ±2	0.59 ±53	0.64 ±4	-	-	2, 4, 33, 53, 54
130	4577.174	0.001 ±0.002	0.000	-0.95 ±0.14	-1.11 ±0.15	✓ X	-1.05 ±33	-1.05 ±55	-1.14 ±2	-1.08 ±53	-	-	-	2, 33, 53, 55
146	4594.124	-0.011 ±0.002	0.069	-0.28 ±0.36	-0.28 ±0.40	✓ ✓	-0.67 ±33	-0.67 ±55	-0.75 ±2	-	-	-	-	33, 55
287	4827.458	0.015 ±0.031	0.040	-1.18 ±0.23	-1.39 ±0.19	✓ X	-1.48 ±33	-1.48 ±55	-1.68 ±2	-	-	-	-	33, 55
651	5626.017	-0.015 ±0.020	1.043	-1.01 ±0.06	-1.21 ±0.06	X X	-1.24 ±33	-1.24 ±55	-1.28 ±2	-1.26 ±53	-	-	-	X
721	5725.641	-0.008 ±0.009	2.365	-0.12 ±0.03	-0.16 ±0.03	✓ ✓	0.01 ±33	-	-0.35 ±2	-	0.04 ±4	-	-	-

Table F.1. $\langle Q \rangle^A$) Quality-assessable (A) Analysis-independent line $^a)$ Paper 1 input list $^b)$ NIST $^c)$ Paper 1 input list $^d)$ VALD3 $^e)$ SpectroWeb $^f)$ CHIANTI $^g)$ TIPbase $^h)$ TOPbase

#	Wavelength (Å) Input	E_{low} (eV) $\Delta\lambda_{grid}$	$\log(gf)$ cog grid	$\log(gf)$ this work grid	Flags QA? AI?	a)	b)	c)	d)	e)	f)	g)	h)	Recommended literature
727	5733.999	0.031 ±0.009	2.359	-0.07 ±0.08	-0.16 ±0.05	✓	X	-0.17 14	-	-1.11 2	-0.17 14	-	-	14
733	5743.447	-0.022 ±0.010	1.081	-0.86 ±0.07	-0.95 ±0.07	✓	X	-0.97 33	-0.97 55	-1.16 2	-	-	-	33, 55
784	5830.675	-0.014 ±0.008	3.113	0.66 ±0.08	0.56 ±0.09	✓	X	0.68 14	-	0.56 2	0.68 14	-	-	2
867	6081.441	-0.001 ±0.002	1.051	-0.60 ±0.05	-0.58 ±0.07	✓	✓	-0.58 55	-0.58 55	-0.60 2	-0.61 53	-	-	2, 53, 55
893	6135.361	0.009 ±0.009	1.051	-0.73 ±0.07	-0.76 ±0.09	✓	✓	-0.75 55	-0.75 55	-0.95 2	-0.76 53	-	-	53, 55
938	6224.529	-0.027 ±0.004	0.287	-1.77 ±0.08	-1.77 ±0.09	✓	✓	-2.01 33	-2.01 54	-1.85 2	-2.01 33	-	-	2
968	6296.487	-0.012 ±0.010	0.301	-1.48 ±0.07	-1.54 ±0.06	✓	X	-1.59 33	-1.59 55	-1.54 2	-1.61 53	-	-	2, 33, 55
821	5928.852	0.012 ±0.010	2.522	-1.60 ±0.06	-1.67 ±0.03	✓	X	-1.68 14	-	-1.60 2	-1.68 14	-	-	14
70	4489.463	0.007 ±0.005	3.556	-0.41 ±0.02	-0.46 ±0.04	✓	X	-0.16 14	-	-0.20 2	-0.16 14	-	-	-
74	4492.306	-0.009 ±0.002	3.375	-0.37 ±0.04	-0.43 ±0.05	✓	X	-0.39 33	-0.39 56	-0.39 2	-0.39 33	-	-	2, 33, 56
86	4511.891	-0.001 ±0.002	3.087	-0.27 ±0.05	-0.42 ±0.05	✓	X	-0.34 33	-0.34 56	-0.43 2	-0.34 33	-0.45 4	X	2, 57
102	4535.136	-0.001 ±0.002	2.544	-0.96 ±0.05	-1.04 ±0.05	✓	X	-1.02 57	-	-1.02 2	-1.02 57	-	-	2, 57
105	4541.061	0.000 ±0.003	2.545	-1.07 ±0.05	-1.14 ±0.06	✓	X	-1.15 57	-	-1.08 2	-1.15 57	-	-	2, 57
109	4545.953	-0.001 ±0.002	0.941	-1.29 ±0.05	-1.37 ±0.04	✓	X	-1.37 57	-1.38 58	-1.04 2	-1.37 57	-	-	57, 58
129	4575.107	-0.005 ±0.001	3.369	-0.84 ±0.02	-0.88 ±0.04	✓	✓	-0.97 33	-	-1.26 2	-0.97 33	-	-	-
133	4580.048	-0.002 ±0.003	0.941	-1.19 ±0.11	-1.49 ±0.08	✓	X	-1.66 57	-1.64 58	-1.30 2	-1.66 57	-	X	2, 57
154	4600.749	-0.002 ±0.003	1.004	-1.20 ±0.06	-1.27 ±0.04	✓	X	-1.25 57	-	-1.30 2	-1.25 57	-	-	2, 57
165	4616.124	-0.005 ±0.001	0.983	-1.17 ±0.04	-1.22 ±0.03	✓	X	-1.19 57	-1.18 58	-1.23 2	-1.19 57	-	-	2, 57
167	4619.533	-0.002 ±0.003	2.987	-0.43 ±0.03	-0.53 ±0.04	✓	X	-0.59 33	-0.59 59	-0.60 2	-0.59 33	-	-	X
169	4621.960	-0.050 ±0.001	2.545	-0.54 ±0.12	-1.06 ±0.05	✓	X	-0.45 14	-	-0.97 2	-0.45 14	-	-	X
172	4626.174	-0.002 ±0.003	0.968	-1.35 ±0.02	-1.32 ±0.04	✓	✓	-1.33 57	-	-1.35 2	-1.33 57	-	-	2, 57
174	4633.255	-0.001 ±0.003	3.125	-1.09 ±0.03	-1.15 ±0.05	✓	X	-1.11 57	-1.24 60	-1.32 2	-1.11 57	-	-	57
183	4646.162	-0.001 ±0.002	1.030	-0.81 ±0.06	-0.71 ±0.06	✓	X	-0.74 57	-0.71 58	-0.70 2	-0.74 57	-0.81 4	-	2, 57, 58
185	4651.284	-0.001 ±0.002	0.983	-1.41 ±0.04	-1.46 ±0.05	✓	X	-1.46 57	-1.46 58	-1.46 2	-1.46 57	-	-	2, 57, 58
209	4689.356	0.010 ±0.013	3.125	-0.23 ±0.05	-0.30 ±0.04	✓	X	-0.40 57	-0.42 33	-0.42 2	-0.40 57	-0.57 4	-	-
212	4693.938	-0.005 ±0.001	2.983	-0.75 ±0.04	-0.86 ±0.05	✓	X	-0.80 57	-0.91 60	-0.85 2	-0.80 57	-	X	2, 33, 56
213	4700.610	-0.003 ±0.003	2.710	-1.35 ±0.09	-1.35 ±0.10	✓	✓	-1.25 33	-	-1.25 2	-1.25 33	-	-	2, 33
218	4708.013	-0.005 ±0.001	3.168	0.02 ±0.04	-0.02 ±0.05	✓	✓	0.07 57	0.11 56	0.11 2	0.07 57	-0.04 4	4	-
221	4718.419	-0.002 ±0.003	3.195	0.25 ±0.04	0.17 ±0.03	✓	X	0.24 57	0.10 60	0.40 2	0.24 57	0.12 4	-	X
228	4730.710	-0.001 ±0.002	3.079	-0.18 ±0.07	-0.25 ±0.06	✓	X	-0.19 33	-0.19 56	-0.19 2	-0.19 33	-0.47 4	-	2, 33, 56
235	4737.348	-0.003 ±0.003	3.087	0.03 ±0.03	-0.15 ±0.05	✓	X	-0.10 33	-0.10 56	-0.10 2	-0.10 33	-0.36 4	X	57
239	4745.307	-0.005 ±0.001	2.708	-1.34 ±0.02	-1.40 ±0.05	✓	X	-1.38 57	-	-1.22 2	-1.38 57	-	-	-
245	4756.112	-0.002 ±0.003	3.104	0.19 ±0.04	0.18 ±0.04	✓	✓	0.09 33	0.09 60	0.09 2	0.09 33	-	-	-
250	4759.910	0.019 ±0.011	3.113	-1.56 ±0.11	-1.70 ±0.06	✓	X	-1.29 14	-	-1.44 2	-1.29 14	-	-	-
252	4764.293	-0.001 ±0.002	3.551	-0.22 ±0.05	-0.24 ±0.05	✓	✓	-0.20 14	-	-0.28 2	-0.20 14	-	-	2, 14
254	4767.855	-0.004 ±0.002	3.556	-0.49 ±0.05	-0.50 ±0.06	✓	✓	-0.88 14	-0.54 60	-0.54 2	-0.53 33	-	-	2, 33, 60

Table F.1. $\langle\mathcal{O}^A\rangle$ Quality-assessable (A) Analysis-independent line ^{a)} Paper 1 input list ^{b)} NIST ^{c)} SpectroWeb ^{d)} VALD3 ^{e)} CHIANTI ^{f)} TIPbase ^{g)} TOPbase

#	Wavelength (Å) Input	E_{low} (eV) $\Delta\lambda_{grid}$	$\log(gf)$ cog	$\log(gf)$ this work grid	Flags QA? AI?	a)	b)	c)	d)	e)	f)	g)	h)	Recommended literature
267	4789.335	-0.011 ±0.002	2.544	-0.34 ±0.04	-0.60 ±0.07	X X	-0.33 57	-0.36 56	-0.36 2	-0.33 57	-0.61 4	-	-	X
268	4790.333	-0.004 ±0.002	2.545	-1.49 ±0.02	-1.60 ±0.03	X X	-1.48 57	-	-1.56 2	-1.48 57	-	-	-	X
276	4801.025	-0.002 ±0.003	3.122	-0.13 ±0.03	-0.15 ±0.04	✓ ✓	-0.13 33	-0.13 56	-0.13 2	-0.13 33	-0.36 4	-	-	2, 33, 56
284	4810.730	0.001 ±0.007	3.079	-1.16 ±0.05	-1.28 ±0.01	X X	-0.64 14	-	-1.30 2	-0.64 14	-	-	-	X
292	4836.852	-0.001 ±0.005	3.104	-0.87 ±0.06	-1.06 ±0.06	X X	-0.60 14	-	-1.14 2	-0.60 14	-	-	-	X
301	4885.770	-0.004 ±0.002	2.544	-0.99 ±0.06	-1.10 ±0.07	✓ X	-1.05 33	-	-1.05 2	-4.54 14	-	-	-	2, 33
335	4936.335	-0.002 ±0.003	3.113	-0.21 ±0.06	-0.26 ±0.05	X X	-0.25 57	-0.34 33	-0.15 2	-0.25 57	-0.23 4	-	-	4, 57
344	4954.806	-0.020 ±0.015	3.122	0.00 ±0.06	-0.13 ±0.03	X X	-0.17 57	-0.31 33	-0.12 2	-0.17 57	-0.23 4	-	-	X
347	4964.927	-0.001 ±0.002	0.941	-2.47 ±0.06	-2.48 ±0.06	✓ ✓	-2.53 61	-2.53 61	-2.53 2	-2.53 33	-	-	-	2, 33, 61
408	5051.897	0.001 ±0.003	0.941	-2.76 ±0.16	-2.94 ±0.05	✓ X	-2.56 14	-	-2.98 2	-2.56 14	-	-	-	2
418	5072.926	-0.001 ±0.002	0.941	-2.55 ±0.12	-2.70 ±0.05	X X	-2.36 14	-	-2.73 2	-2.36 14	-	-	-	2
428	5091.883	-0.010 ±0.003	1.004	-3.06 ±0.05	-3.28 ±0.04	X X	-2.65 14	-	-3.34 2	-2.65 14	-	-	-	X
470	5221.751	-0.001 ±0.002	3.375	-0.46 ±0.04	-0.49 ±0.03	✓ ✓	-0.35 14	-	-0.87 2	-0.35 14	-	-	-	-
479	5237.833	0.011 ±0.006	3.648	-1.08 ±0.04	-1.17 ±0.05	X X	-0.93 14	-	-1.03 2	-0.93 14	-	-	-	-
480	5238.961	-0.001 ±0.002	2.709	-1.34 ±0.03	-1.34 ±0.04	✓ ✓	-1.27 57	-1.30 56	-1.36 2	-1.27 57	-	-	-	2, 56
482	5240.473	-0.029 ±0.008	3.668	-0.53 ±0.02	-0.57 ±0.03	✓ ✓	-0.71 14	-	-0.70 2	-0.71 14	-	-	-	-
483	5241.458	0.001 ±0.005	2.710	-1.99 ±0.09	-2.04 ±0.09	X X	-1.92 57	-2.08 60	-2.24 2	-1.92 57	-	-	-	60
485	5243.354	-0.010 ±0.009	3.395	-0.39 ±0.12	-0.55 ±0.02	X X	-0.58 57	-	-0.74 2	-0.54 14	-0.83 4	-	-	X
490	5247.565	0.000 ±0.001	0.961	-1.56 ±0.05	-1.56 ±0.08	✓ ✓	-1.59 57	-1.63 58	-1.64 2	-1.59 57	-	-	-	2, 57, 58
502	5272.000	-0.004 ±0.002	3.449	-0.37 ±0.06	-0.45 ±0.04	X X	-0.42 57	-0.42 56	-0.40 2	-0.42 57	-0.28 4	-	-	56, 57
505	5275.747	0.004 ±0.002	2.889	0.06 ±0.08	-0.10 ±0.03	X X	-0.02 14	-	-0.05 2	-0.02 14	-	-	-	X
512	5287.178	-0.001 ±0.002	3.438	-0.83 ±0.04	-0.89 ±0.03	✓ X	-0.87 57	-0.91 56	-0.91 2	-0.87 57	-0.49 4	-	-	2, 56, 57
519	5296.691	0.000 ±0.001	0.983	-1.31 ±0.04	-1.28 ±0.04	✓ ✓	-1.36 57	-1.41 58	-1.40 2	-1.36 57	-	-	-	-
520	5298.271	0.006 ±0.002	0.983	-0.96 ±0.08	-1.25 ±0.07	X X	-1.14 57	-1.16 58	-1.15 2	-1.14 57	-	-	-	X
522	5300.745	-0.001 ±0.002	0.983	-2.04 ±0.06	-2.10 ±0.07	✓ X	-2.00 57	-	-2.11 2	-2.02 14	-	-	-	2
523	5304.180	-0.003 ±0.003	3.464	-0.66 ±0.03	-0.66 ±0.04	✓ ✓	-0.67 57	-0.69 56	-0.69 2	-0.67 57	-0.60 4	-	-	2, 56, 57
530	5312.856	-0.004 ±0.002	3.449	-0.53 ±0.01	-0.53 ±0.03	✓ ✓	-0.55 57	-0.56 56	-0.56 2	-0.55 57	-0.49 4	-	-	2, 56, 57
534	5318.771	-0.004 ±0.002	3.438	-0.67 ±0.03	-0.67 ±0.05	✓ ✓	-0.67 57	-0.69 56	-0.69 2	-0.67 57	-0.56 4	-	-	2, 56, 57
542	5329.138	0.001 ±0.003	2.914	0.04 ±0.06	-0.07 ±0.03	X X	-0.06 33	-	-0.06 2	-0.01 14	-	-	-	X
543	5329.784	0.001 ±0.002	2.914	-0.81 ±0.52	-0.78 ±0.04	✓ ✓	-0.80 33	-0.80 56	-0.80 2	-0.80 33	-	-	-	2, 33, 56
548	5344.756	-0.001 ±0.003	3.449	-0.96 ±0.02	-1.00 ±0.03	✓ ✓	-0.99 57	-1.06 60	-1.06 2	-0.99 57	-	-	-	57
549	5348.314	0.004 ±0.002	1.004	-1.17 ±0.04	-1.15 ±0.04	✓ ✓	-1.21 57	-1.29 58	-1.29 2	-1.21 57	-	-	-	-
653	5628.642	-0.005 ±0.001	3.422	-0.76 ±0.06	-0.76 ±0.06	✓ ✓	-0.74 57	-0.77 56	-0.76 2	-0.74 57	-	-	-	-
662	5642.359	0.006 ±0.004	3.857	-0.75 ±0.05	-0.79 ±0.03	✓ ✓	-0.90 14	-0.84 60	-0.84 2	-0.83 33	-	-	-	-
667	5648.261	-0.004 ±0.004	3.826	-0.89 ±0.03	-0.94 ±0.03	X X	-0.90 14	-1.00 60	-1.02 2	-1.00 33	-	-	-	-
669	5649.386	-0.006 ±0.002	3.839	-0.66 ±0.03	-0.70 ±0.04	✓ ✓	-0.77 33	-0.77 60	-1.16 2	-0.77 33	-	-	-	-
682	5664.581	-0.012 ±0.004	3.826	-0.83 ±0.08	-0.87 ±0.07	✓ ✓	-0.63 14	-	-0.79 2	-0.63 14	-	-	-	-
699	5694.740	-0.005 ±0.003	3.857	-0.19 ±0.02	-0.24 ±0.03	✓ X	-0.24 14	-	-0.27 2	-0.24 14	-	-	-	2, 14

Table F.1. ^(*a*) Quality-assessable (^(*b*)) Analysis-independent line ^(*c*) Paper 1 input list ^(*d*) NIST ^(*e*) VALD3 ^(*f*) SpectroWeb ^(*g*) CHIANTI ^(*h*) TIPbase ^(*i*) TOPbase

#	Wavelength (Å) Input	E_{low} (eV) $\Delta\lambda_{grid}$	$\log(gf)$ cog grid	$\log(gf)$ this work grid	Flags QA? AI?	a)	b)	c)	d)	e)	f)	g)	h)	Recommended literature
714	5712.771	-0.016 ±0.010	3.011	-1.01 ±0.04	-1.11 ±0.03	X	X	-1.05 ¹⁴	-	-1.30 ²	-1.05 ¹⁴	-	-	X
719	5719.815	-0.004 ±0.004	3.013	-1.62 ±0.08	-1.64 ±0.07	✓	✓	-1.58 ⁵⁷	-1.66 ⁵⁶	-1.74 ⁴²	-1.58 ⁵⁷	-	-	56, 57
723	5729.206	-0.012 ±0.008	3.845	-1.11 ±0.08	-1.07 ±0.10	✓	✓	-1.05 ¹⁴	-	-1.06 ²	-1.05 ¹⁴	-	-	2, 14
729	5738.530	0.000 ±0.003	3.551	-1.33 ±0.09	-1.36 ±0.06	✓	✓	-1.37 ¹⁴	-	-1.47 ²	-1.37 ¹⁴	-	-	14
755	5781.751	-0.001 ±0.005	3.323	-0.61 ±0.06	-0.70 ±0.02	X	X	-0.73 ¹⁴	-	-0.64 ²	-0.73 ¹⁴	-	-	X
756	5783.065	-0.005 ±0.001	3.323	-0.41 ±0.02	-0.42 ±0.02	✓	✓	-0.38 ¹⁴	-0.50 ⁶⁰	-1.82 ²	-0.50 ³³	-	-	-
757	5783.850	0.001 ±0.002	3.322	-0.16 ±0.04	-0.24 ±0.03	X	X	-0.29 ³³	-0.29 ⁵⁶	-0.18 ²	-0.29 ³³	-	-	X
759	5784.969	-0.003 ±0.003	3.321	-0.38 ±0.02	-0.40 ±0.02	✓	✓	-0.38 ³³	-0.38 ⁵⁶	-0.37 ²	-0.38 ³³	-	-	33, 56
761	5787.919	-0.006 ±0.002	3.322	-0.14 ±0.03	-0.15 ±0.02	✓	✓	-0.08 ³³	-0.08 ⁵⁶	-0.13 ²	-0.08 ³³	-	-	2
762	5788.381	-0.004 ±0.007	3.013	-1.45 ±0.01	-1.47 ±0.02	✓	✓	-1.49 ⁵⁷	-	-1.83 ²	-1.49 ⁵⁷	-	-	57
789	5844.595	-0.002 ±0.005	3.013	-1.66 ±0.04	-1.70 ±0.06	✓	✓	-1.77 ⁵⁷	-1.76 ⁶⁰	-1.76 ²	-1.77 ⁵⁷	-	-	2, 60
984	6330.091	-0.001 ±0.002	0.941	-2.85 ±0.05	-2.87 ±0.05	✓	✓	-2.79 ¹⁴	-2.91 ⁶⁰	-2.92 ²	-2.92 ³³	-	-	2, 33, 60
1040	6630.010	-0.001 ±0.003	1.030	-3.44 ±0.03	-3.46 ±0.05	✓	✓	-3.56 ³³	-3.56 ⁶⁰	-3.86 ²	-3.56 ³³	-	-	-
1048	6661.075	-0.006 ±0.002	4.193	-0.08 ±0.05	-0.12 ±0.04	✓	✓	-0.11 ¹⁴	-	-0.19 ²	-0.11 ¹⁴	-	-	14
1053	6669.281	-0.003 ±0.004	4.175	-0.40 ±0.04	-0.48 ±0.03	X	X	-0.56 ¹⁴	-	-0.56 ²	-0.56 ¹⁴	-	-	X
1072	6729.734	-0.011 ±0.007	4.389	-0.55 ±0.04	-0.57 ±0.05	✓	✓	-0.56 ¹⁴	-	-0.71 ²	-0.56 ¹⁴	-	-	14
140	4588.199	-0.005 ±0.001	4.071	-0.64 ±0.05	-0.63 ±0.04	✓	✓	-0.63 ⁶²	-	-0.59 ²	-0.63 ⁶²	-	-	2, 62
144	4592.049	0.000 ±0.001	4.074	-1.14 ±0.04	-1.36 ±0.08	X	X	-1.22 ⁶²	-	-1.19 ²	-1.22 ⁶²	-	-	X
175	4634.070	-0.001 ±0.004	4.072	-0.80 ±0.08	-0.96 ±0.04	X	X	-0.99 ⁶³	-	-0.98 ²	-0.99 ⁶³	-	-	X
478	5237.328	-0.008 ±0.003	4.073	-1.07 ±0.06	-1.19 ±0.01	X	X	-1.14 ¹⁴	-1.16 ⁴⁹	-1.16 ²	-1.35 ⁶⁴	-	-	X
487	5246.768	0.004 ±0.002	3.714	-2.34 ±0.06	-2.42 ±0.02	✓	✓	-2.47 ⁶²	-	-2.44 ²	-2.47 ⁶²	-	-	2
504	5274.964	0.039 ±0.012	4.071	-0.86 ±0.14	-1.02 ±0.09	✓	✓	-1.56 ⁶⁴	-	-1.29 ²	-1.56 ⁶⁴	-	-	-
508	5279.876	-0.003 ±0.003	4.073	-1.89 ±0.03	-1.97 ±0.03	X	X	-1.94 ¹⁴	-2.10 ⁴⁹	-1.91 ²	-2.11 ⁶⁴	-	-	X
524	5305.853	0.009 ±0.002	3.827	-1.98 ±0.03	-2.02 ±0.02	✓	✓	-2.36 ¹⁴	-	-2.16 ²	-2.16 ⁶⁴	-	-	-
528	5310.686	0.004 ±0.006	4.072	-2.12 ±0.09	-2.19 ±0.06	✓	✓	-2.20 ¹⁴	-2.27 ⁴⁹	-2.14 ²	-2.28 ³³	-	-	2, 14
531	5313.563	0.015 ±0.003	4.074	-1.54 ±0.04	-1.58 ±0.02	✓	✓	-1.53 ¹⁴	-1.65 ⁴⁹	-1.65 ²	-1.78 ⁶⁴	-	-	-
603	5502.067	0.012 ±0.004	4.168	-1.81 ±0.06	-1.91 ±0.01	X	X	-2.09 ¹⁴	-1.99 ⁴⁹	-1.99 ²	-2.12 ⁶⁴	-	-	X
858	6053.466	0.025 ±0.022	4.745	-1.82 ±0.18	-2.01 ±0.06	✓	✓	-2.23 ⁶²	-	-2.20 ²	-2.23 ⁶²	-	-	-
11	4257.654	-0.001 ±0.002	2.953	-0.36 ±0.10	-0.45 ±0.10	✓	✓	-0.70 ³³	-0.47 ²	-0.70 ³³	-0.70 ⁴	-	-	2
12	4265.918	-0.001 ±0.002	2.941	-0.36 ±0.05	-0.40 ±0.07	✓	✓	-0.27 ³³	-0.27 ⁶⁵	-0.27 ²	-0.27 ³³	-	-	4
54	4451.581	0.001 ±0.004	2.888	0.40 ±0.08	0.35 ±0.07	X	X	0.28 ³³	0.28 ⁶⁵	0.28 ²	0.28 ³³	-	-	2, 33, 65
56	4452.999	-0.004 ±0.002	2.941	-0.46 ±0.10	-0.54 ±0.09	✓	✓	-0.49 ³³	-0.49 ⁶⁵	-0.49 ²	-0.49 ³³	-	-	2, 33, 65
58	4457.034	-0.004 ±0.002	3.073	-0.55 ±0.08	-0.69 ±0.06	✓	✓	-0.56 ³³	-0.56 ⁶⁵	-0.56 ²	-0.56 ³³	-	-	-
59	4458.248	-0.001 ±0.002	3.073	0.10 ±0.08	-0.12 ±0.09	X	X	0.04 ³³	0.04 ⁶⁵	0.04 ²	0.04 ³³	-	-	X
78	4498.891	-0.001 ±0.002	2.941	-0.39 ±0.04	-0.49 ±0.04	X	X	-0.34 ³³	-0.34 ⁶⁵	-0.34 ²	-0.34 ³³	-	-	X
79	4502.213	-0.004 ±0.002	2.920	-0.37 ±0.05	-0.44 ±0.06	✓	✓	-0.34 ³³	-0.34 ⁶⁵	-0.50 ²	-0.34 ³³	-	-	2

Table F.1. $\langle g \rangle$) Quality-assessable (A^l) Analysis-independent line $a)$ Paper 1 input list $b)$ NIST $c)$ SpectroWeb $d)$ VALD3 $e)$ CHIANTI $f)$ TIPbase $g)$ TOPbase

#	Wavelength (Å) Input	E_{low} (eV) $\Delta\lambda_{grid}$	$\log(gf)$ cog grid	Flags QA? AI?	a)	b)	c)	d)	e)	f)	g)	h)	Recommended literature
199	4671.670	-0.001 ±0.003	2.888	-1.53 ±0.04	-1.64 ±0.05	X	X	-1.67 66	-1.67 33	-1.67 2	-1.68 66	-	-
220	4709.710	-0.005 ±0.001	2.888	-0.24 ±0.10	-0.31 ±0.11	✓	X	-0.49 66	-0.34 65	-0.33 2	-0.49 66	-0.69 4	-
236	4739.090	0.010 ±0.001	2.941	-0.39 ±0.10	-0.49 ±0.11	✓	X	-0.61 66	-0.49 65	-0.49 2	-0.61 66	-	-
526	5308.922	0.001 ±0.011	5.405	0.35 ±0.04	0.20 ±0.07	X	X	0.26 14	-	0.30 2	0.26 14	-	-
561	5399.475	-0.001 ±0.002	3.853	-0.07 ±0.09	-0.20 ±0.07	✓	X	-0.34 14	-	-0.29 2	-0.34 14	-	-
Fe I													
1	4207.127	-0.003 ±0.003	2.832	-1.54 ±0.11	-1.52 ±0.10	✓	✓	-1.46 67	-	-1.46 2	-	-2.51 68	2,67
2	4208.604	-0.007 ±0.004	3.397	-1.04 ±0.12	-0.99 ±0.14	✓	X	-1.36 14	-	-	-	-	-
3	4217.546	-0.006 ±0.003	3.430	-0.57 ±0.13	-0.78 ±0.20	✓	X	-0.48 69	-	-0.51 2	-	-0.27 4	-
4	4220.341	-0.004 ±0.002	3.071	-1.25 ±0.11	-1.37 ±0.10	✓	X	-1.31 69	-1.31 69	-1.37 2	-1.31 69	-1.17 68	2,69
5	4222.213	-0.004 ±0.002	2.450	-1.09 ±0.05	-1.11 ±0.06	✓	✓	-0.97 67	-	-0.97 2	-	-0.93 4	-
6	4232.726	-0.003 ±0.003	0.110	-4.67 ±0.08	-4.88 ±0.08	X	X	-4.93 67	-4.93 70	-5.13 2	-4.93 67	-	X
7	4241.114	0.003 ±0.004	2.832	-2.35 ±0.15	-2.52 ±0.06	✓	X	-2.51 67	-	-2.51 2	-2.51 67	-	2,67
8	4243.816	-0.004 ±0.002	3.884	-1.39 ±0.07	-1.44 ±0.09	✓	X	-1.50 67	-1.48 71	-1.50 2	-1.50 67	-	2,67,71
10	4256.805	-0.004 ±0.002	4.256	-1.43 ±0.04	-1.45 ±0.05	✓	✓	-1.56 67	-	-1.57 2	-	-	-
13	4266.964	-0.001 ±0.003	2.728	-1.36 ±0.12	-1.75 ±0.14	X	X	-1.81 69	-1.78 2	-1.81 69	-	-2.49 68	X
17	4291.463	-0.001 ±0.002	0.052	-3.91 ±0.05	-3.95 ±0.07	✓	✓	-4.08 69	-4.08 69	-4.80 2	-4.08 69	-	-
23	4365.896	-0.001 ±0.002	2.990	-2.27 ±0.06	-2.25 ±0.07	✓	✓	-2.25 69	-2.25 69	-2.25 2	-2.25 69	-	2,69
24	4367.903	-0.001 ±0.002	1.608	-2.76 ±0.05	-2.83 ±0.06	✓	X	-2.89 69	-2.89 69	-2.65 2	-2.89 69	-	69
25	4373.561	-0.002 ±0.003	3.018	-1.75 ±0.10	-1.98 ±0.08	X	X	-1.83 69	-	-2.29 2	-	-2.25 68	X
27	4387.891	-0.001 ±0.002	3.071	-1.42 ±0.03	-1.48 ±0.05	✓	X	-1.52 69	-1.52 69	-1.52 2	-1.52 69	-1.02 68	2,69
28	4389.244	-0.001 ±0.002	0.052	-4.48 ±0.07	-4.50 ±0.09	✓	✓	-4.58 67	-4.58 70	-4.58 2	-4.58 67	-	2,67,70
33	4412.426	0.025 ±0.027	2.176	-4.26 ±0.10	-4.58 ±0.01	X	X	-3.21 14	-	-4.50 2	-3.21 14	-	X
34	4413.396	-0.033 ±0.010	4.076	-2.33 ±0.08	-2.78 ±0.05	X	X	-1.53 67	-	-3.50 2	-	-	X
38	4422.568	-0.025 ±0.005	2.845	-0.92 ±0.77	-1.34 ±0.22	✓	X	-1.12 69	-	-1.67 2	-	-1.75 68	69
39	4423.841	-0.005 ±0.001	3.654	-1.60 ±0.04	-1.61 ±0.06	✓	✓	-1.61 72	-	-1.76 2	-1.61 67	-	67,72
41	4432.568	-0.003 ±0.003	3.573	-1.68 ±0.04	-1.72 ±0.06	✓	✓	-1.60 67	-1.56 71	-1.85 2	-1.60 67	-	-
44	4438.343	-0.006 ±0.002	3.686	-1.56 ±0.04	-1.65 ±0.06	✓	X	-1.58 73	-	-1.79 2	-	-	-
45	4439.634	-0.005 ±0.001	3.047	-2.94 ±0.04	-2.92 ±0.04	✓	✓	-2.84 67	-	-3.06 2	-	-	-
46	4439.881	-0.001 ±0.002	2.279	-2.96 ±0.05	-2.94 ±0.05	✓	✓	-3.00 67	-	-3.00 2	-3.00 67	-	-
47	4442.339	0.006 ±0.002	2.198	-1.09 ±0.04	-1.27 ±0.05	X	X	-1.25 67	-1.25 74	-1.25 2	-1.25 67	-1.31 68	X
48	4442.831	-0.004 ±0.002	2.176	-2.56 ±0.08	-2.69 ±0.09	✓	X	-2.79 67	-2.79 74	-2.79 2	-2.79 67	-	-
49	4447.130	-0.011 ±0.002	2.198	-2.55 ±0.05	-2.76 ±0.08	X	X	-2.73 69	-2.73 69	-2.84 2	-2.73 69	-	X
51	4450.316	-0.005 ±0.001	3.111	-1.64 ±0.17	-2.03 ±0.04	X	X	-1.99 69	-1.99 69	-2.10 2	-1.99 69	-1.50 68	X
60	4461.653	-0.001 ±0.002	0.087	-3.17 ±0.04	-3.25 ±0.04	✓	X	-3.21 67	-3.21 70	-3.21 2	-3.21 67	-	2,67,70
61	4466.551	0.002 ±0.003	2.832	-0.42 ±0.07	-0.57 ±0.04	X	X	-0.60 69	-	-0.96 2	-	-0.42 4	X
65	4479.962	-0.005 ±0.001	3.984	-1.31 ±0.04	-1.45 ±0.06	X	X	-1.52 67	-	-1.55 2	-1.52 67	-	X
66	4481.609	-0.006 ±0.002	3.686	-1.50 ±0.03	-1.59 ±0.06	✓	X	-1.53 72	-	-1.74 2	-	-	72

Table F.1. ^(*a*) Quality-assessable (^(*A*)) Analysis-independent line ^(*a*) Paper 1 input list ^(*b*) NIST ^(*c*) Paper 1 input list ^(*d*) VALD3 ^(*e*) SpectroWeb ^(*f*) CHIANTI ^(*g*) TIPbase ^(*h*) TOPbase

#	Wavelength (Å) Input	E_{low} (eV) $\Delta\lambda_{grid}$	$\log(gf)$ cog	$\log(gf)$ this work grid	Flags QA? AI?	Flags a) b)	Flags c) d)	Flags e) d)	Flags f) g)	Flags h)	Recommended literature
67	4484.220	-0.001 ±0.002	3.603	-0.82 ±0.06	-0.82 ±0.07	✓	✓	-0.67 73	-0.86 2	-	-
68	4485.970	-0.005 ±0.001	3.654	-2.36 ±0.03	-2.40 ±0.04	✓	✓	-2.35 67	-2.52 2	-	-
71	4489.739	-0.001 ±0.002	0.121	-3.89 ±0.05	-3.91 ±0.06	✓	✓	-3.97 70	-3.97 67	-	2, 67, 70
72	4490.084	-0.004 ±0.002	3.017	-1.43 ±0.04	-1.59 ±0.08	X	X	-1.58 67	-1.51 2	-	X
75	4492.678	0.000 ±0.003	3.984	-1.60 ±0.04	-1.71 ±0.05	X	X	-1.65 67	-1.83 2	-1.65 67	X
77	4495.953	-0.005 ±0.001	3.654	-1.62 ±0.03	-1.72 ±0.05	X	X	-1.69 73	-1.87 2	-	X
80	4502.591	-0.006 ±0.002	3.573	-2.20 ±0.03	-2.21 ±0.03	✓	✓	-2.35 67	-2.31 71	-2.27 2	-2.35 67
81	4504.210	0.006 ±0.008	3.960	-3.16 ±0.05	-3.22 ±0.04	✓	X	-3.06 14	-4.20 2	-3.09 14	-
82	4504.831	-0.014 ±0.002	3.266	-1.99 ±0.10	-2.13 ±0.04	✓	X	-2.27 67	-2.22 71	-2.28 2	-2.27 67
84	4508.685	-0.004 ±0.004	4.283	-1.87 ±0.03	-1.94 ±0.04	✓	X	-2.05 14	-	-	-
85	4509.735	-0.006 ±0.002	4.220	-1.40 ±0.05	-1.37 ±0.04	✓	✓	-1.29 14	-	-	-
90	4514.184	-0.004 ±0.002	3.047	-1.99 ±0.03	-2.09 ±0.05	X	X	-2.05 67	-	-2.04 2	X
97	4523.399	-0.004 ±0.002	3.654	-1.86 ±0.04	-1.86 ±0.04	✓	✓	-1.99 67	-2.09 2	-	-
98	4525.864	0.001 ±0.003	2.882	-3.04 ±0.04	-3.11 ±0.04	✓	X	-3.20 67	-	-3.34 2	-
104	4537.671	-0.001 ±0.002	3.267	-2.84 ±0.03	-2.89 ±0.04	✓	X	-2.88 67	-2.98 71	-2.88 2	2, 67
107	4543.221	-0.019 ±0.006	3.640	-3.03 ±0.03	-3.08 ±0.03	X	X	-3.33 14	-	-5.74 2	-
111	4551.647	-0.001 ±0.002	3.943	-1.92 ±0.04	-1.93 ±0.05	✓	✓	-2.06 67	-2.03 71	-1.92 2	2
115	4556.924	-0.004 ±0.002	3.252	-2.60 ±0.03	-2.65 ±0.04	✓	X	-2.71 67	-	-2.69 2	2
116	4560.088	-0.001 ±0.002	3.603	-1.73 ±0.05	-1.85 ±0.06	X	X	-1.92 67	-	-1.92 2	X
117	4561.198	-0.017 ±0.005	4.320	-2.20 ±0.06	-2.47 ±0.07	X	X	-1.28 14	-	-	X
121	4566.515	-0.005 ±0.001	3.301	-2.09 ±0.04	-2.17 ±0.05	✓	X	-2.38 69	-	-2.17 2	-2.38 69
122	4566.865	-0.012 ±0.006	4.313	-1.08 ±0.10	-1.30 ±0.07	X	X	-0.93 14	-	-	X
127	4574.216	-0.003 ±0.003	3.211	-2.33 ±0.04	-2.34 ±0.04	✓	✓	-2.38 73	-2.45 71	-2.47 2	-2.50 67
128	4574.718	-0.002 ±0.003	2.279	-2.81 ±0.05	-2.82 ±0.04	✓	✓	-2.97 67	-	-2.92 2	-
132	4579.820	0.000 ±0.007	3.071	-2.68 ±0.04	-2.83 ±0.03	X	X	-2.83 67	-	-3.12 2	-2.83 67
135	4583.128	0.000 ±0.008	4.371	-1.93 ±0.07	-2.04 ±0.10	✓	X	-1.76 14	-	-	-
137	4585.339	-0.004 ±0.002	4.608	-1.52 ±0.02	-1.57 ±0.04	✓	X	-1.08 14	-	-	-
138	4587.127	-0.001 ±0.002	3.573	-1.57 ±0.06	-1.68 ±0.05	✓	X	-1.74 69	-	-1.69 2	-1.17 68
139	4587.720	-0.016 ±0.008	3.984	-2.07 ±0.05	-2.20 ±0.03	X	X	-2.15 67	-	-2.36 2	X
143	4590.789	-0.006 ±0.002	4.387	-1.36 ±0.06	-1.44 ±0.04	✓	X	-1.77 14	-	-1.77 2	-
145	4593.525	0.004 ±0.007	3.943	-1.91 ±0.05	-1.98 ±0.07	X	X	-2.06 67	-2.03 71	-2.18 2	-2.06 67
148	4597.250	0.000 ±0.013	4.387	-1.51 ±0.05	-1.68 ±0.02	X	X	-1.12 14	-	-	X
149	4598.117	-0.002 ±0.003	3.283	-1.48 ±0.05	-1.50 ±0.07	✓	✓	-1.57 67	-	-1.71 2	-1.57 67
150	4598.324	0.030 ±0.003	0.958	-4.80 ±0.06	-5.25 ±0.09	X	X	-4.71 14	-	-5.36 2	-4.78 14
151	4598.740	-0.006 ±0.002	3.654	-2.50 ±0.03	-2.56 ±0.04	✓	X	-2.66 67	-	-2.88 2	-2.66 67
152	4599.841	-0.010 ±0.001	4.313	-0.85 ±0.04	-0.88 ±0.03	✓	✓	-1.24 14	-	-2.33 2	-1.23 14
155	4602.001	-0.003 ±0.003	1.608	-3.15 ±0.05	-3.13 ±0.05	✓	✓	-3.13 69	-3.15 75	-3.13 2	-3.15 67
156	4602.941	-0.001 ±0.002	1.485	-2.23 ±0.04	-2.21 ±0.03	✓	✓	-2.21 69	-2.22 75	-2.31 2	-2.21 69
157	4603.342	-0.006 ±0.002	2.845	-3.16 ±0.08	-3.26 ±0.04	✓	X	-3.04 71	-	-3.44 2	-3.14 67

Table F.1. ^(*a*) Quality-assessable (^(*A*)) Analysis-independent line ^(*a*) Paper 1 input list ^(*b*) NIST ^(*c*) Paper 1 input list ^(*d*) VALD3 ^(*e*) SpectroWeb ^(*f*) CHIANTI ^(*g*) TIPbase ^(*h*) TOPbase

#	Wavelength (Å) Input	E_{low} (eV) $\Delta\lambda_{grid}$	$\log(gf)$ cog grid	$\log(gf)$ this work grid	Flags QA? AI?	a)	b)	c)	d)	e)	f)	g)	h)	Recommended literature
158	4604.557	-0.007 ±0.003	4.473	-1.05 ±0.03	-1.11 ±0.04	✓	X	-1.06 14	-	-2.83 2	-1.06 14	-	-	-
160	4605.588	-0.012 ±0.003	4.320	-1.04 ±0.07	-1.11 ±0.03	✓	X	-1.16 14	-	-1.66 2	-	-	-	-
163	4614.205	-0.006 ±0.002	3.301	-2.36 ±0.06	-2.49 ±0.04	X	X	-2.52 71	-	-2.62 2	-	-	-	X
164	4615.565	-0.007 ±0.003	4.580	-1.19 ±0.07	-1.25 ±0.04	✓	X	-1.31 14	-	-1.32 2	-	-	-	-
166	4619.288	-0.002 ±0.003	3.603	-1.07 ±0.07	-1.05 ±0.04	✓	✓	-1.07 73	-	-1.01 2	-	-	-	-4.57 68
170	4623.578	-0.001 ±0.003	4.415	-1.74 ±0.04	-1.81 ±0.03	X	X	-1.86 14	-	-	-	-	-	2, 73
171	4625.045	-0.005 ±0.001	3.241	-1.27 ±0.05	-1.30 ±0.03	✓	✓	-1.30 73	-	-1.35 2	-1.34 67	-	-	73
173	4630.120	-0.003 ±0.003	2.279	-2.49 ±0.04	-2.49 ±0.04	✓	✓	-2.59 69	-	-2.73 2	-	-	-	-
177	4635.846	-0.005 ±0.001	2.845	-2.35 ±0.04	-2.33 ±0.04	✓	✓	-2.36 69	-2.36 69	-2.41 2	-2.36 69	-	-	69
178	4637.503	-0.004 ±0.002	3.283	-1.29 ±0.06	-1.32 ±0.07	✓	✓	-1.29 73	-1.34 71	-1.39 2	-1.39 67	-	-	-
181	4643.463	-0.002 ±0.003	3.654	-1.23 ±0.07	-1.20 ±0.05	✓	✓	-1.15 69	-	-1.29 2	-	-	-	69
189	4657.585	-0.004 ±0.002	2.845	-2.85 ±0.04	-2.89 ±0.05	✓	✓	-2.80 71	-	-3.14 2	-	-	-	-
190	4660.426	-0.007 ±0.003	4.435	-1.64 ±0.04	-1.68 ±0.04	✓	✓	-1.71 14	-	-1.46 14	-	-	-	14
191	4660.887	0.011 ±0.002	4.473	-1.51 ±0.04	-1.56 ±0.03	✓	X	-1.75 14	-	-1.77 14	-	-	-	-
192	4661.534	-0.005 ±0.001	4.559	-1.18 ±0.05	-1.18 ±0.04	✓	✓	-1.17 71	-	-1.27 2	-1.27 67	-	-	71
193	4661.970	0.004 ±0.002	2.990	-2.28 ±0.09	-2.46 ±0.05	X	X	-2.50 69	-	-2.63 2	-	-	-	X
194	4665.255	-0.050 ±0.001	4.387	-1.95 ±0.12	-2.18 ±0.11	✓	X	-1.28 14	-	-1.35 14	-	-	-	-
196	4669.171	-0.006 ±0.002	3.654	-1.12 ±0.09	-1.20 ±0.06	✓	X	-1.24 73	-	-1.26 2	-1.21 69	-	-	2, 69, 73
200	4672.830	-0.002 ±0.003	1.608	-3.99 ±0.12	-4.16 ±0.14	✓	X	-4.24 67	-	-4.24 2	-4.24 67	-	-	2, 67
201	4678.846	-0.005 ±0.001	3.603	-0.76 ±0.08	-0.75 ±0.07	✓	✓	-0.70 73	-	-0.66 2	-	-	-	73
203	4681.473	-0.014 ±0.004	4.607	-1.23 ±0.04	-1.26 ±0.04	✓	✓	-1.35 14	-	-	-	-	-	-
205	4683.560	-0.005 ±0.001	2.832	-2.32 ±0.05	-2.38 ±0.04	✓	X	-2.32 69	-	-2.53 2	-	-	-	-
208	4688.176	-0.004 ±0.002	4.607	-0.95 ±0.05	-0.95 ±0.03	✓	✓	-1.54 14	-	-1.54 2	-	-	-	-
210	4690.138	-0.005 ±0.001	3.686	-1.55 ±0.06	-1.56 ±0.05	✓	✓	-1.64 69	-	-1.68 2	-	-	-	-
217	4704.948	-0.004 ±0.002	3.686	-1.42 ±0.06	-1.46 ±0.07	✓	✓	-1.32 73	-	-1.57 2	-	-	-	-4.09 68
224	4726.137	-0.001 ±0.002	2.998	-3.04 ±0.03	-3.06 ±0.04	✓	✓	-2.90 73	-	-3.24 2	-	-	-	-
225	4728.546	-0.005 ±0.001	3.654	-1.08 ±0.07	-1.11 ±0.05	✓	✓	-1.17 69	-	-1.14 2	-	-	-	2
226	4729.019	-0.004 ±0.002	4.076	-1.52 ±0.06	-1.57 ±0.06	✓	X	-1.61 69	-	-1.66 2	-1.61 69	-	-	69
233	4733.591	-0.004 ±0.002	1.485	-2.93 ±0.05	-3.05 ±0.05	X	X	-2.99 69	-2.99 75	-2.92 2	-2.99 69	-	-	X
234	4735.843	0.002 ±0.005	4.076	-1.09 ±0.09	-1.19 ±0.08	✓	X	-1.33 69	-1.32 69	-1.23 2	-1.32 69	-	-	2
240	4745.800	-0.005 ±0.001	3.654	-1.18 ±0.07	-1.23 ±0.05	✓	X	-1.34 73	-	-1.19 2	-	-	-	2
242	4749.948	-0.006 ±0.002	4.559	-1.15 ±0.03	-1.22 ±0.03	X	X	-1.24 71	-	-1.35 2	-	-	-	X
247	4757.578	-0.004 ±0.002	3.274	-1.97 ±0.06	-2.03 ±0.07	✓	X	-2.04 14	-	-2.02 2	-	-	-	2, 14
257	4776.067	-0.004 ±0.002	3.301	-2.52 ±0.04	-2.58 ±0.02	✓	X	-2.60 71	-	-2.71 2	-	-	-	71
258	4779.439	-0.002 ±0.003	3.415	-2.07 ±0.08	-2.15 ±0.04	✓	X	-2.02 69	-2.02 2	-2.02 2	-2.02 69	-	-	-
261	4785.957	-0.005 ±0.001	4.143	-1.75 ±0.03	-1.76 ±0.03	✓	X	-1.83 71	-	-1.93 2	-1.93 67	-	-	-
264	4786.807	-0.004 ±0.002	3.017	-1.38 ±0.04	-1.50 ±0.03	X	X	-1.61 69	-	-1.74 2	-	-	-	-2.22 68
265	4787.827	0.000 ±0.003	2.998	-2.51 ±0.03	-2.59 ±0.03	X	X	-2.60 73	-	-2.77 2	-	-	-	-
266	4788.757	-0.005 ±0.001	3.237	-1.67 ±0.03	-1.74 ±0.04	✓	X	-1.76 69	-1.76 69	-1.80 2	-1.76 69	-	-	-0.75 68

Table F1. ^(*a*) Quality-assessable (*AI*) Analysis-independent line ^(*a*) Paper 1 input list ^(*b*) NIST ^(*c*) Paper 1 input list ^(*d*) VALD3 ^(*e*) SpectroWeb ^(*f*) CHIANTI ^(*g*) TIPbase ^(*h*) TOPbase

#	Wavelength (Å) Input	E_{low} (eV) $\Delta\lambda_{grid}$	$\log(gf)$ cog grid	$\log(gf)$ this work grid	Flags QA? AI?	a)	b)	c)	d)	e)	f)	g)	h)	Recommended literature
269	4794.354	0.000 ±0.003	2.424	-3.83 ±0.03	-3.87 ±0.03	✓	✓	-3.95 71	-	-4.05 2	-	-	-	-
270	4798.265	-0.002 ±0.003	4.186	-1.39 ±0.05	-1.40 ±0.04	✓	✓	-1.17 69	-	-1.54 2	-	-	-	-
272	4798.731	-0.002 ±0.003	1.608	-4.04 ±0.03	-4.10 ±0.05	✓	✓	-4.15 71	-	-4.24 2	-	-	-	71
273	4799.406	-0.004 ±0.002	3.640	-2.04 ±0.03	-2.10 ±0.05	✓	✓	-2.13 71	-2.19 71	-2.23 2	-2.23 67	-	-2.75 68	-
274	4800.128	-0.004 ±0.002	3.039	-3.05 ±0.02	-3.12 ±0.04	✗	✗	-2.64 71	-	-3.29 2	-	-	-	X
275	4800.649	-0.008 ±0.003	4.143	-0.88 ±0.08	-1.13 ±0.05	✗	✗	-1.03 69	-1.03 69	-1.25 2	-1.03 69	-	-	X
277	4802.880	-0.003 ±0.003	3.642	-1.59 ±0.10	-1.67 ±0.09	✗	✗	-1.51 69	-1.51 69	-1.67 2	-1.51 69	-	-2.01 68	2
278	4804.517	0.000 ±0.003	3.573	-2.30 ±0.04	-2.43 ±0.03	✗	✗	-2.59 67	-	-2.59 2	-2.59 67	-	-	X
280	4807.708	-0.005 ±0.001	3.368	-1.95 ±0.04	-2.01 ±0.04	✗	✗	-2.15 72	-2.15 71	-2.21 2	-2.20 67	-	-	-
281	4808.148	-0.005 ±0.001	3.252	-2.57 ±0.04	-2.59 ±0.04	✓	✓	-2.69 71	-	-2.80 2	-	-	-2.40 68	-
283	4809.137	0.011 ±0.006	3.695	-2.39 ±0.05	-2.51 ±0.02	✗	✗	-2.23 14	-	-2.77 2	-	-	-2.54 68	X
285	4813.113	-0.011 ±0.005	3.274	-2.61 ±0.05	-2.67 ±0.03	✗	✗	-2.79 71	-	-2.92 2	-2.89 67	-	-	-
289	4833.375	-0.001 ±0.026	4.559	-2.28 ±0.30	-2.56 ±0.14	✗	✗	-1.47 14	-	-	-	-	-	X
290	4834.507	0.007 ±0.005	2.424	-3.03 ±0.09	-3.22 ±0.05	✗	✗	-3.31 71	-	-3.41 2	-	-	-	-
291	4835.868	-0.004 ±0.002	4.103	-1.29 ±0.05	-1.33 ±0.05	✓	✓	-1.40 71	-1.47 71	-1.50 2	-1.50 67	-	-	-
293	4839.544	-0.001 ±0.002	3.267	-1.68 ±0.07	-1.77 ±0.07	✗	✗	-1.82 69	-1.82 69	-1.82 2	-1.82 69	-	-2.69	-
295	4843.143	-0.004 ±0.002	3.397	-1.52 ±0.08	-1.65 ±0.08	✗	✗	-1.65 73	-1.79 71	-1.84 2	-1.84 67	-	-	73
297	4875.877	-0.001 ±0.002	3.332	-1.75 ±0.05	-1.84 ±0.07	✗	✗	-1.90 72	-1.97 71	-2.02 2	-2.02 67	-	-	72
300	4885.430	-0.003 ±0.003	3.882	-1.01 ±0.06	-1.02 ±0.05	✗	✗	-0.97 72	-	-1.09 2	-	-	-	72
302	4886.332	-0.005 ±0.001	4.154	-0.75 ±0.07	-0.74 ±0.05	✗	✗	-0.61 14	-	-0.56 2	-	-	-1.50 68	-
303	4888.166	-0.009 ±0.002	4.559	-2.04 ±0.11	-2.32 ±0.19	✗	✗	-1.01 14	-	-	-1.77 14	-	-	-
304	4892.859	-0.005 ±0.001	4.218	-1.16 ±0.05	-1.18 ±0.06	✓	✓	-1.29 67	-	-	-1.29 2	-1.29 67	-	-
305	4894.562	-0.012 ±0.003	4.143	-2.24 ±0.04	-2.30 ±0.05	✗	✗	-2.00 14	-	-2.51 2	-2.28 14	-	-	14
306	4896.439	0.000 ±0.003	3.884	-1.74 ±0.06	-1.87 ±0.05	✗	✗	-1.89 73	-	-2.05 2	-	-	-	X
310	4902.233	0.004 ±0.025	4.559	-1.62 ±0.05	-1.82 ±0.02	✗	✗	-1.38 14	-	-	-	-	-	X
311	4903.310	-0.002 ±0.003	2.882	-1.42 ±1.15	-1.00 ±0.06	✗	✗	-0.90 76	-	-1.07 2	-	-0.79 4	-	-
313	4905.133	-0.009 ±0.002	3.929	-1.77 ±0.02	-1.90 ±0.04	✗	✗	-1.73 72	-	-2.05 2	-	-	-	X
314	4907.320	-0.006 ±0.011	4.143	-3.08 ±0.27	-3.44 ±0.20	✗	✗	-1.89 14	-	-	-1.59 14	-	-	-
315	4907.732	-0.003 ±0.003	3.430	-1.71 ±0.04	-1.75 ±0.05	✗	✗	-1.70 73	-	-	-1.84 2	-1.84 67	-	73
316	4909.383	-0.003 ±0.003	3.929	-1.17 ±0.05	-1.20 ±0.04	✗	✗	-1.23 14	-	-1.27 2	-	-	-	14
317	4910.325	-0.005 ±0.001	4.191	-0.76 ±0.10	-0.83 ±0.10	✗	✗	-0.46 14	-	-0.76 2	-0.46 14	-	-	2
319	4911.529	-0.001 ±0.002	4.256	-1.65 ±0.04	-1.71 ±0.04	✗	✗	-1.84 72	-	-1.88 2	-2.24 67	-	-	-
320	4911.779	-0.005 ±0.001	3.929	-1.58 ±0.04	-1.63 ±0.04	✗	✗	-1.79 72	-	-1.79 2	-	-	-	-
325	4915.850	-0.010 ±0.010	4.143	-2.33 ±0.12	-2.70 ±0.11	✗	✗	-2.02 14	-	-2.80 2	-	-	-	X
326	4917.230	-0.003 ±0.003	4.191	-0.96 ±0.07	-0.99 ±0.05	✗	✗	-1.08 71	-1.16 71	-1.18 2	-1.18 67	-	-1.55 68	-
327	4918.012	-0.001 ±0.002	4.231	-1.13 ±0.04	-1.21 ±0.07	✗	✗	-1.26 71	-1.34 71	-1.36 2	-1.36 67	-	-	71
331	4926.816	-0.031 ±0.023	3.634	-2.72 ±0.12	-3.15 ±0.04	✗	✗	-2.17 14	-	-3.32 2	-2.18 14	-	-	X
332	4930.315	-0.014 ±0.002	3.960	-0.79 ±0.07	-1.08 ±0.07	✗	✗	-1.20 77	-	-1.35 2	-	-	-	X

Table F.1. $\langle\mathcal{O}^A\rangle$ Quality-assessable (A) Analysis-independent line ^{a)} Paper 1 input list ^{b)} NIST ^{c)} SpectroWeb ^{d)} VALD3 ^{e)} CHIANTI ^{f)} TIPbase ^{g)} TOPbase

#	Wavelength (Å) Input	E_{low} (eV) $\Delta\lambda_{grid}$	$\log(gf)$ cog	$\log(gf)$ this work grid	Flags QA? AI?	a)	b)	c)	d)	e)	f)	g)	h)	Recommended literature
336	4939.687	-0.001 ±0.002	0.859	-3.21 ±0.05	-3.26 ±0.04	✓ X	X	-3.34 78	-3.34 2	-3.34 67	-	-3.15 68	-	-
338	4945.636	-0.002 ±0.004	4.209	-1.30 ±0.03	-1.39 ±0.03	✗ X	X	-1.41 71	-1.49 71	-1.51 2	-1.51 67	-	-	X
341	4950.105	-0.007 ±0.006	3.417	-1.46 ±0.05	-1.54 ±0.07	✓ ✓	X	-1.49 73	-	-1.67 2	-1.67 67	-	-	73
345	4962.572	-0.004 ±0.002	4.178	-1.21 ±0.06	-1.18 ±0.03	✓ ✓	X	-1.18 69	-1.18 69	-1.23 2	-1.18 69	-	-	69
349	4969.917	-0.002 ±0.003	4.218	-0.74 ±0.05	-0.71 ±0.03	✓ ✓	X	-0.71 79	-	-0.62 2	-0.71 67	-	-2.40 68	67,79
350	4970.496	-0.004 ±0.002	3.635	-1.41 ±0.16	-1.62 ±0.04	✗ X	X	-1.74 69	-1.74 69	-1.69 2	-1.74 69	-	-1.78 68	X
352	4973.102	-0.004 ±0.002	3.960	-0.65 ±0.05	-0.78 ±0.03	✗ X	X	-0.73 72	-	-0.95 2	-	-0.87 4	-	X
356	4980.540	0.000 ±0.004	4.186	-2.29 ±0.07	-2.53 ±0.08	✗ X	X	-2.00 14	-	-2.82 2	-2.56 14	-	-	X
357	4982.499	-0.001 ±0.002	4.103	-0.18 ±0.07	-0.13 ±0.05	✓ X	X	0.16 14	-	0.14 2	0.16 14	-	-	-
359	4983.853	-0.005 ±0.001	4.103	-0.24 ±0.10	-0.29 ±0.11	✓ X	X	-0.01 14	-	-0.07 2	-0.01 14	-	-0.92 68	-
360	4985.547	-0.001 ±0.002	2.865	-1.43 ±0.05	-1.48 ±0.04	✓ X	X	-1.33 69	-	-1.51 2	-	-	-	2
361	4986.223	-0.003 ±0.003	4.218	-1.24 ±0.03	-1.27 ±0.03	✓ ✓	X	-1.29 71	-1.37 71	-1.39 2	-1.39 67	-	-	71
362	4987.620	-0.003 ±0.003	4.178	-2.65 ±0.09	-2.74 ±0.05	✓ X	X	-2.09 14	-	-2.72 2	-2.72 67	-	-	2,67
363	4988.352	0.011 ±0.010	4.638	-2.02 ±0.12	-2.29 ±0.10	✗ X	X	-1.24 14	-	-	-	-	-	X
364	4988.950	-0.004 ±0.002	4.154	-0.58 ±0.07	-0.62 ±0.06	✓ ✓	X	-0.89 67	-0.86 80	-0.89 2	-	-0.82 4	-	-
365	4992.785	-0.001 ±0.002	4.260	-2.15 ±0.05	-2.20 ±0.03	✓ X	X	-2.35 67	-	-2.34 2	-2.35 67	-	-	-
367	4993.680	0.016 ±0.003	4.209	-1.01 ±0.10	-1.19 ±0.06	✗ X	X	-1.37 71	-1.45 71	-1.47 2	-	-	-	X
368	4995.408	-0.004 ±0.002	4.260	-1.94 ±0.04	-2.00 ±0.03	✓ X	X	-1.79 71	-1.87 71	-2.22 2	-	-	-	-
370	4995.871	0.043 ±0.016	4.231	-2.71 ±0.07	-2.76 ±0.14	✓ X	X	-2.41 14	-	-2.82 2	-2.41 14	-	-1.80 68	2
373	4999.112	-0.009 ±0.005	4.186	-1.56 ±0.04	-1.68 ±0.05	✗ X	X	-1.64 71	-	-1.74 2	-	-	-	X
374	5002.583	-0.004 ±0.003	4.186	-1.59 ±0.16	-1.98 ±0.01	✗ X	X	-1.14 14	-	-2.45 2	-	-	-	X
375	5002.792	0.004 ±0.005	3.397	-1.38 ±0.05	-1.48 ±0.05	✓ X	X	-1.46 72	-1.53 71	-1.58 2	-1.58 67	-	-	71,72
377	5004.044	-0.004 ±0.002	4.209	-1.20 ±0.04	-1.26 ±0.04	✓ X	X	-1.30 71	-1.38 71	-1.40 2	-1.40 67	-	-	71
378	5008.642	-0.008 ±0.003	4.559	-1.69 ±0.06	-1.71 ±0.05	✓ ✓	X	-1.51 14	-	-	-	-	-	-
382	5012.695	-0.002 ±0.003	4.283	-1.30 ±0.02	-1.41 ±0.03	✗ X	X	-1.69 71	-	-1.79 2	-	-	-	X
383	5015.315	-0.019 ±0.013	4.076	-1.93 ±0.20	-2.41 ±0.04	✗ X	X	-1.74 14	-	-2.29 14	-	-	-	X
385	5016.477	-0.007 ±0.003	4.256	-1.51 ±0.05	-1.53 ±0.05	✓ ✓	X	-1.37 14	-	-1.68 2	-	-1.85 68	-	-
387	5020.494	-0.007 ±0.005	4.607	-1.74 ±0.13	-1.92 ±0.11	✓ X	X	-1.33 14	-	-	-	-	-	-
388	5023.186	-0.003 ±0.003	4.283	-1.40 ±0.03	-1.41 ±0.03	✓ ✓	X	-1.50 71	-1.58 71	-1.60 2	-1.60 67	-	-	-
389	5023.498	-0.001 ±0.002	4.313	-1.49 ±0.04	-1.54 ±0.03	✗ X	X	-1.67 72	-1.69 71	-1.71 2	-1.71 67	-	-	X
391	5025.081	-0.005 ±0.003	4.260	-1.77 ±0.03	-1.84 ±0.03	✗ X	X	-1.99 67	-	-1.99 2	-	-	-	X
392	5025.303	0.001 ±0.003	4.284	-1.84 ±0.03	-1.87 ±0.02	✓ ✓	X	-2.00 14	-	-2.04 2	-2.04 67	-	-	-
394	5027.757	-0.005 ±0.001	4.209	-0.94 ±0.07	-1.10 ±0.03	✗ X	X	-1.15 71	-1.23 71	-1.25 2	-	-	-	X
395	5028.126	-0.001 ±0.002	3.573	-1.15 ±0.08	-1.20 ±0.06	✗ X	X	-1.04 76	-1.12 69	-1.12 2	-1.12 69	-	-1.00 68	-
396	5029.618	-0.004 ±0.002	3.415	-1.91 ±0.03	-1.97 ±0.03	✗ X	X	-1.95 71	-	-2.05 2	-	-	-	71
398	5031.914	-0.010 ±0.006	4.371	-1.50 ±0.06	-1.60 ±0.02	✗ X	X	-1.57 71	-1.65 71	-1.67 2	-1.67 67	-	-	X
405	5047.698	0.022 ±0.031	3.695	-3.14 ±0.11	-3.29 ±0.15	✗ X	X	-2.68 14	-	-3.85 2	-	-	-	-
406	5048.436	-0.002 ±0.003	3.960	-1.00 ±0.07	-1.07 ±0.05	✓ X	X	-1.00 73	-	-1.26 2	-	-1.26 2	-	-

Table F1. ^(*a*) Quality-assessable (*AI*) Analysis-independent line ^(*a*) Paper 1 input list ^(*b*) NIST ^(*c*) Paper 1 input list ^(*d*) VALD3 ^(*e*) SpectroWeb ^(*f*) CHIANTI ^(*g*) TIPbase ^(*h*) TOPbase

#	Wavelength (Å) Input	E_{low} (eV) $\Delta\lambda_{grid}$	$\log(gf)$ cog grid	$\log(gf)$ this work grid	Flags QA? AI?	a)	b)	c)	d)	e)	f)	g)	h)	Recommended literature
407	5051.277	-0.002 ±0.006	4.220	-2.48 ±0.10	-2.53 ±0.01	✓ X	-1.11 14	-	-3.63 2	-	-	-1.83 68	-	-
410	5054.642	-0.003 ±0.003	3.640	-1.92 ±0.06	-2.05 ±0.04	X	-1.92 69	-	-2.14 2	-	-	-	-	X
411	5057.481	-0.001 ±0.002	4.191	-1.87 ±0.04	-1.94 ±0.04	✓ X	-1.58 14	-	-2.14 2	-1.59 14	-	-	-	-
412	5058.496	-0.004 ±0.002	3.642	-2.65 ±0.09	-2.68 ±0.06	✓	-2.83 67	-	-2.83 2	-	-	-	-	-
414	5067.150	-0.001 ±0.004	4.220	-0.81 ±0.05	-0.81 ±0.06	✓	-0.97 67	-	-0.97 2	-0.97 67	-	-	-	-
416	5072.078	-0.004 ±0.002	4.283	-0.55 ±0.08	-0.60 ±0.09	✓ X	-0.68 14	-	-0.38 2	-	-	-1.63 68	-	14
417	5072.672	-0.004 ±0.002	4.220	-0.93 ±0.04	-1.02 ±0.07	✓ X	-0.84 14	-	-0.88 2	-0.83 14	-	-	-	-
419	5079.223	0.000 ±0.003	2.198	-1.92 ±0.05	-2.04 ±0.03	X X	-2.07 74	-2.07 74	-2.07 2	-2.07 67	-	-1.93 68	-	X
420	5079.740	-0.002 ±0.003	0.990	-3.07 ±0.09	-3.22 ±0.05	X X	-3.22 78	-3.22 78	-3.22 2	-3.22 67	-	-3.20 68	-	X
423	5083.338	0.000 ±0.001	0.958	-2.96 ±0.04	-2.98 ±0.05	✓	-2.94 78	-2.96 78	-2.96 2	-2.96 67	-	-2.60 68	-	2, 67, 78
426	5088.153	-0.001 ±0.002	4.154	-1.48 ±0.06	-1.61 ±0.03	X X	-1.68 71	-1.75 71	-1.77 2	-1.78 67	-	-1.62 68	-	X
432	5104.030	0.001 ±0.005	3.017	-2.57 ±0.12	-2.80 ±0.05	X X	-2.77 71	-	-2.87 2	-	-	-	-	X
433	5104.190	0.000 ±0.004	4.178	-1.59 ±0.05	-1.74 ±0.04	X X	-1.87 71	-1.94 71	-1.97 2	-1.97 67	-	-	-	X
434	5104.438	-0.004 ±0.002	4.283	-1.41 ±0.07	-1.50 ±0.04	✓ X	-1.59 71	-1.67 71	-1.70 2	-1.69 67	-	-3.12 68	-	-
435	5109.652	-0.006 ±0.002	4.301	-0.64 ±0.05	-0.67 ±0.05	✓	-0.98 67	-	-0.98 2	-	-	-2.02 68	-	-
438	5123.720	0.001 ±0.002	1.011	-2.94 ±0.06	-3.09 ±0.06	X X	-3.07 78	-3.07 78	-3.07 2	-3.07 67	-	-2.90 68	-	X
439	5127.359	-0.001 ±0.002	0.915	-3.25 ±0.05	-3.40 ±0.05	X X	-3.31 78	-3.31 78	-3.31 2	-3.31 67	-	-3.15 68	-	X
442	5131.468	-0.003 ±0.003	2.223	-2.29 ±0.08	-2.44 ±0.04	X X	-2.52 69	-2.52 69	-2.56 2	-2.52 69	-	-2.40 68	-	X
445	5137.382	0.000 ±0.003	4.178	-0.29 ±0.09	-0.23 ±0.07	✓ X	-0.40 67	-0.43 80	-0.41 2	-0.40 67	-0.49 4	-	-2.53 68	-
446	5143.723	-0.004 ±0.002	2.198	-3.64 ±0.11	-3.79 ±0.06	✓ X	-3.69 71	-3.69 71	-3.99 2	-3.79 67	-	-	-	67
447	5145.094	0.000 ±0.003	2.198	-3.00 ±0.12	-3.17 ±0.05	✓ X	-2.88 69	-	-3.23 2	-2.88 69	-	-	-	-
450	5148.229	-0.002 ±0.003	4.256	-0.33 ±1.34	-0.56 ±0.09	✓ X	-0.24 14	-	-0.27 2	-0.24 14	-	-	-	-
451	5151.911	-0.001 ±0.002	1.011	-3.05 ±0.10	-3.30 ±0.04	X X	-3.32 78	-3.32 78	-3.32 2	-3.32 67	-	-3.20 68	-	X
456	5159.058	-0.004 ±0.004	4.283	-0.77 ±0.07	-0.76 ±0.05	✓	-0.82 67	-	-0.82 2	-0.82 67	-	-	-	-
460	5196.059	-0.001 ±0.002	4.256	-0.77 ±0.03	-0.82 ±0.05	✓ X	-0.49 14	-	-0.49 2	-0.49 14	-	-	-	-
462	5197.936	-0.003 ±0.003	4.301	-1.43 ±0.03	-1.44 ±0.03	✓	-1.54 71	-1.62 71	-1.64 2	-1.64 67	-	-	-	-
466	5217.919	-0.016 ±0.003	3.640	-1.80 ±0.06	-1.89 ±0.05	X X	-1.72 69	-1.72 69	-2.10 2	-1.72 69	-	-1.99 68	-	X
469	5221.036	-0.003 ±0.003	4.294	-1.72 ±0.04	-1.82 ±0.02	X X	-1.58 14	-	-	-	-	-	-	X
471	5222.395	0.001 ±0.003	2.279	-3.66 ±0.04	-3.80 ±0.03	X X	-3.83 14	-	-3.98 2	-	-	-	-	X
472	5223.183	-0.001 ±0.002	3.635	-2.20 ±0.03	-2.21 ±0.03	✓	-1.78 69	-1.78 69	-2.39 2	-1.78 69	-	-2.34 68	-	-
474	5225.526	-0.001 ±0.002	0.110	-4.64 ±0.10	-4.68 ±0.09	✓ ✓	-4.79 70	-4.79 70	-4.79 2	-4.79 67	-	-	-	-
475	5228.376	-0.003 ±0.003	4.220	-1.00 ±0.04	-1.04 ±0.04	✓ ✓	-1.19 71	-1.26 71	-1.29 2	-1.29 67	-	-	-	-
477	5236.202	-0.006 ±0.002	4.186	-1.58 ±0.04	-1.63 ±0.04	✓ X	-1.50 69	-	-1.73 2	-	-	-2.80 68	-	-
484	5242.491	-0.001 ±0.002	3.634	-0.96 ±0.06	-0.93 ±0.04	✓	-0.97 69	-0.97 69	-0.96 2	-0.97 69	-0.91 4	-1.12 68	-	2, 4, 69
486	5243.776	-0.004 ±0.002	4.256	-0.99 ±0.05	-1.01 ±0.04	✓	-1.05 71	-1.12 71	-1.15 2	-1.15 68	-	-1.83 68	-	-
488	5247.050	-0.001 ±0.002	0.087	-4.88 ±0.06	-4.90 ±0.07	✓	-4.95 70	-4.95 70	-4.95 2	-4.95 67	-	-	-	71
492	5249.105	-0.014 ±0.002	4.473	-1.20 ±0.07	-1.32 ±0.02	X	-1.38 71	-1.46 71	-1.59 2	-1.48 67	-	-2.13 68	-	X
493	5250.209	-0.001 ±0.002	0.121	-4.77 ±0.09	-4.76 ±0.10	✓	-4.93 70	-4.94 70	-4.94 2	-4.94 67	-	-	-	-
494	5250.646	-0.001 ±0.002	2.198	-2.05 ±0.05	-2.05 ±0.02	✓	-2.18 69	-2.18 69	-2.05 2	-2.18 69	-	-1.91 68	-	-

Table F.1. $\langle\mathcal{O}^A\rangle$ Quality-assessable (A^I) Analysis-independent line $a)$ Paper 1 input list $b)$ NIST $c)$ SpectroWeb $d)$ VALD3 $e)$ CHIANTI $f)$ TIPbase $g)$ TOPbase

#	Wavelength (Å) Input	E_{low} (eV) $\Delta\lambda_{grid}$	$\log(gf)$ cog grid	$\log(gf)$ this work grid	Flags QA? AI?	a)	b)	c)	d)	e)	f)	g)	h)	Recommended literature
495	5253.021	-0.001 ±0.002	2.279	-3.79 ±0.03	-3.80 ±0.03	✓	✓	-3.84 71	-	-3.94 2	-	-	-	-
498	5262.881	0.000 ±0.003	3.252	-2.75 ±0.07	-2.89 ±0.04	X	X	-2.56 71	-	-3.17 2	-	-3.78 68	X	
501	5267.269	-0.001 ±0.002	4.371	-1.45 ±0.11	-1.62 ±0.04	X	X	-1.60 77	-1.77 2	-1.60 77	-	-	X	
503	5272.268	-0.006 ±0.009	5.033	-1.06 ±0.05	-1.21 ±0.03	X	X	-1.04 14	-	-	-	-	-	
506	5277.306	0.002 ±0.005	4.415	-2.12 ±0.03	-2.18 ±0.03	✓	X	-1.05 14	-	-3.50 2	-1.05 14	-	-	
507	5279.650	0.003 ±0.008	3.301	-3.41 ±0.03	-3.50 ±0.06	✓	X	-3.34 71	-	-3.50 2	-3.44 67	-	2.67	
510	5284.609	-0.003 ±0.003	4.186	-1.82 ±0.19	-1.83 ±0.03	✓	✓	-2.01 71	-	-2.11 2	-	-3.54 68	-	
511	5285.127	-0.001 ±0.002	4.435	-1.44 ±0.04	-1.50 ±0.03	✓	X	-1.66 72	-1.62 71	-1.64 2	-1.64 67	-2.13 68	-	
513	5288.525	0.003 ±0.003	3.695	-1.53 ±0.05	-1.60 ±0.03	✓	X	-1.49 76	-	-1.75 2	-	-2.25 68	-	
515	5292.597	-0.019 ±0.002	4.991	-0.83 ±0.03	-0.86 ±0.02	✓	✓	-0.59 14	-	-0.59 2	-	-	-	
516	5294.547	-0.003 ±0.003	3.640	-2.58 ±0.02	-2.62 ±0.03	✓	✓	-2.76 71	-2.81 71	-2.86 2	-2.86 67	-	-	
517	5295.312	-0.003 ±0.003	4.415	-1.49 ±0.04	-1.49 ±0.03	✓	✓	-1.59 71	-1.67 71	-1.69 2	-1.69 67	-	-	
521	5300.403	-0.007 ±0.005	4.593	-2.19 ±0.03	-2.38 ±0.05	X	X	-1.65 71	-	-4.15 2	-1.75 67	X	-	
525	5308.679	-0.006 ±0.003	4.256	-2.30 ±0.05	-2.36 ±0.02	✓	X	-1.99 14	-	-2.50 2	-2.50 67	-	-	
527	5310.463	0.004 ±0.005	5.086	-1.63 ±0.07	-1.70 ±0.06	✓	X	-1.69 14	-	-	-	-	14	
532	5315.070	-0.011 ±0.005	4.371	-1.40 ±0.04	-1.46 ±0.02	✓	X	-1.65 71	-	-1.55 2	-1.55 67	-	-	
533	5315.775	0.004 ±0.005	3.640	-3.03 ±0.04	-3.11 ±0.02	X	X	-2.84 14	-	-3.90 2	-	X	X	
535	5319.035	-0.014 ±0.007	4.835	-1.75 ±0.02	-1.85 ±0.06	X	X	-1.82 14	-	-	-1.81 14	X	X	
536	5320.036	0.011 ±0.013	3.642	-2.44 ±0.03	-2.48 ±0.07	✓	✓	-2.44 71	-	-2.54 2	-	2.71	-	
537	5321.108	-0.001 ±0.002	4.435	-1.22 ±0.03	-1.23 ±0.03	✓	✓	-1.09 69	-1.09 69	-1.44 2	-0.95 69	-	-	
538	5322.041	0.000 ±0.003	2.279	-2.85 ±0.04	-2.90 ±0.05	✓	X	-2.80 69	-	-3.04 2	-	-	-	
540	5326.142	0.000 ±0.003	3.573	-2.11 ±0.04	-2.20 ±0.06	✓	X	-2.07 77	-2.07 77	-2.30 2	-2.07 77	-	-	
541	5326.790	0.021 ±0.002	4.415	-1.77 ±0.15	-1.95 ±0.04	✓	X	-1.32 14	-	-2.10 2	-2.10 67	-	-	
544	5329.989	-0.002 ±0.003	4.076	-1.15 ±0.04	-1.22 ±0.04	✓	X	-1.20 81	-	-1.29 2	-1.19 77	77.81	-	
545	5332.900	-0.001 ±0.002	1.557	-2.81 ±0.05	-2.79 ±0.03	✓	✓	-2.78 69	-2.78 69	-2.94 2	-2.78 69	-2.95 68	69	
547	5339.929	0.000 ±0.001	3.266	-0.72 ±0.04	-0.65 ±0.02	X	X	-0.63 73	-	-0.68 2	-	-0.53 4	X	
553	5373.709	-0.003 ±0.003	4.473	-0.77 ±0.03	-0.76 ±0.05	✓	✓	-0.71 72	-0.84 71	-0.86 2	-0.86 67	-	-3.93 68	
554	5379.574	-0.002 ±0.003	3.695	-1.47 ±0.05	-1.48 ±0.04	✓	✓	-1.51 69	-	-1.52 2	-	-1.38 68	2.69	
556	5385.575	0.006 ±0.004	3.695	-3.01 ±0.03	-3.07 ±0.03	X	X	-2.87 71	-	-3.20 2	-	-	-	
557	5386.333	-0.004 ±0.002	4.154	-1.67 ±0.03	-1.67 ±0.03	✓	✓	-1.67 71	-	-1.77 2	-	-1.42 68	71	
559	5395.217	-0.001 ±0.002	4.446	-1.63 ±0.04	-1.67 ±0.02	✓	✓	-2.07 71	-2.15 71	-2.17 67	-	-1.88 68	-	
560	5398.279	0.000 ±0.003	4.446	-0.62 ±0.05	-0.63 ±0.05	✓	✓	-0.63 71	-0.71 71	-0.67 2	-	-	2.71	
562	5401.266	-0.003 ±0.003	4.320	-1.63 ±0.04	-1.70 ±0.03	X	X	-1.82 71	-1.89 71	-1.92 2	-1.92 67	-	-	
564	5406.775	-0.001 ±0.002	4.371	-1.35 ±0.04	-1.40 ±0.03	X	X	-1.62 71	-	-1.52 2	-1.72 67	-	-	
565	5409.133	-0.002 ±0.003	4.371	-0.98 ±0.03	-1.08 ±0.03	X	X	-1.20 71	-1.27 71	-1.12 2	-1.30 67	X	-	
566	5410.910	-0.001 ±0.002	4.473	0.13 ±0.07	0.23 ±0.04	✓	X	0.40 69	0.40 69	0.28 2	0.40 69	0.40 4	-	
567	5412.784	-0.006 ±0.002	4.435	-1.68 ±0.03	-1.77 ±0.05	X	X	-1.72 77	-1.72 77	-1.88 2	-1.72 77	-	X	
569	5417.033	0.000 ±0.001	4.415	-1.38 ±0.03	-1.43 ±0.03	✓	X	-1.58 71	-	-1.68 2	-1.68 67	-	-	

Table F1. ^(*a*) Quality-assessable (*AI*) Analysis-independent line ^(*b*) NIST ^(*c*) Paper 1 input list ^(*d*) VALD3 ^(*e*) SpectroWeb ^(*f*) CHIANTI ^(*g*) TIPbase ^(*h*) TOPbase

#	Wavelength (Å) Input	E_{low} (eV) $\Delta\lambda_{grid}$	$\log(gf)$ cog	$\log(gf)$ this work grid	Flags QA? AI?	a)	b)	c)	d)	e)	f)	g)	h)	Recommended literature
572	5421.850	-0.014 ±0.004	4.549	-1.75 ±0.05	-1.87 ±0.07	✓ X	-1.68 71	-	-2.08 2	-1.78 67	-	-	-	-
574	5432.948	-0.011 ±0.002	4.446	-0.65 ±0.09	-0.82 ±0.06	✗ X	-0.94 71	-1.02 71	-1.04 2	-	-	-2.43 68	-	X
576	5436.295	-0.001 ±0.002	4.387	-1.27 ±0.03	-1.30 ±0.03	✓ ✓	-1.44 71	-1.51 71	-1.54 2	-1.54 67	-	-	-	-
577	5436.588	-0.004 ±0.002	2.279	-3.20 ±0.05	-3.27 ±0.04	✗ X	-2.96 69	-	-3.39 2	-	-	-	-	-
578	5441.339	-0.002 ±0.003	4.313	-1.52 ±0.03	-1.58 ±0.03	✗ X	-1.63 71	-	-1.73 2	-	-	-	-	-
581	5461.550	-0.005 ±0.001	4.446	-1.51 ±0.04	-1.56 ±0.03	✗ X	-1.80 71	-1.88 71	-1.80 2	-1.90 67	-	-	-	-
583	5462.960	-0.005 ±0.001	4.473	-0.29 ±0.10	-0.29 ±0.08	✓ ✓	-0.05 14	-	-0.16 2	-0.13 14	-	-	-	-
584	5464.280	-0.004 ±0.002	4.143	-1.55 ±0.04	-1.57 ±0.03	✓ ✓	-1.40 69	-1.40 69	-1.72 2	-1.40 69	-	-	-	-
585	5466.396	-0.004 ±0.002	4.371	-0.58 ±0.05	-0.57 ±0.04	✓ ✓	-0.63 67	-	-0.63 2	-	-	-	-	-
587	5473.163	0.001 ±0.003	4.191	-1.94 ±0.02	-2.00 ±0.03	✗ X	-2.04 71	-	-2.14 2	-	-	-1.63 68	-	X
589	5473.900	-0.005 ±0.001	4.154	-0.72 ±0.05	-0.71 ±0.02	✓ ✓	-0.72 72	-	-0.76 2	-	-0.75 4	-	-	-
591	5483.099	-0.004 ±0.002	4.154	-1.37 ±0.04	-1.38 ±0.03	✓ ✓	-1.39 73	-	-1.57 2	-	-	-	-	73
592	5487.145	-0.009 ±0.002	4.415	-1.31 ±0.02	-1.39 ±0.03	✗ X	-1.43 71	-1.51 71	-1.53 2	-	-	-2.27 68	-	X
593	5487.745	-0.004 ±0.002	4.320	-0.48 ±0.11	-1.05 ±0.09	✗ X	-0.32 14	-	-0.36 2	-0.32 14	-	-1.35 68	-	X
597	5491.832	-0.004 ±0.002	4.186	-2.16 ±0.03	-2.20 ±0.03	✓ ✓	-2.19 77	-2.19 77	-2.38 2	-2.19 77	-	-5.06 68	-	77
599	5493.499	0.014 ±0.010	4.103	-1.54 ±0.02	-1.73 ±0.06	✗ X	-1.48 72	-	-1.84 2	-	-	-	-	X
600	5494.463	-0.001 ±0.002	4.076	-1.84 ±0.02	-1.89 ±0.03	✓ X	-1.99 71	-	-2.10 2	-2.09 67	-	-	-	-
602	5497.516	0.004 ±0.004	1.011	-2.67 ±0.09	-2.95 ±0.08	✗ X	-2.84 78	-2.85 78	-2.85 2	-2.85 67	-	-2.86 68	-	X
605	5512.257	-0.012 ±0.004	4.371	-1.15 ±0.08	-1.37 ±0.04	✗ X	-1.32 71	-1.39 71	-1.42 2	-	-	-2.26 68	-	X
608	5516.482	-0.001 ±0.004	3.547	-3.20 ±0.08	-3.32 ±0.05	✓ X	-3.04 14	-	-3.40 2	-	-	-	-	-
609	5517.065	-0.002 ±0.003	4.209	-1.96 ±0.02	-1.99 ±0.03	✓ ✓	-2.27 71	-	-2.16 2	-	-	-	-	-
611	5521.280	0.016 ±0.007	4.435	-2.14 ±0.04	-2.40 ±0.08	✗ X	-0.81 14	-	-2.39 2	-2.39 67	-	-	-	X
612	5522.446	-0.004 ±0.002	4.209	-1.39 ±0.03	-1.41 ±0.03	✓ ✓	-1.45 71	-	-1.56 2	-	-	-	-	-
613	5523.980	-0.008 ±0.004	4.559	-1.88 ±0.04	-2.29 ±0.07	✗ X	-1.35 14	-	-	-	-	-2.86 68	-	X
616	5535.418	0.026 ±0.010	4.186	-0.47 ±0.20	-0.69 ±0.08	✗ X	-1.16 69	-1.16 69	-1.15 2	-1.16 69	-	-1.49 68	-	-
617	5538.516	-0.005 ±0.001	4.218	-1.49 ±0.03	-1.52 ±0.03	✓ ✓	-1.54 72	-	-1.67 2	-	-	-2.22 68	-	72
618	5539.280	-0.002 ±0.003	3.642	-2.49 ±0.03	-2.57 ±0.03	✗ X	-2.56 71	-	-2.66 2	-	-	-	-	X
619	5543.147	0.035 ±0.001	3.695	-1.40 ±0.05	-1.50 ±0.03	✗ X	-1.47 71	-	-1.57 2	-	-	-	-	X
620	5543.936	-0.004 ±0.002	4.218	-1.02 ±0.04	-1.04 ±0.03	✓ ✓	-1.04 71	-	-0.92 2	-	-	71	-	-
622	5546.506	-0.001 ±0.002	4.371	-1.08 ±0.03	-1.09 ±0.03	✓ ✓	-1.21 71	-1.28 71	-1.31 2	-1.31 67	-	-	-	-
623	5549.949	-0.005 ±0.003	3.695	-2.73 ±0.03	-2.78 ±0.03	✗ X	-2.81 71	-	-3.01 2	-	-	-	-	71
624	5552.692	-0.006 ±0.002	4.956	-1.69 ±0.03	-1.72 ±0.03	✓ ✓	-1.89 71	-	-1.99 2	-	-	-	-	-
625	5559.893	-0.017 ±0.009	4.638	-2.17 ±0.06	-2.46 ±0.11	✗ X	-1.66 14	-	-	-	-	-	-	X
626	5560.212	-0.005 ±0.001	4.435	-1.04 ±0.05	-1.02 ±0.03	✓ ✓	-1.09 71	-1.16 71	-1.19 2	-1.19 67	-	-	-	-
627	5561.243	-0.005 ±0.005	4.607	-1.87 ±0.02	-1.95 ±0.02	✗ X	-1.21 14	-	-	-	-	-	-	X
628	5562.706	-0.001 ±0.002	4.435	-0.87 ±0.06	-0.91 ±0.06	✓ ✓	-0.64 14	-	-0.96 2	-0.64 14	-	2	-	-
629	5577.025	-0.005 ±0.001	5.033	-1.41 ±0.03	-1.44 ±0.03	✓ ✓	-1.54 14	-	-1.55 2	-	-	-	-	-
632	5584.765	0.003 ±0.003	3.573	-2.07 ±0.05	-2.21 ±0.03	✗ X	-2.22 71	-2.27 71	-2.33 2	-2.32 67	-	-	-	X

Table F.1. ^(*a*) Quality-assessable (*AI*) Analysis-independent line ^(*a*) Paper 1 input list ^(*b*) NIST ^(*c*) Paper 1 input list ^(*d*) VALD3 ^(*e*) SpectroWeb ^(*f*) CHIANTI ^(*g*) TIPbase ^(*h*) TOPbase

#	Wavelength (Å) Input	E_{low} (eV) $\Delta\lambda_{grid}$	$\log(gf)$ cog	$\log(gf)$ this work grid	Flags QA? AI?	a)	b)	c)	d)	e)	f)	g)	h)	Recommended literature
633	5587.574	-0.001 ±0.002	4.143	-1.54 ±0.02	-1.64 ±0.04	X	X	-1.75 71	-	-1.84 2	-	-	-	X
637	5592.645	-0.004 ±0.003	4.294	-2.41 ±0.05	-2.50 ±0.05	✓	X	-2.0 14	-	-2.74 2	-	-	-	-
640	5608.972	-0.002 ±0.003	4.209	-2.19 ±0.03	-2.30 ±0.03	✓	X	-1.49 14	-	-2.58 2	-	-	-	X
641	5611.672	-0.025 ±0.005	5.070	-1.90 ±0.07	-2.02 ±0.05	✓	X	-1.11 14	-	-2.79 2	-	-	-	-
643	5618.632	-0.003 ±0.003	4.209	-1.25 ±0.03	-1.25 ±0.02	✓	✓	-1.25 73	-	-1.28 2	-	-	-	73
644	5619.225	0.008 ±0.008	3.695	-3.02 ±0.02	-3.12 ±0.01	X	X	-2.64 14	-	-3.34 2	-	-	-	X
645	5619.595	-0.003 ±0.003	4.387	-1.39 ±0.03	-1.46 ±0.02	X	X	-1.60 71	-1.67 71	-1.70 2	-1.70 67	-	-	X
646	5620.027	-0.001 ±0.006	4.143	-2.44 ±0.04	-2.49 ±0.03	✓	X	-2.31 14	-	-2.72 2	-	-	-	-
648	5624.022	-0.003 ±0.003	4.387	-1.07 ±0.03	-1.13 ±0.03	✓	X	-1.38 71	-1.45 71	-1.48 2	-1.48 67	-	-	-
649	5624.542	0.000 ±0.001	3.417	-0.77 ±0.04	-0.74 ±0.03	✓	✓	-0.77 82	-	-0.79 2	-	-0.83 4	-	82
654	5633.946	-0.005 ±0.001	4.991	-0.18 ±0.03	-0.22 ±0.02	✓	✓	-0.23 71	-	-0.27 2	-	-	-	71
655	5635.822	-0.005 ±0.001	4.256	-1.53 ±0.03	-1.54 ±0.03	✓	✓	-1.79 71	-	-1.69 2	-	-	-	-
656	5636.696	-0.004 ±0.002	3.640	-2.47 ±0.04	-2.47 ±0.03	✓	✓	-2.51 71	-	-2.67 2	-	-	-	-3.23 68
657	5638.262	-0.004 ±0.002	4.220	-0.74 ±0.04	-0.78 ±0.03	✓	✓	-0.72 72	-	-0.82 2	-	-	-	-
658	5640.307	-0.018 ±0.007	4.638	-1.49 ±0.07	-1.57 ±0.05	✓	X	-1.37 14	-	-	-	-	-	-
660	5641.434	-0.001 ±0.002	4.256	-0.92 ±0.05	-1.00 ±0.03	✓	X	-1.08 71	-	-1.18 2	-	-	-	-
663	5642.751	-0.004 ±0.002	4.608	-1.83 ±0.03	-1.91 ±0.03	X	X	-2.02 71	-2.10 71	-2.18 2	-2.12 67	-	-	X
666	5645.833	-0.007 ±0.004	4.607	-1.75 ±0.02	-1.83 ±0.03	X	X	-0.96 14	-	-	-	-	-	X
670	5649.987	-0.005 ±0.001	5.100	-0.70 ±0.03	-0.72 ±0.02	✓	✓	-0.82 71	-	-0.63 2	-	-	-	-
671	5650.705	-0.022 ±0.003	5.086	-0.70 ±0.04	-0.73 ±0.03	✓	✓	-0.86 71	-	-0.91 2	-	-	-	-
672	5651.469	-0.004 ±0.002	4.473	-1.71 ±0.02	-1.72 ±0.02	✓	✓	-1.90 71	-	-1.95 2	-2.00 67	-	-	X
673	5652.318	-0.005 ±0.001	4.260	-1.71 ±0.02	-1.72 ±0.02	✓	✓	-1.85 71	-	-1.90 2	-	-	-	-
674	5653.865	-0.001 ±0.002	4.387	-1.33 ±0.03	-1.33 ±0.02	✓	✓	-1.54 71	-1.61 71	-1.64 2	-1.64 67	-	-	-
676	5655.176	-0.005 ±0.001	5.064	-0.47 ±0.06	-0.47 ±0.03	✓	✓	-0.60 71	-	-0.65 2	-	-	-	-
678	5661.021	-0.010 ±0.009	4.580	-2.25 ±0.03	-2.34 ±0.04	X	X	-1.96 14	-	-2.53 2	-2.43 67	-	-	X
679	5661.345	-0.004 ±0.002	4.284	-1.78 ±0.02	-1.81 ±0.02	✓	✓	-1.76 77	-	-2.04 2	-	-	-	-
681	5662.516	-0.003 ±0.003	4.178	-0.71 ±0.09	-0.66 ±0.08	✓	X	-0.45 73	-	-0.54 2	-	-	-	-
688	5677.684	-0.001 ±0.004	4.103	-2.56 ±0.03	-2.57 ±0.04	✓	✓	-2.34 14	-	-2.83 2	-	-	-	-
689	5679.023	-0.005 ±0.001	4.652	-0.71 ±0.04	-0.72 ±0.02	✓	✓	-0.82 71	-	-0.93 2	-0.92 67	-	-	-
694	5686.120	0.055 ±0.001	3.635	-2.26 ±0.09	-2.44 ±0.12	✓	X	-2.93 14	-	-2.75 2	-	-	-	-4.02 68
695	5686.530	-0.006 ±0.002	4.549	-0.60 ±0.09	-0.54 ±0.06	✓	X	-0.44 69	-0.45 69	-0.66 2	-0.45 69	-	-	-
698	5691.497	-0.005 ±0.001	4.301	-1.36 ±0.04	-1.39 ±0.03	✓	✓	-1.45 73	-	-1.54 2	-	-	-	-
701	5696.089	-0.001 ±0.002	4.549	-1.81 ±0.04	-1.82 ±0.02	✓	✓	-1.72 77	-1.72 77	-2.17 2	-1.72 77	-	-	-
702	5698.020	-0.011 ±0.007	3.640	-2.57 ±0.04	-2.64 ±0.04	✓	X	-2.58 71	-	-2.84 2	-	-	-	-3.54 68
703	5699.409	-0.014 ±0.016	4.956	-1.80 ±0.04	-1.88 ±0.06	✓	X	-2.06 14	-	-2.06 14	-	-	-	-
705	5701.544	0.002 ±0.003	2.559	-2.13 ±0.03	-2.20 ±0.03	X	X	-2.19 83	-	-2.37 2	-	-	-	-2.65 68
707	5704.733	-0.005 ±0.001	5.033	-1.16 ±0.03	-1.15 ±0.02	✓	X	-1.41 14	-	-	-	-	-	-
708	5705.464	-0.003 ±0.003	4.301	-1.40 ±0.02	-1.41 ±0.02	✓	✓	-1.36 77	-	-1.58 2	-	-	-	-
709	5705.992	0.016 ±0.004	4.608	-0.14 ±0.10	-0.29 ±0.06	X	X	-0.46 72	-	-0.77 2	-	-	-	-

Table F1. $\langle Q_A \rangle$ Quality-assessable (A^I) Analysis-independent line $^{(a)}$ Paper 1 input list $^{(b)}$ NIST $^{(c)}$ VALD3 $^{(d)}$ SpectroWeb $^{(e)}$ CHIANTI $^{(g)}$ TIPbase $^{(h)}$ TOPbase

#	Wavelength (Å) Input	E_{low} (eV) $\Delta\lambda_{grid}$	$\log(gf)$ cog	$\log(gf)$ this work grid	Flags QA? AI?	a)	b)	c)	d)	e)	f)	g)	h)	Recommended literature
710	5708.094	-0.001 ±0.002	4.435	-1.17 ±0.07	-1.33 ±0.02	X	X	-1.47 71	-1.54 71	-1.59 2	-1.57 67	-	-	X
712	5709.378	0.001 ±0.003	3.368	-1.89 ±1.07	-1.36 ±0.01	X	X	-1.02 82	-	-1.09 2	-	-	-	-
713	5712.131	-0.003 ±0.003	3.417	-1.95 ±0.03	-2.00 ±0.03	X	X	-1.98 82	-	-2.05 2	-	-	-	82
716	5714.551	-0.009 ±0.002	5.086	-1.65 ±0.02	-1.69 ±0.03	X	X	-1.71 14	-	-	-	-	-	14
718	5717.833	-0.005 ±0.001	4.284	-0.97 ±0.05	-0.97 ±0.02	X	X	-0.99 72	-	-1.18 2	-	-	-	72
720	5721.707	-0.005 ±0.004	4.154	-2.59 ±0.04	-2.70 ±0.04	X	X	-2.53 14	-	-3.05 2	-	-	-	X
724	5730.854	-0.006 ±0.003	4.913	-1.74 ±0.03	-1.78 ±0.02	X	X	-1.45 14	-	-	-	-	-	-
725	5731.762	-0.005 ±0.001	4.256	-1.08 ±0.03	-1.08 ±0.02	X	X	-1.20 71	-	-1.17 2	-	-	-	-
726	5732.296	-0.001 ±0.004	4.991	-1.32 ±0.01	-1.37 ±0.02	X	X	-1.46 71	-	-1.59 2	-	-	-	X
728	5734.564	-0.006 ±0.004	4.956	-1.73 ±0.01	-1.77 ±0.02	X	X	-1.57 14	-	-	-	-	-	X
731	5741.848	-0.004 ±0.002	4.256	-1.59 ±0.03	-1.60 ±0.02	X	X	-1.67 69	-	-1.67 2	-	-	-	-
732	5742.960	0.001 ±0.005	4.178	-2.22 ±0.02	-2.24 ±0.02	X	X	-2.41 71	-	-3.75 2	-2.51 67	-	-	-
734	5743.933	-0.017 ±0.005	5.067	-1.83 ±0.08	-1.93 ±0.06	X	X	-1.25 14	-	-	-	-	-	-
736	5747.954	-0.011 ±0.002	4.608	-1.12 ±0.05	-1.25 ±0.01	X	X	-1.33 71	-1.41 71	-1.50 2	-1.43 67	-	-	X
738	5750.030	0.018 ±0.006	5.010	-2.08 ±0.13	-2.12 ±0.08	X	X	-2.25 14	-	-2.27 14	-	-	-	-
739	5752.032	-0.004 ±0.002	4.549	-0.92 ±0.06	-0.89 ±0.04	X	X	-1.18 14	-	-1.07 2	-1.17 14	-	-	-
740	5753.122	-0.003 ±0.003	4.260	-0.70 ±0.05	-0.67 ±0.03	X	X	-0.62 73	-	-0.69 2	-	-	-	2
743	5755.347	-0.009 ±0.011	3.640	-3.50 ±0.16	-3.51 ±0.10	X	X	-2.76 14	-	-3.61 2	-	-	-	2
744	5760.344	0.004 ±0.008	3.642	-2.38 ±0.02	-2.41 ±0.03	X	X	-2.39 71	-	-2.54 2	-	-	-	71
746	5762.413	-0.004 ±0.002	3.642	-2.08 ±0.05	-2.25 ±0.03	X	X	-2.18 71	-2.23 71	-2.42 2	-2.28 67	-	-	X
747	5762.992	-0.009 ±0.002	4.209	-0.18 ±0.14	-0.24 ±0.06	X	X	-0.36 72	-	-0.37 2	-	-	-	-
749	5769.323	0.004 ±0.008	4.608	-1.96 ±0.04	-2.01 ±0.03	X	X	-2.26 14	-	-2.28 2	-2.25 14	-	-	-
750	5769.674	-0.015 ±0.007	4.103	-2.93 ±0.07	-3.10 ±0.07	X	X	-2.90 14	-	-3.21 2	-	-0.29 68	-	X
752	5775.081	-0.005 ±0.001	4.220	-1.18 ±0.07	-1.16 ±0.05	X	X	-1.13 73	-	-1.30 2	-	-	-	73
753	5776.224	0.001 ±0.003	3.695	-3.47 ±0.08	-3.48 ±0.07	X	X	-3.37 14	-	-3.69 2	-	-	-	-
754	5778.453	-0.002 ±0.003	2.588	-3.44 ±0.03	-3.44 ±0.03	X	X	-3.43 77	-	-3.43 2	-	-	-	2.77
758	5784.658	-0.001 ±0.002	3.397	-2.52 ±0.02	-2.55 ±0.03	X	X	-2.55 82	-	-2.64 2	-	-	-	82
763	5791.524	-0.001 ±0.003	4.584	-1.91 ±0.01	-1.96 ±0.02	X	X	-1.88 14	-	-2.23 2	-1.89 14	-	-	X
765	5793.915	-0.004 ±0.002	4.220	-1.58 ±0.03	-1.59 ±0.02	X	X	-1.60 71	-	-1.83 2	-	-	-	71
767	5796.431	-0.009 ±0.010	4.607	-2.55 ±0.11	-2.63 ±0.07	X	X	-2.48 14	-	-3.29 2	-	-	-	-
769	5798.171	-0.003 ±0.003	3.929	-1.67 ±0.03	-1.77 ±0.02	X	X	-1.79 71	-1.84 71	-2.02 2	-1.89 67	-	-	X
770	5804.034	-0.001 ±0.002	3.882	-2.08 ±0.03	-2.18 ±0.02	X	X	-2.19 71	-2.24 71	-2.29 2	-2.29 67	-	-	X
773	5806.725	-0.004 ±0.002	4.608	-0.84 ±0.05	-0.88 ±0.03	X	X	-0.95 71	-1.03 71	-1.05 2	-1.05 67	-	-	X
774	5807.783	-0.001 ±0.002	3.292	-3.20 ±0.01	-3.28 ±0.02	X	X	-3.41 67	-	-3.53 2	-	-	-	X
775	5807.975	-0.006 ±0.003	4.608	-2.26 ±0.04	-2.35 ±0.05	X	X	-2.47 67	-	-2.62 2	-	-	-	-
776	5809.217	-0.002 ±0.003	3.884	-1.60 ±0.03	-1.67 ±0.01	X	X	-1.74 71	-1.79 71	-1.95 2	-1.84 67	-	-	X
778	5811.914	-0.002 ±0.003	4.143	-2.30 ±0.04	-2.32 ±0.03	X	X	-2.33 71	-	-2.52 2	-	-	-	71
779	5814.807	-0.005 ±0.001	4.283	-1.77 ±0.03	-1.78 ±0.02	X	X	-1.87 71	-	-1.97 2	-	-	-	-

Table F.1. $\langle\mathcal{O}^A\rangle$ Quality-assessable (A) Analysis-independent line ^{a)} Paper 1 input list ^{b)} NIST ^{c)} SpectroWeb ^{d)} VALD3 ^{e)} CHIANTI ^{f)} TIPbase ^{g)} TOPbase

#	Wavelength (Å) Input	E_{low} (eV) $\Delta\lambda_{grid}$	$\log(gf)$ cog grid	$\log(gf)$ this work grid	Flags QA? AI?	Flags a) b)	Flags c) d)	Flags e) f)	Flags g) h)	Recommended literature
780	5815.626	-0.011 ±0.006	4.956	-1.95 ±0.06	-2.03 ±0.05	✓ X	-1.51 14	-	-	-
781	5821.888	-0.023 ±0.004	4.988	-1.66 ±0.04	-1.75 ±0.03	X X	-1.62 14	-	-	X
782	5827.454	-0.029 ±0.004	4.956	-1.63 ±0.06	-1.76 ±0.05	X X	-1.34 14	-	-	X
783	5827.877	-0.005 ±0.001	3.283	-3.08 ±0.02	-3.10 ±0.02	✓ X	-3.31 71	-3.33 2	-	-
786	5835.100	-0.004 ±0.002	4.256	-2.05 ±0.02	-2.06 ±0.02	✓ X	-2.27 71	-2.36 2	-	-
787	5837.701	-0.001 ±0.002	4.294	-2.17 ±0.03	-2.22 ±0.02	✓ X	-2.24 71	-2.52 2	-	-2.93 68
788	5838.372	-0.006 ±0.002	3.943	-2.18 ±0.02	-2.21 ±0.03	✓ X	-2.24 71	-2.46 2	-2.34 67	-
790	5844.918	0.001 ±0.002	4.154	-2.74 ±0.03	-2.80 ±0.04	✓ X	-3.05 14	-2.94 2	-	-
792	5849.683	-0.002 ±0.003	3.695	-2.89 ±0.04	-2.90 ±0.03	✓ X	-2.89 71	-3.19 2	-	71
793	5851.204	-0.006 ±0.007	4.956	-1.88 ±0.05	-1.94 ±0.05	✓ X	-2.12 14	-	-	-
794	5852.219	-0.005 ±0.001	4.549	-1.14 ±0.03	-1.18 ±0.03	✓ X	-1.23 71	-1.30 71	-1.36 2	-1.33 67
795	5853.148	-0.002 ±0.003	1.485	-5.03 ±0.03	-5.09 ±0.03	✓ X	-5.18 71	-	-5.29 2	-5.28 67
796	5855.076	-0.001 ±0.002	4.608	-1.49 ±0.02	-1.49 ±0.02	✓ X	-1.48 77	-1.48 77	-1.48 2	-1.48 77
797	5856.088	-0.005 ±0.001	4.294	-1.51 ±0.02	-1.52 ±0.02	✓ X	-1.33 69	-	-1.68 2	-
798	5858.778	0.003 ±0.004	4.220	-2.12 ±0.02	-2.20 ±0.03	X X	-2.16 71	-	-2.26 2	-2.26 67
800	5859.586	-0.005 ±0.001	4.549	-0.62 ±0.08	-0.61 ±0.07	✓ X	-0.42 14	-	-0.42 2	-0.42 14
801	5861.109	-0.004 ±0.003	4.283	-2.28 ±0.03	-2.32 ±0.02	✓ X	-2.30 14	-	-2.45 2	-
802	5864.244	0.001 ±0.003	4.301	-2.32 ±0.05	-2.39 ±0.03	✓ X	-2.52 67	-	-2.52 2	-
805	5871.304	-0.015 ±0.014	4.154	-2.68 ±0.03	-2.74 ±0.06	✓ X	-2.67 14	-	-2.99 2	-
806	5873.212	-0.015 ±0.003	4.256	-1.87 ±0.03	-1.94 ±0.02	X X	-2.04 71	-	-2.14 2	-
807	5876.276	-0.007 ±0.013	4.301	-2.31 ±0.07	-2.37 ±0.05	✓ X	-2.65 67	-	-3.11 2	-
808	5877.788	-0.004 ±0.002	4.178	-2.05 ±0.03	-2.10 ±0.03	✓ X	-2.13 71	-	-2.39 2	-2.23 67
809	5879.487	0.004 ±0.008	4.607	-1.79 ±0.07	-1.85 ±0.04	✓ X	-2.04 71	-2.12 71	-2.12 2	-2.14 67
810	5880.027	-0.001 ±0.004	4.559	-1.82 ±0.04	-1.86 ±0.03	✓ X	-1.84 71	-	-2.13 2	-
812	5883.816	-0.001 ±0.002	3.960	-1.19 ±0.08	-1.18 ±0.04	✓ X	-1.26 71	-1.31 71	-1.36 2	-1.36 67
813	5885.054	-0.005 ±0.006	4.988	-1.75 ±0.06	-1.84 ±0.07	✓ X	-1.46 14	-	-1.48 14	-
815	5902.473	-0.003 ±0.003	4.593	-1.73 ±0.03	-1.77 ±0.03	✓ X	-1.71 71	-	-1.98 2	-1.81 67
817	5905.671	-0.004 ±0.002	4.652	-0.74 ±0.04	-0.73 ±0.02	✓ X	-0.69 71	-0.77 71	-0.92 2	-0.73 67
818	5916.247	-0.002 ±0.003	2.453	-2.85 ±0.03	-2.87 ±0.04	✓ X	-2.99 74	-2.99 74	-2.99 2	-2.99 67
820	5927.789	0.001 ±0.004	4.652	-1.03 ±0.04	-1.09 ±0.03	✓ X	-0.99 71	-1.07 71	-1.21 2	-1.09 67
822	5929.676	-0.004 ±0.002	4.549	-1.15 ±0.03	-1.17 ±0.02	✓ X	-1.31 71	-1.38 71	-1.41 2	-
823	5930.180	-0.001 ±0.002	4.652	-0.25 ±0.07	-0.21 ±0.04	✓ X	-0.23 67	-	-0.23 2	-0.23 67
824	5934.654	-0.002 ±0.003	3.929	-1.11 ±0.04	-1.10 ±0.02	✓ X	-1.07 71	-1.12 71	-1.19 2	-1.17 67
826	5940.991	-0.004 ±0.022	4.178	-1.93 ±0.05	-1.86 ±0.08	✓ X	-2.05 71	-	-2.19 2	-
828	5943.578	0.000 ±0.005	2.198	-4.18 ±0.04	-4.26 ±0.02	X X	-4.18 14	-	-4.52 2	-4.19 14
831	5952.718	-0.004 ±0.002	3.984	-1.34 ±0.04	-1.35 ±0.02	✓ X	-1.34 71	-1.39 71	-1.44 2	-1.44 67
833	5956.694	-0.004 ±0.002	0.859	-4.53 ±0.05	-4.54 ±0.05	✓ X	-4.60 84	-4.61 85	-4.61 2	-4.61 67
834	5958.333	-0.033 ±0.013	2.176	-3.81 ±0.19	-4.05 ±0.05	✓ X	-4.16 14	-	-4.49 2	-4.18 14

Table F.1. ^(*a*) Quality-assessable (*AI*) Analysis-independent line ^(*a*) Paper 1 input list ^(*b*) NIST ^(*c*) Paper 1 input list ^(*d*) VALD3 ^(*e*) SpectroWeb ^(*f*) CHIANTI ^(*g*) TIPbase ^(*h*) TOPbase

#	Wavelength (Å) Input	E_{low} (eV) $\Delta\lambda_{grid}$	$\log(gf)$ cog grid	$\log(gf)$ this work grid	Flags QA? AI?	a)	b)	c)	d)	e)	f)	g)	h)	Recommended literature
835	5959.915	-0.015 ±0.022	4.143	-2.80 ±0.11	-2.78 ±0.10	✓	✓	-2.49 14	--	-3.05 2	-2.50 14	--	--	-
836	5963.239	-0.012 ±0.006	2.223	-4.69 ±0.04	-4.76 ±0.04	✓	✓	-4.59 14	--	-4.86 2	-4.59 14	--	--	-
838	5976.439	0.022 ±0.009	4.178	-2.21 ±0.07	-2.38 ±0.09	✓	✓	-2.33 14	--	-2.75 2	--	-0.48 68	--	X
839	5976.777	-0.004 ±0.002	3.943	-1.24 ±0.06	-1.22 ±0.04	✓	✓	-1.24 14	--	-1.31 2	-1.24 14	--	--	14
841	5982.310	-0.016 ±0.004	4.913	-2.04 ±0.05	-2.11 ±0.06	✓	✓	-1.47 14	--	-	-	--	--	-
842	5983.680	-0.003 ±0.003	4.549	-0.68 ±0.06	-0.65 ±0.04	✓	✓	-1.47 14	--	-0.78 2	--	--	--	-
843	5984.815	-0.001 ±0.002	4.733	-0.32 ±0.07	-0.29 ±0.04	✓	✓	-0.20 14	--	-0.34 2	-0.20 14	--	--	-
844	5987.065	-0.004 ±0.002	4.796	-0.48 ±0.05	-0.46 ±0.04	✓	✓	-0.43 14	--	-0.56 2	-0.43 14	--	--	14
847	5999.171	0.033 ±0.003	4.220	-2.40 ±0.06	-2.47 ±0.05	✓	✓	-2.25 14	--	-	-	--	--	-
848	6003.011	-0.001 ±0.002	3.882	-1.03 ±0.03	-1.01 ±0.02	✓	✓	-1.10 72	--	-1.15 2	-1.12 67	--	--	-
850	6007.960	-0.003 ±0.003	4.652	-0.72 ±0.06	-0.71 ±0.03	✓	✓	-0.60 14	--	-0.97 2	-0.60 14	--	--	-
851	6008.556	-0.001 ±0.002	3.884	-1.00 ±0.04	-0.97 ±0.03	✓	✓	-0.98 72	--	-1.08 2	-0.98 14	--	--	14, 72
852	6020.169	-0.039 ±0.015	4.608	-0.21 ±0.10	0.03 ±0.01	✓	✓	-0.27 67	--	-0.28 2	-0.27 67	--	--	X
855	6027.051	-0.004 ±0.002	4.076	-1.20 ±0.09	-1.18 ±0.07	✓	✓	-1.09 69	-1.09 69	-1.23 2	-1.09 69	--	--	2
856	6034.035	-0.005 ±0.003	4.313	-2.24 ±0.03	-2.28 ±0.02	✓	✓	-2.31 14	--	-2.48 2	--	--	--	-
857	6035.337	-0.004 ±0.002	4.294	-2.40 ±0.03	-2.44 ±0.03	✓	✓	-2.40 14	--	-3.02 2	--	--	--	-
860	6055.402	0.003 ±0.006	4.956	-2.00 ±0.04	-2.16 ±0.06	✓	✓	-1.52 14	--	-	-	--	--	X
861	6056.005	-0.005 ±0.001	4.733	-0.43 ±0.06	-0.41 ±0.04	✓	✓	-0.32 72	--	-0.33 2	-0.46 67	--	-0.20 68	-
862	6057.253	-0.010 ±0.006	4.991	-1.67 ±0.05	-1.79 ±0.04	✓	✓	-1.28 14	--	-	-	--	--	X
865	6078.491	-0.004 ±0.002	4.796	-0.35 ±0.07	-0.34 ±0.04	✓	✓	-0.32 14	--	-0.42 2	-0.32 14	--	-0.36 68	-
866	6079.008	-0.004 ±0.002	4.652	-0.95 ±0.03	-0.96 ±0.03	✓	✓	-1.02 71	-1.10 71	-1.13 2	-	--	--	-
868	6082.710	-0.004 ±0.002	2.223	-3.51 ±0.02	-3.53 ±0.03	✓	✓	-3.58 83	-3.57 74	-3.65 2	-3.57 67	--	--	-
874	6093.643	-0.004 ±0.002	4.608	-1.30 ±0.03	-1.31 ±0.01	✓	✓	-1.40 71	-1.47 71	-1.50 2	-1.50 67	--	--	-
875	6094.373	-0.004 ±0.002	4.652	-1.53 ±0.03	-1.56 ±0.01	✓	✓	-1.84 71	-1.92 71	-1.76 2	-1.94 67	--	--	-
876	6096.664	-0.005 ±0.003	3.984	-1.75 ±0.02	-1.82 ±0.03	✓	✓	-1.83 71	-1.88 71	-2.00 2	-1.93 67	--	--	X
877	6097.081	0.002 ±0.010	2.176	-4.76 ±0.07	-4.84 ±0.05	✓	✓	-4.65 14	--	-4.85 2	-4.75 14	--	--	2
878	6098.244	-0.002 ±0.003	4.559	-1.70 ±0.02	-1.74 ±0.02	✓	✓	-1.86 14	--	-1.99 2	-1.88 67	--	-0.53 68	-
880	6102.171	0.002 ±0.003	4.835	-0.28 ±0.06	-0.27 ±0.04	✓	✓	-0.52 14	--	-0.63 2	-0.52 14	--	--	-
887	6127.906	-0.004 ±0.002	4.143	-1.41 ±0.06	-1.39 ±0.03	✓	✓	-1.40 69	-1.40 69	-1.52 2	-1.40 69	--	--	69
894	6136.994	-0.001 ±0.002	2.198	-2.82 ±0.06	-2.93 ±0.02	✓	✓	-2.95 74	-2.95 74	-3.21 2	-2.95 67	--	-3.26 68	X
897	6145.410	-0.012 ±0.011	3.368	-3.56 ±0.03	-3.66 ±0.04	✓	✓	-2.78 14	--	-3.90 2	--	--	--	X
899	6151.617	-0.003 ±0.003	2.176	-3.27 ±0.03	-3.27 ±0.03	✓	✓	-3.29 83	-3.30 74	-3.30 2	-3.30 67	--	-3.61 68	-
903	6157.728	-0.004 ±0.002	4.076	-1.23 ±0.08	-1.22 ±0.06	✓	✓	-1.16 71	-1.22 71	-1.27 2	-1.26 67	--	-5.65 68	-
904	6159.374	-0.009 ±0.002	4.608	-1.79 ±0.03	-1.89 ±0.03	✓	✓	-0.55 14	--	-2.09 2	-2.09 2	--	--	X
908	6165.360	-0.004 ±0.002	4.143	-1.49 ±0.06	-1.48 ±0.05	✓	✓	-1.47 69	-1.47 69	-1.67 2	-1.47 69	--	--	69
911	6170.506	-0.004 ±0.002	4.796	-0.21 ±0.04	-0.37 ±0.02	✓	✓	-0.44 67	--	-0.65 2	-0.44 67	--	--	X
912	6173.334	-0.001 ±0.002	2.223	-2.83 ±0.03	-2.85 ±0.03	✓	✓	-2.88 74	-2.88 74	-2.88 2	-2.88 67	--	-3.14 68	2, 67, 74
916	6180.203	-0.001 ±0.002	2.728	-2.61 ±0.03	-2.65 ±0.03	✓	✓	-2.59 81	-2.65 69	-2.62 2	-2.59 77	--	--	2, 67, 71
917	6183.558	0.028 ±0.004	5.033	-1.28 ±0.02	-1.39 ±0.02	✓	✓	-1.26 14	--	-	-	--	--	X

Table F.1. ^(*a*) Quality-assessable (^(*A*)) Analysis-independent line ^(*a*) Paper 1 input list ^(*b*) NIST ^(*c*) SpectroWeb ^(*d*) VALD3 ^(*e*) CHIANTI ^(*f*) TIPbase ^(*h*) TOPbase

#	Wavelength (Å) Input	E_{low} (eV) $\Delta\lambda_{grid}$	$\log(gf)$ cog grid	$\log(gf)$ this work grid	Flags QA? AI?	a)	b)	c)	d)	e)	f)	g)	h)	Recommended literature
919	6187.398	-0.008 ±0.004	2.832	-4.00 ±0.04	-4.02 ±0.04	✓	✓	-4.15 14	-	-4.34 2	-4.16 14	-	-4.63 68	-
920	6187.989	-0.002 ±0.003	3.943	-1.61 ±0.02	-1.63 ±0.02	✓	✓	-1.62 71	-1.67 71	-1.92 2	-1.72 67	-	-	71
921	6190.399	-0.011 ±0.005	5.273	-1.70 ±0.05	-1.94 ±0.10	x	x	-1.52 14	-	-	-	-	-	X
926	6199.506	-0.001 ±0.004	2.559	-4.24 ±0.06	-4.30 ±0.03	✓	x	-4.43 14	-	-4.60 2	-	-	-	-
927	6200.312	0.000 ±0.001	2.609	-2.35 ±0.03	-2.36 ±0.03	✓	✓	-2.43 74	-	-2.44 2	-	-	-2.79 68	-
929	6208.212	-0.018 ±0.015	5.100	-1.89 ±0.08	-2.12 ±0.06	x	x	-1.14 14	-	-	-	-	-	X
931	6213.429	-0.001 ±0.002	2.223	-2.52 ±0.03	-2.54 ±0.03	✓	✓	-2.48 69	-2.48 69	-2.73 2	-2.48 69	-	-2.78 68	-
933	6217.683	-0.019 ±0.007	5.033	-1.88 ±0.04	-1.97 ±0.04	x	x	-1.67 14	-	-	-	-	-	X
936	6220.780	-0.002 ±0.003	3.882	-2.25 ±0.02	-2.29 ±0.02	✓	✓	-2.06 14	-	-2.54 2	-2.46 67	-	-	-
939	6226.734	-0.001 ±0.002	3.884	-2.03 ±0.03	-2.06 ±0.02	✓	✓	-2.12 71	-	-2.22 2	-2.22 67	-	-	-
940	6229.226	-0.002 ±0.003	2.845	-2.83 ±0.04	-2.90 ±0.03	✓	x	-2.81 86	-2.81 86	-2.81 2	-2.81 86	-	-3.45 68	-
942	6232.640	-0.001 ±0.002	3.654	-1.26 ±0.03	-1.26 ±0.02	✓	✓	-1.24 87	-	-1.75 2	-	-	-	87
945	6240.310	-0.007 ±0.004	4.143	-2.10 ±0.03	-2.13 ±0.02	✓	✓	-2.08 14	-	-2.37 2	-1.92 14	-	-6.83 68	-
946	6240.646	-0.002 ±0.003	2.223	-3.25 ±0.03	-3.26 ±0.03	✓	✓	-3.23 88	-3.17 69	-3.17 2	-3.23 86	-	-	86, 88
951	6253.828	0.004 ±0.007	4.733	-1.43 ±0.02	-1.52 ±0.02	x	x	-1.30 14	-	-1.66 2	-1.66 67	-	-	X
952	6256.361	-0.005 ±0.001	2.453	-2.13 ±0.08	-2.27 ±0.06	✓	x	-2.41 69	-2.41 69	-2.92 2	-2.41 69	-	-2.78 68	-
957	6265.132	-0.002 ±0.003	2.176	-2.52 ±0.03	-2.55 ±0.02	✓	✓	-2.55 74	-2.55 74	-2.55 2	-2.55 67	-	-2.77 68	2, 67, 74
959	6270.223	-0.002 ±0.003	2.858	-2.57 ±0.03	-2.58 ±0.03	✓	✓	-2.47 88	-2.61 69	-2.46 2	-2.46 86	-	-3.33 68	69
960	6271.278	-0.001 ±0.002	3.332	-2.68 ±0.02	-2.70 ±0.03	✓	✓	-2.70 77	-	-3.04 2	-	-	-	77
965	6280.617	-0.009 ±0.007	0.859	-4.26 ±0.06	-4.25 ±0.21	✓	✓	-4.39 84	-4.39 85	-4.39 2	-4.39 67	-	-	2, 67, 84, 85
966	6290.965	0.015 ±0.009	4.733	-0.56 ±0.05	-0.70 ±0.04	x	x	-0.77 14	-	-0.77 2	-0.77 14	-	-	X
967	6293.924	-0.001 ±0.004	4.835	-1.53 ±0.04	-1.59 ±0.02	✓	x	-1.72 14	-	-1.91 2	-1.72 14	-	-	-
969	6297.793	-0.001 ±0.002	2.223	-2.72 ±0.02	-2.71 ±0.03	✓	✓	-2.74 83	-2.74 74	-2.87 2	-2.74 67	-	-2.89 68	67, 74, 83
972	6302.493	0.001 ±0.005	3.686	-1.23 ±0.05	-1.09 ±0.13	✓	x	-0.97 14	-	-1.20 2	-	-	-3.45 68	2, 14
974	6311.499	-0.003 ±0.003	2.832	-3.07 ±0.02	-3.10 ±0.03	✓	✓	-3.14 77	-3.14 77	-3.39 2	-3.14 77	-	-3.45 68	-
976	6315.811	-0.002 ±0.003	4.076	-1.63 ±0.05	-1.65 ±0.04	✓	✓	-1.63 72	-1.66 71	-1.68 2	-1.71 67	-	-	2, 71, 72
982	6322.685	0.001 ±0.002	2.588	-2.34 ±0.03	-2.36 ±0.02	✓	✓	-2.43 74	-	-2.78 2	-	-	-2.79 68	-
985	6330.848	-0.004 ±0.002	4.733	-1.13 ±0.03	-1.13 ±0.02	✓	✓	-1.64 71	-1.72 71	-1.36 2	-	-	-	-
987	6338.876	-0.004 ±0.002	4.796	-0.87 ±0.05	-0.90 ±0.02	✓	✓	-0.96 71	-1.04 71	-1.12 2	-1.06 67	-	-	-
989	6344.148	-0.001 ±0.002	2.433	-2.72 ±0.04	-2.82 ±0.04	x	x	-2.92 74	-2.92 74	-3.09 2	-2.92 67	-	-2.78 68	X
992	6355.028	0.010 ±0.005	2.845	-2.07 ±0.11	-2.23 ±0.04	x	x	-2.34 81	-2.29 69	-2.35 2	-2.35 77	-	-2.97 68	X
993	6364.364	-0.004 ±0.002	4.796	-1.15 ±0.03	-1.20 ±0.02	✓	x	-1.33 71	-1.41 71	-1.43 2	-1.43 67	-	-	-
994	6364.695	0.000 ±0.003	4.584	-1.74 ±0.04	-1.87 ±0.03	x	x	-1.49 14	-	-1.77 2	-	-	-	X
999	6380.743	-0.004 ±0.002	4.186	-1.33 ±0.07	-1.32 ±0.03	✓	✓	-1.38 69	-1.38 69	-1.42 2	-1.38 69	-	-5.93 68	-
1000	6385.718	-0.002 ±0.003	4.733	-1.74 ±0.03	-1.76 ±0.03	✓	✓	-0.98 14	-	-2.01 2	-	-	-	-
1002	6400.317	-0.001 ±0.002	0.915	-4.06 ±0.28	-4.39 ±0.03	x	x	-4.32 69	-4.32 69	-4.32 2	-4.32 69	-	-	X
1003	6408.017	-0.001 ±0.002	3.686	-1.05 ±0.04	-1.00 ±0.02	✓	x	-1.01 82	-	-1.23 2	-	-	-	82
1007	6419.949	-0.005 ±0.001	4.733	-0.24 ±0.05	-0.25 ±0.03	✓	✓	-0.20 71	-0.27 71	-0.44 2	-0.24 67	-	-	67, 71

Table F1. ^(*a*) Quality-assessable (*AI*) Analysis-independent line ^(*a*) Paper 1 input list ^(*b*) NIST ^(*c*) Paper 1 input list ^(*d*) VALD3 ^(*e*) SpectroWeb ^(*f*) CHIANTI ^(*g*) TIPbase ^(*h*) TOPbase

#	Wavelength (Å) Input	E_{low} (eV) $\Delta\lambda_{grid}$	$\log(gf)$ cog grid	$\log(gf)$ this work grid	Flags QA? AI?	Flags a) b)	Flags c) d)	Flags e) f)	Flags g) h)	Recommended literature
1010	6436.406	0.000 ±0.003	4.186	-2.32 ±0.03	✓ ✓	-2.58 ¹⁴ -0.73 ⁷¹	-2.73 ² -0.89 ²	-2.73 ² -0.77 ⁶⁷	-	-
1017	6469.192	-0.004 ±0.002	4.835	-0.59 ±0.04	✓ X	-2.72 ±0.07	✓ ✓	-2.94 ⁶⁹ -2.98 ⁸³	-2.94 ² -3.08 ²	-7.66 ⁶⁸
1019	6475.624	0.000 ±0.006	2.559	-2.72 ±0.07	✓ ✓	-2.90 ±0.03	✓ X	-0.53 ⁷¹ -0.12 ¹⁴	-0.61 ⁷¹ -0.12 ¹⁴	-
1021	6481.870	-0.001 ±0.002	2.279	-2.90 ±0.03	✓ ✓	-0.58 ±0.04	✓ X	-0.53 ⁷¹ -0.12 ¹⁴	-0.61 ⁷¹ -0.12 ¹⁴	67, 71
1023	6496.466	-0.005 ±0.001	4.796	-0.52 ±0.04	✓ X	-1.56 ±0.08	✓ X	-0.12 ¹⁴ -2.49 ¹⁴	-1.91 ² -3.21 ²	X
1025	6504.182	-0.023 ±0.010	4.733	-1.82 ±0.07	✓ X	-2.85 ±0.06	✓ X	-0.12 ¹⁴ -2.49 ¹⁴	-1.91 ² -3.21 ²	-
1026	6509.615	-0.006 ±0.002	4.076	-2.89 ±0.05	✓ X	-2.49 ±0.03	✓ X	-0.91 ±0.03 -0.97 ⁷¹	-1.05 ⁷¹ -1.05 ⁷¹	-
1028	6518.366	0.001 ±0.005	2.832	-2.49 ±0.03	✓ X	-2.54 ±0.03	✓ X	-2.44 ⁸¹ -2.42 ⁷⁴	-2.30 ⁶⁹ -2.42 ⁷⁴	-2.46 ⁷⁷
1031	6533.928	-0.004 ±0.005	4.559	-1.15 ±0.07	✓ X	-1.20 ±0.04	✓ X	-1.36 ⁷¹ -2.42 ⁷⁴	-1.36 ⁷¹ -2.42 ⁷⁴	-1.26 ⁶⁸
1033	6593.869	0.004 ±0.002	2.433	-2.30 ±0.03	✓ X	-2.33 ±0.03	✓ X	-0.97 ⁷¹ -3.93 ⁷¹	-1.05 ⁷¹ -4.16 ²	-
1034	6597.559	-0.004 ±0.002	4.796	-0.87 ±0.03	✓ X	-0.91 ±0.03	✓ X	-0.97 ⁷¹ -3.93 ⁷¹	-1.05 ⁷¹ -4.16 ²	-
1036	6608.025	-0.002 ±0.003	2.279	-3.89 ±0.03	✓ X	-3.91 ±0.03	✓ X	-1.39 ⁷¹ -0.80 ⁶⁹	-1.39 ⁷¹ -0.80 ⁶⁹	-
1037	6609.110	0.001 ±0.002	2.559	-2.59 ±0.04	✓ X	-2.66 ±0.03	✓ X	-2.69 ⁷⁴ -5.34 ⁸⁵	-2.69 ⁷⁴ -5.34 ⁸⁵	-2.91 ²
1038	6625.021	-0.004 ±0.002	1.011	-5.22 ±0.03	✓ X	-5.24 ±0.05	✓ X	-5.34 ⁸⁵ -1.59 ⁷²	-5.34 ⁸⁵ -1.59 ⁷²	-5.35 ⁶⁷
1039	6627.544	-0.003 ±0.003	4.549	-1.42 ±0.02	✓ X	-1.45 ±0.02	✓ X	-1.59 ⁷² -1.39 ⁷¹	-1.61 ² -1.41 ²	-
1041	6633.412	-0.002 ±0.004	4.835	-1.13 ±0.03	✓ X	-1.20 ±0.02	✓ X	-1.39 ⁷¹ -0.80 ⁶⁹	-1.49 ⁶⁷ -0.88 ²	-
1042	6633.749	-0.004 ±0.002	4.559	-0.70 ±0.05	✓ X	-0.70 ±0.03	✓ X	-1.39 ⁷¹ -0.80 ⁶⁹	-1.49 ⁶⁷ -0.88 ²	-0.96 ⁶⁸
1043	6634.106	0.001 ±0.004	4.796	-1.03 ±0.07	✓ X	-1.13 ±0.05	✓ X	-1.33 ⁷¹ -2.42 ¹⁴	-1.40 ² -2.21 ¹⁴	-1.43 ⁶⁷
1047	6653.851	-0.002 ±0.004	4.154	-2.30 ±0.05	✓ X	-2.37 ±0.03	✓ X	-1.20 ⁷² -2.47 ⁸³	-1.20 ⁷² -2.47 ⁸³	-2.52 ⁶⁷
1050	6663.231	-0.002 ±0.003	4.559	-1.17 ±0.05	✓ X	-1.34 ±0.02	✓ X	-1.20 ⁷² -4.18 ¹⁴	-1.62 ² -4.18 ¹⁴	-1.62 ²
1051	6663.441	0.000 ±0.003	2.424	-2.34 ±0.09	✓ X	-2.49 ±0.03	✓ X	-2.47 ⁸³ -4.18 ¹⁴	-2.55 ² -4.40 ⁶⁷	-2.26 ⁶⁸
1052	6667.418	-0.001 ±0.006	2.453	-4.21 ±0.07	✓ X	-4.28 ±0.03	✓ X	-2.47 ⁸³ -4.18 ¹⁴	-2.55 ² -4.40 ⁶⁷	-
1054	6687.491	-0.007 ±0.009	4.143	-2.68 ±0.08	✓ X	-2.82 ±0.06	✓ X	-2.53 ¹⁴ -2.36 ¹⁴	-3.22 ² -2.95 ²	-
1055	6692.271	-0.021 ±0.013	4.076	-2.91 ±0.06	✓ X	-3.00 ±0.06	✓ X	-2.36 ¹⁴ -2.10 ⁷⁷	-2.10 ⁷⁷ -3.06 ⁷¹	-3.05 ⁶⁸
1058	6699.141	-0.002 ±0.003	4.593	-2.00 ±0.07	✓ X	-2.12 ±0.04	✓ X	-2.10 ⁷⁷ -3.06 ⁷¹	-2.28 ² -3.16 ⁶⁷	X
1059	6703.566	-0.001 ±0.002	2.759	-2.98 ±0.02	✓ X	-2.98 ±0.03	✓ X	-2.38 ¹⁴ -2.38 ¹⁴	-2.38 ¹⁴ -2.66 ⁶⁷	-3.06 ⁶⁸
1060	6704.480	-0.002 ±0.005	4.218	-2.49 ±0.05	✓ X	-2.56 ±0.03	✓ X	-2.38 ¹⁴ -2.38 ¹⁴	-2.38 ¹⁴ -2.66 ⁶⁷	-
1061	6705.101	-0.004 ±0.002	4.607	-1.02 ±0.02	✓ X	-1.05 ±0.02	✓ X	-0.87 ⁷² -2.20 ²	-1.65 ² -2.20 ²	-2.01 ⁶⁸
1062	6707.431	0.014 ±0.028	4.608	-2.03 ±0.03	✓ X	-4.75 ±0.02	✓ X	-4.76 ¹⁴ -1.48 ⁷¹	-4.76 ¹⁴ -1.48 ⁷¹	-4.88 ⁶⁷
1063	6710.318	-0.001 ±0.003	1.485	-4.75 ±0.02	✓ X	-2.01 ±0.06	✓ X	-0.88 ¹⁴ -1.48 ⁷¹	-1.50 ⁷¹ -1.48 ⁷¹	-5.05 ²
1064	6711.820	0.007 ±0.009	4.956	-1.26 ±0.09	✓ X	-1.42 ±0.02	✓ X	-0.88 ¹⁴ -1.48 ⁷¹	-1.66 ² -1.48 ⁷¹	-1.66 ²
1065	6713.046	0.006 ±0.006	4.607	-1.37 ±0.02	✓ X	-1.38 ±0.02	✓ X	-1.50 ⁷¹ -1.54 ⁷¹	-1.59 ² -1.54 ⁷¹	-1.60 ⁶⁷
1066	6713.743	-0.006 ±0.002	4.796	-1.37 ±0.02	✓ X	-1.47 ±0.02	✓ X	-1.54 ⁷¹ -1.84 ¹⁴	-1.66 ² -1.84 ¹⁴	-1.66 ²
1067	6715.382	-0.005 ±0.003	4.608	-1.39 ±0.03	✓ X	-1.49 ±0.02	✓ X	-1.54 ⁷¹ -1.84 ¹⁴	-1.66 ² -1.84 ¹⁴	-1.66 ²
1068	6716.236	-0.001 ±0.002	4.580	-1.69 ±0.04	✓ X	-1.80 ±0.03	✓ X	-1.84 ¹⁴ -2.17 ⁰³	-2.10 ⁷² -2.10 ⁷²	-1.92 ⁶⁷
1070	6725.356	-0.006 ±0.002	4.103	-2.14 ±0.02	✓ X	-2.17 ±0.03	✓ X	-2.10 ⁷² -1.13 ¹⁴	-2.30 ² -1.21 ²	-2.30 ⁶⁷
1071	6726.666	-0.001 ±0.002	4.607	-1.01 ±0.02	✓ X	-1.02 ±0.01	✓ X	-1.13 ¹⁴ -0.62 ¹⁴	-1.21 ² -0.62 ¹⁴	-1.28 ⁶⁸
1073	6730.291	-0.006 ±0.005	4.913	-2.01 ±0.12	✓ X	-1.99 ±0.08	✓ X	-0.62 ¹⁴ -	-	-

Table F.1. (g) Quality-assessable (A) Analysis-independent line ^{a)} Paper 1 input list ^{b)} NIST ^{c)} SpectroWeb ^{d)} VALD3 ^{e)} CHIANTI ^{f)} TIPbase ^{g)} TOPbase

#	Wavelength (Å) Input	E_{low} (eV) $\Delta\lambda_{grid}$	$\log(gf)$ cog	$\log(gf)$ this work grid	Flags QA? AI?	a)	b)	c)	d)	e)	f)	g)	h)	Recommended literature
1074	6732.065	-0.006 ±0.004	4.584	-2.05 ±0.05	-2.12 ±0.04	✓ X	-2.02 14	-	-2.31 2	-2.21 67	-	-	-	-
1075	6733.150	0.000 ±0.003	4.638	-1.38 ±0.03	-1.40 ±0.02	✓ ✓	-1.15 73	-	-1.59 2	-	-	-	-	-
1076	6737.985	-0.001 ±0.005	4.559	-1.54 ±0.04	-1.58 ±0.02	✓ ✓	-2.05 14	-	-1.91 2	-	-	-	-	-
1077	6739.520	-0.001 ±0.002	1.557	-4.82 ±0.07	-4.86 ±0.03	✓ ✓	-4.79 86	-4.79 86	-4.79 86	-	-	-	-	-
1080	6745.956	0.000 ±0.006	4.076	-2.56 ±0.12	-2.65 ±0.05	✓ X	-2.50 14	-	-2.77 2	-2.77 67	-	-	-	-
1081	6746.953	0.002 ±0.004	2.609	-4.29 ±0.11	-4.27 ±0.06	✓ ✓	-4.30 14	-	-4.46 2	-	-	-	-	14
1082	6750.151	-0.001 ±0.002	2.424	-2.58 ±0.04	-2.60 ±0.03	✓ ✓	-2.62 83	-	-2.72 2	-	-	-	-2.38 68	83
1083	6752.707	-0.002 ±0.003	4.638	-1.19 ±0.02	-1.21 ±0.02	✓ ✓	-1.20 77	-	-1.26 2	-	-	-	-	77
1084	6753.464	-0.004 ±0.005	4.559	-2.15 ±0.06	-2.17 ±0.04	✓ ✓	-1.78 14	-	-3.23 2	-	-	-	-	-
1088	6786.425	-0.024 ±0.015	3.241	-3.50 ±0.07	-3.58 ±0.09	✓ X	-3.77 14	-	-3.70 2	-3.76 14	-	-	-	-
1089	6786.858	-0.005 ±0.003	4.191	-1.85 ±0.02	-1.87 ±0.02	✓ ✓	-1.97 71	-2.02 71	-2.09 2	-2.07 67	-	-	-	-
1090	6793.258	-0.005 ±0.003	4.076	-2.30 ±0.02	-2.32 ±0.03	✓ ✓	-2.33 77	-2.33 77	-2.61 2	-2.33 77	-	-	-	77
Fe II														
35	4416.819	-0.005 ±0.001	2.778	-2.34 ±0.09	-2.61 ±0.04	✓ X	-2.41 89	-2.60 90	-2.61 2	-2.41 89	-	-	-4.27 68	X
73	4491.397	0.006 ±0.004	2.856	-2.55 ±0.04	-2.61 ±0.04	✓ X	-2.70 91	-2.64 92	-2.70 2	-2.70 91	-	-	-2.73 68	92
83	4508.280	-0.001 ±0.002	2.856	-2.40 ±0.05	-2.34 ±0.03	✓ X	-2.25 93	-2.30 90	-2.31 2	-2.25 93	-	-	-3.09 68	2
106	4541.516	-0.009 ±0.004	2.856	-2.77 ±0.06	-2.98 ±0.02	✓ X	-2.79 89	-3.00 90	-2.85 2	-2.79 89	-	-	-3.48 68	X
114	4555.887	-0.004 ±0.002	2.828	-2.26 ±0.05	-2.57 ±0.07	✓ X	-2.16 89	-2.25 92	-2.28 2	-2.16 89	-	-	-2.44 68	X
134	4582.830	-0.016 ±0.004	2.844	-3.08 ±0.07	-3.37 ±0.08	✓ X	-3.09 93	-3.06 92	-3.09 2	-3.09 93	-	-	-3.20 68	X
168	4620.513	0.002 ±0.004	2.828	-3.23 ±0.04	-3.40 ±0.04	✓ X	-3.24 93	-3.19 92	-3.29 2	-3.24 93	-	-	-3.48 68	X
176	4635.317	-0.001 ±0.008	5.956	-1.31 ±0.05	-1.43 ±0.04	✓ X	-1.65 67	-	-1.65 2	-1.65 67	-	-	-1.57 68	X
187	4656.976	-0.003 ±0.003	2.891	-3.58 ±0.04	-3.62 ±0.03	✓ X	-3.61 93	-3.57 92	-3.75 2	-3.61 93	-	-	-	93
197	4670.170	-0.004 ±0.002	2.583	-3.95 ±0.05	-4.11 ±0.04	✓ X	-4.06 93	-4.10 90	-4.30 2	-4.06 93	-	-	-	X
230	4731.448	0.003 ±0.006	2.891	-2.47 ±0.17	-2.91 ±0.17	✓ X	-3.00 94	-3.10 90	-2.75 2	-3.00 94	-	-	-	X
366	4993.350	-0.001 ±0.003	2.807	-3.53 ±0.17	-3.68 ±0.02	✓ X	-3.68 64	-3.68 64	-3.85 2	-3.64 93	-	-	-64, 90	
461	5197.568	0.001 ±0.002	3.230	-2.24 ±0.05	-2.30 ±0.06	✓ X	-2.22 95	-2.05 92	-2.35 2	-2.10 91	-	-	-2.36 68	2, 68
499	5264.802	-0.001 ±0.002	3.230	-3.00 ±0.07	-3.07 ±0.03	✓ X	-3.13 95	-3.23 92	-3.30 2	-3.12 93	-	-	-	-
509	5284.103	0.000 ±0.001	2.891	-2.92 ±0.11	-3.13 ±0.03	✓ X	-3.19 64	-3.20 90	-3.30 2	-2.99 89	-	-	-	X
539	5325.552	-0.001 ±0.002	3.221	-3.08 ±0.08	-3.18 ±0.02	✓ X	-3.16 95	-3.26 96	-3.22 2	-3.12 89	-	-	-3.04 68	95
568	5414.070	-0.002 ±0.003	3.221	-3.48 ±0.04	-3.56 ±0.02	✓ X	-3.58 95	-3.48 92	-3.79 2	-3.54 93	-	-	-	X
573	5425.248	-0.001 ±0.003	3.199	-3.18 ±0.04	-3.25 ±0.02	✓ X	-3.22 95	-3.40 90	-3.37 2	-3.16 89	-	-	-3.15 68	X
615	5534.838	0.001 ±0.002	3.245	-2.72 ±0.03	-2.83 ±0.02	✓ X	-2.87 64	-2.90 90	-3.00 2	-2.73 89	-	-	-	X
845	5991.371	-0.002 ±0.003	3.153	-3.49 ±0.03	-3.57 ±0.02	✓ X	-3.65 64	-3.60 90	-3.76 2	-3.54 89	-	-	-	X
869	6084.102	-0.001 ±0.002	3.199	-3.74 ±0.02	-3.77 ±0.03	✓ ✓	-3.88 64	-3.90 90	-4.01 2	-3.78 89	-	-	-	89
898	6149.246	-0.005 ±0.001	3.889	-2.69 ±0.02	-2.73 ±0.03	✓ ✓	-2.84 64	-2.80 90	-2.92 2	-2.72 89	-	-	-2.99 68	89
944	6239.943	-0.008 ±0.006	3.889	-3.35 ±0.04	-3.41 ±0.02	✓ ✓	-3.57 64	-3.60 90	-3.70 2	-3.57 64	-	-	-3.69 68	-
950	6247.557	-0.001 ±0.002	3.892	-2.30 ±0.03	-2.35 ±0.02	✓ X	-2.43 64	-2.40 90	-2.44 2	-2.31 89	-	-	-2.58 68	-
958	6269.959	0.001 ±0.004	3.245	-4.27 ±0.07	-4.36 ±0.03	✓ X	-4.50 64	-	-4.62 2	-4.50 64	-	-	-	-
996	6369.459	-0.002 ±0.004	2.891	-4.09 ±0.03	-4.15 ±0.03	✓ X	-4.11 95	-4.29 96	-4.32 2	-4.16 89	-	-	-	89

Table F.1. $\langle g \rangle A$) Quality-assessable (A) Analysis-independent line $a)$ Paper 1 input list $b)$ NIST $c)$ Paper 1 input list $d)$ VALD3 $e)$ SpectroWeb $f)$ CHIANTI $g)$ TIPbase $h)$ TOPbase

#	Wavelength (Å) Input	E_{low} (eV) $\Delta\lambda_{grid}$	$\log(gf)$ cog grid	Flags QA? AI?	Flags a)	Flags b)	Flags c)	Flags d)	Flags e)	Flags f)	Flags g)	Flags h)	Recommended literature
1009	6432.676	0.002 ±0.003	2.891	-3.53 ±0.03	-3.60 ±0.03	X	X	-3.57 95	-3.50 92	-3.78 2	-3.52 93	-	-
1011	6446.407	-0.016 ±0.005	6.223	-1.89 ±0.09	-1.96 ±0.05	✓	X	-1.96 89	-2.08 90	-2.11 2	-1.96 89	-	X
1015	6456.380	-0.001 ±0.002	3.903	-2.08 ±0.03	-2.11 ±0.03	✓	✓	-2.18 64	-2.20 90	-2.38 2	-2.10 89	-	20, 89
1027	6516.077	0.001 ±0.005	2.891	-3.21 ±0.05	-3.31 ±0.04	X	X	-3.31 95	-3.37 92	-3.61 2	-3.32 93	-	89
													X
91	4517.094	0.040 ±0.001	3.128	-0.07 ±0.05	-0.15 ±0.03	✓	X	-0.74 14	-	-0.10 2	-0.74 14	-	-
124	4570.024	-0.021 ±0.005	3.632	-0.46 ±0.06	-0.59 ±0.06	✓	X	-0.40 14	-	-0.42 2	-0.40 14	-	X
141	4588.729	-0.043 ±0.005	0.432	-3.24 ±0.10	-3.33 ±0.12	✓	X	-3.82 14	-	-3.28 2	-3.82 14	-	2
147	4594.632	-0.004 ±0.002	3.632	-0.23 ±0.09	-0.35 ±0.10	✓	X	-0.04 14	-	-0.38 2	-0.04 14	-	2
211	4693.188	-0.001 ±0.002	3.231	-0.28 ±0.05	-0.47 ±0.05	X	X	-0.50 14	-	-0.55 2	-0.50 14	-	X
													X
255	4768.075	-0.001 ±0.004	3.191	-0.63 ±0.13	-0.77 ±0.07	✓	X	-0.59 14	-	-0.67 2	-0.59 14	-	-
256	4771.083	0.008 ±0.013	3.133	-0.30 ±0.15	-0.49 ±0.09	✓	X	-0.43 14	-	-0.50 2	-0.43 14	-	2, 14
260	4781.428	-0.006 ±0.003	1.883	-2.03 ±0.07	-2.26 ±0.07	X	X	-2.15 67	-2.16 67	-2.35 2	-2.15 67	-	X
307	4899.514	-0.008 ±0.003	2.042	-1.78 ±0.12	-1.98 ±0.10	✓	X	-1.60 14	-	-1.96 2	-1.60 14	-	2
476	5235.183	-0.007 ±0.006	2.137	-1.23 ±0.07	-1.45 ±0.07	X	X	-1.47 67	-1.46 67	-1.45 2	-1.47 67	-	X
													X
491	5247.920	-0.002 ±0.003	1.785	-1.87 ±0.08	-1.97 ±0.07	✓	X	-2.07 67	-2.08 67	-2.01 2	-2.07 67	-	2
529	5312.648	0.001 ±0.006	4.209	0.08 ±0.03	0.01 ±0.04	✓	X	-0.19 14	-	-0.84 2	-0.19 14	-	-
579	5454.570	0.003 ±0.003	4.072	0.24 ±0.06	0.11 ±0.05	X	X	0.24 14	-	0.14 2	0.24 14	-	X
991	6347.842	-0.009 ±0.002	4.395	-0.01 ±0.05	-0.19 ±0.07	X	X	-0.06 14	-	-0.12 2	-0.06 14	-	X
1020	6477.860	-0.006 ±0.006	3.775	-0.70 ±0.10	-0.76 ±0.06	✓	X	-0.61 14	-	-0.71 2	-0.61 14	-	2
													2
32	4410.518	0.001 ±0.002	3.306	-0.99 ±0.08	-1.13 ±0.08	✓	X	-1.08 67	-1.08 97	-1.08 2	-1.08 67	-	-
42	4437.566	-0.006 ±0.002	3.679	-1.10 ±0.07	-1.21 ±0.05	✓	X	-1.24 67	-	-1.19 2	-1.24 67	-	2, 67, 97
63	4470.472	0.004 ±0.002	3.399	-0.32 ±0.05	-0.39 ±0.06	✓	X	-0.31 98	-	-0.31 2	-0.30 99	-	2, 67
89	4512.990	-0.004 ±0.002	3.706	-1.40 ±0.06	-1.42 ±0.06	✓	✓	-1.47 67	-1.47 97	-1.55 2	-1.47 67	-	67, 97
94	4519.983	0.002 ±0.004	1.676	-2.90 ±0.04	-2.95 ±0.06	✓	X	-2.88 67	-2.88 100	-2.88 2	-3.08 99	-	-
													X
103	4537.411	-0.012 ±0.006	4.089	-1.77 ±0.05	-1.76 ±0.05	✓	✓	-1.93 14	-	-	-1.93 14	-	-
153	4600.359	-0.002 ±0.003	3.597	-0.49 ±0.13	-0.65 ±0.06	✓	X	-0.61 67	-0.61 97	-0.61 2	-0.61 67	-	-
159	4604.982	-0.008 ±0.003	3.480	-0.18 ±0.07	-0.49 ±0.07	X	X	-0.25 98	-	-0.24 2	-0.24 99	-	X
184	4648.646	0.004 ±0.002	3.420	-0.22 ±0.05	-0.25 ±0.08	✓	✓	-0.10 98	-	-0.15 2	-0.09 99	-	-
195	4667.759	0.000 ±0.003	3.706	-0.76 ±0.05	-0.97 ±0.06	X	X	-0.85 14	-	-1.01 2	-0.85 14	-	X
													X
207	4686.207	0.004 ±0.002	3.597	-0.55 ±0.07	-0.71 ±0.06	X	X	-0.58 98	-	-0.63 2	-0.59 99	-	-
214	4701.352	-0.004 ±0.002	3.480	-1.09 ±0.05	-1.21 ±0.07	✓	X	-1.22 67	-1.22 97	-1.22 2	-1.22 67	-	2, 67, 97
215	4701.530	-0.005 ±0.001	4.088	-0.34 ±0.07	-0.43 ±0.08	✓	X	-0.39 67	-0.38 97	-0.38 2	-0.39 67	-	2, 67, 97
216	4703.807	-0.004 ±0.002	3.658	-0.56 ±0.06	-0.72 ±0.11	X	X	-0.52 14	-	-0.73 2	-0.52 14	-	2
231	4731.798	0.004 ±0.005	3.833	-0.79 ±0.07	-0.94 ±0.09	✓	X	-0.85 67	-0.85 97	-0.85 2	-0.85 67	-	2, 67, 97
													X
232	4732.457	-0.001 ±0.002	4.105	-0.53 ±0.05	-0.57 ±0.06	✓	✓	-0.55 67	-0.55 97	-0.55 2	-0.55 67	-	2, 67, 97
243	4752.420	0.002 ±0.003	3.658	-0.56 ±0.07	-0.65 ±0.06	✓	X	-0.70 67	-0.69 97	-0.69 2	-0.70 67	-	2, 67, 97

Table F.1. \mathcal{Q}^A) Quality-assessable (A^I) Analysis-independent line $a)$ Paper 1 input list $b)$ NIST $c)$ SpectroWeb $d)$ VALD3 $e)$ CHIANTI $f)$ TIPbase $g)$ TOPbase

#	Wavelength (Å) Input	E_{low} (eV) $\Delta\lambda_{grid}$	$\log(gf)$ cog	$\log(gf)$ this work grid	Flags QA? AI?	a)	b)	c)	d)	e)	f)	g)	h)	Recommended literature
244	4754.756	-0.005 ±0.001	3.635	-0.84 ±0.07	-0.94 ±0.06	✓	X	-0.97 98	-	-0.94 2	-0.98 99	-	-	2, 98, 99
246	4756.510	0.000 ±0.001	3.480	-0.35 ±0.06	-0.30 ±0.05	✓	X	-0.27 98	-	-0.30 2	-0.27 99	-	-	2, 98, 99
262	4786.281	-0.001 ±0.002	1.676	-2.91 ±0.04	-3.02 ±0.05	X	X	-3.12 67	-3.12 100	-3.12 2	-3.14 99	-	-	X
263	4786.531	0.001 ±0.002	3.420	-0.13 ±0.08	-0.23 ±0.05	✓	X	-0.16 98	-	-0.24 2	-0.18 99	-0.17 4	-	2, 99
279	4806.987	-0.001 ±0.002	3.679	-0.56 ±0.06	-0.61 ±0.06	✓	X	-1.02 14	-	-0.64 2	-0.64 67	-	-	2, 67
282	4808.874	-0.011 ±0.006	3.706	-1.28 ±0.06	-1.36 ±0.05	✓	X	-1.41 67	-1.41 97	-1.41 2	-1.41 67	-	-	2, 67, 97
288	4829.023	-0.004 ±0.002	3.542	-0.34 ±0.09	-0.32 ±0.08	✓	X	-0.14 14	-0.33 97	-0.21 2	-0.33 67	-	-	67, 97
296	4873.438	0.001 ±0.002	3.699	-0.45 ±0.12	-0.56 ±0.09	✓	X	-0.38 99	-	-0.47 2	-0.38 99	-	-	2
312	4904.412	-0.001 ±0.002	3.542	-0.17 ±0.04	-0.19 ±0.06	✓	✓	-0.02 14	-0.17 97	-0.12 2	-0.17 67	-	-	67, 97
321	4912.018	-0.004 ±0.002	3.768	-0.71 ±0.07	-0.83 ±0.06	✓	X	-0.54 14	-0.79 97	-0.79 2	-0.80 67	-	-	2, 67, 97
323	4913.973	-0.002 ±0.003	3.743	-0.61 ±0.07	-0.63 ±0.06	✓	✓	-0.50 14	-0.62 97	-0.59 2	-0.63 67	-	-	2, 67, 97
328	4918.364	-0.002 ±0.003	3.841	-0.11 ±0.06	-0.26 ±0.07	X	X	-0.08 14	-0.23 97	-0.11 2	-0.24 67	-	-	X
329	4925.559	0.004 ±0.002	3.655	-0.50 ±0.09	-0.73 ±0.06	X	X	-0.77 98	-	-0.82 2	-0.78 99	-	-	X
333	4930.802	-0.004 ±0.002	3.847	-1.22 ±0.04	-1.30 ±0.06	✓	X	-1.56 14	-	-1.36 2	-1.56 14	-	-	2
334	4935.831	-0.002 ±0.003	3.941	-0.34 ±0.06	-0.37 ±0.06	✓	✓	-0.21 14	-0.36 97	-0.24 2	-0.35 67	-	-	67, 97
337	4945.444	-0.004 ±0.002	3.796	-0.72 ±0.06	-0.76 ±0.04	✓	✓	-0.82 67	-0.82 97	-0.82 2	-0.82 67	-	-	-
339	4946.032	-0.004 ±0.002	3.796	-1.15 ±0.07	-1.23 ±0.06	✓	X	-1.15 14	-1.29 97	-1.29 2	-1.29 67	-	-	2, 67, 97
342	4952.280	-0.004 ±0.002	3.606	-1.23 ±0.05	-1.27 ±0.04	✓	✓	-1.66 14	-	-1.22 2	-1.69 14	-	-	-
343	4953.200	0.009 ±0.004	3.740	-0.62 ±0.05	-0.70 ±0.07	✓	X	-0.58 99	-	-0.66 2	-0.58 99	-	-	2
348	4965.167	-0.004 ±0.002	3.796	-1.14 ±0.05	-1.21 ±0.05	✓	X	-1.21 14	-	-1.14 2	-1.21 14	-	-	14
351	4971.345	-0.002 ±0.003	3.658	-0.66 ±0.05	-0.73 ±0.06	✓	X	-0.55 14	-	-	-0.55 14	-	-	-
353	4976.130	0.001 ±0.002	3.606	-1.23 ±0.04	-1.29 ±0.05	✓	X	-1.26 99	-	-1.36 2	-1.26 99	-	-	99
354	4976.325	-0.001 ±0.002	1.676	-2.91 ±0.04	-2.97 ±0.06	✓	X	-3.00 99	-3.10 100	-3.10 2	-3.00 99	-	-	99
369	4995.650	-0.001 ±0.002	3.635	-1.49 ±0.02	-1.51 ±0.03	✓	✓	-1.12 14	-1.58 97	-1.58 2	-1.58 67	-	-	-
372	4998.218	0.006 ±0.002	3.606	-0.75 ±0.05	-0.83 ±0.06	✓	X	-0.69 98	-	-0.78 2	-0.70 99	-	-	2
376	5003.741	-0.001 ±0.002	1.676	-2.95 ±0.09	-3.01 ±0.07	✓	X	-3.07 99	-2.80 100	-3.00 2	-3.07 99	-	-	2, 99
380	5010.022	-0.002 ±0.003	3.768	-0.99 ±0.03	-1.05 ±0.05	✓	X	-0.98 98	-	-1.04 2	-0.98 99	-	-	2
381	5010.938	-0.003 ±0.003	3.635	-0.87 ±0.05	-0.86 ±0.05	✓	✓	-0.68 14	-0.87 97	-0.72 2	-0.87 67	-	-	67, 97
399	5032.727	-0.004 ±0.009	3.898	-1.08 ±0.11	-1.20 ±0.04	✓	X	-1.40 14	-1.27 97	-1.27 2	-1.27 67	-	-	-
403	5042.186	-0.002 ±0.003	3.658	-0.57 ±0.05	-0.64 ±0.08	✓	✓	-0.58 67	-0.57 97	-0.50 2	-0.58 67	-	-	67, 97
421	5080.528	0.004 ±0.002	3.655	0.31 ±0.09	0.20 ±0.07	✓	X	0.33 98	-	0.43 2	0.32 99	0.22 4	-	4
422	5082.344	-0.002 ±0.003	3.658	-0.51 ±0.06	-0.56 ±0.06	✓	X	-0.44 14	-0.54 97	-0.52 2	-0.54 67	-	-	2, 67, 97
424	5084.096	-0.001 ±0.002	3.679	-0.02 ±0.10	0.02 ±0.08	✓	✓	-0.08 14	-	0.10 2	0.03 67	-	-	2, 67
427	5088.538	-0.002 ±0.004	3.847	-0.87 ±0.25	-1.09 ±0.05	✓	X	-0.91 14	-	-0.98 2	-0.91 14	-	-	-
429	5094.411	-0.001 ±0.004	3.833	-1.05 ±0.05	-1.07 ±0.05	✓	✓	-1.00 14	-1.08 97	-1.08 2	-1.08 67	-	-	2, 67, 97
430	5099.930	-0.002 ±0.003	3.679	-0.07 ±0.10	-0.17 ±0.09	✓	X	-0.10 67	-	-0.10 2	-0.10 67	-	-	2, 67
431	5102.966	-0.004 ±0.002	1.676	-2.70 ±0.10	-2.80 ±0.06	✓	X	-2.62 67	-2.62 100	-2.62 2	-2.87 99	-	-	-
437	5115.392	-0.001 ±0.002	3.834	-0.14 ±0.07	-0.13 ±0.05	✓	✓	-0.11 67	-0.04 2	-0.11 67	-0.11 67	-	-	67, 97
441	5129.371	-0.004 ±0.002	3.679	-0.37 ±0.08	-0.58 ±0.05	X	X	-0.63 67	-	-0.63 2	-0.63 67	-0.77 4	-	X

Table F1. $\langle Q_A \rangle$ Quality-assessable (A^1) Analysis-independent line $^{(a)}$ Paper 1 input list $^{(b)}$ NIST $^{(c)}$ Paper 1 input list $^{(d)}$ VALD3 $^{(e)}$ Spectr-W 3 $^{(f)}$ CHIANTI $^{(g)}$ TIPbase $^{(h)}$ TOPbase

#	Wavelength (Å) Input	E_{low} (eV) $\Delta\lambda_{grid}$	$\log(gf)$ cog grid	$\log(gf)$ this work grid	Flags QA? AI?	a)	b)	c)	d)	e)	f)	g)	h)	Recommended literature
443	5131.768	-0.004 ±0.002	3.699	-0.77 ±0.10	-0.94 ±0.07	✓	X	-0.74 ±14	-	-0.81 ±2	-0.74 ±14	-	-	-
444	5137.074	-0.004 ±0.002	1.676	-1.64 ±0.07	-1.70 ±0.08	✓	X	-1.94 ±99	-1.99 ±100	-1.93 ±2	-1.94 ±99	-	-	-
448	5146.482	-0.001 ±0.002	3.706	-0.04 ±0.04	-0.10 ±0.07	✓	X	0.06 ±14	-	-0.06 ±2	0.06 ±14	-	-	2
453	5155.126	-0.001 ±0.003	3.898	-0.53 ±0.08	-0.66 ±0.06	✓	X	-0.56 ±14	-0.66 ±97	-0.58 ±2	-0.65 ±67	-	-	67, 97
454	5155.764	-0.002 ±0.003	3.898	-0.04 ±0.05	-0.13 ±0.07	✓	X	0.07 ±14	-0.09 ±97	0.01 ±2	0.07 ±14	-	-	97
455	5157.976	0.003 ±0.003	3.606	-1.53 ±0.06	-1.58 ±0.06	✓	X	-1.51 ±99	-	-1.51 ±2	-1.51 ±99	-	-	-
457	5176.560	-0.001 ±0.003	3.898	-0.38 ±0.06	-0.48 ±0.05	✓	X	-0.30 ±14	-0.44 ±97	-0.44 ±2	-0.44 ±67	-	-	2, 67, 97
468	5220.291	-0.003 ±0.003	3.740	-1.19 ±0.04	-1.26 ±0.04	✓	X	-1.31 ±67	-1.31 ±97	-1.31 ±2	-1.31 ±67	-	-	-
558	5392.331	-0.004 ±0.002	4.154	-1.22 ±0.08	-1.30 ±0.06	✓	X	-1.32 ±14	-1.32 ±97	-1.26 ±2	-1.32 ±67	-	-	2, 14, 67, 97
575	5435.858	-0.002 ±0.003	1.986	-2.39 ±0.06	-2.45 ±0.05	✓	X	-2.58 ±99	-2.60 ±100	-2.40 ±2	-2.58 ±99	-	-	2
582	5462.493	-0.003 ±0.003	3.847	-0.80 ±0.05	-0.90 ±0.05	✓	X	-0.82 ±14	-0.93 ±97	-0.93 ±2	-0.93 ±67	-	-	2, 67, 97
601	5494.880	-0.006 ±0.002	4.105	-1.06 ±0.04	-1.12 ±0.04	✓	X	-1.16 ±67	-1.16 ±97	-1.16 ±2	-1.16 ±67	-	-	2, 67, 97
630	5578.718	-0.001 ±0.002	1.676	-2.63 ±0.09	-2.71 ±0.07	✓	X	-2.83 ±99	-2.64 ±100	-2.64 ±2	-2.83 ±99	-	-	2, 100
634	5587.858	-0.002 ±0.003	1.935	-2.33 ±0.05	-2.42 ±0.05	✓	X	-2.39 ±99	-2.14 ±100	-2.14 ±2	-2.39 ±99	-	-	99
635	5589.358	-0.001 ±0.002	3.898	-1.07 ±0.05	-1.16 ±0.05	✓	X	-0.94 ±14	-1.14 ±97	-1.14 ±2	-1.14 ±67	-	-	2, 67, 97
638	5593.735	-0.002 ±0.003	3.898	-0.78 ±0.06	-0.84 ±0.04	✓	X	-0.68 ±14	-0.84 ±97	-0.84 ±2	-0.84 ±67	-	-	2, 67, 97
639	5606.998	-0.013 ±0.009	3.898	-2.04 ±0.04	-2.16 ±0.04	✓	X	-1.70 ±14	-	-2.10 ±2	-1.70 ±14	-	-	X
642	5614.773	-0.002 ±0.003	4.154	-0.51 ±0.03	-0.62 ±0.04	✓	X	-0.57 ±14	-	-0.51 ±2	-0.57 ±14	-	-	X
650	5625.317	-0.001 ±0.002	4.089	-0.65 ±0.04	-0.69 ±0.04	✓	✓	-0.55 ±14	-0.70 ±97	-0.60 ±2	-0.70 ±67	-	-	67, 97
652	5628.342	-0.004 ±0.002	4.089	-1.27 ±0.06	-1.29 ±0.05	✓	✓	-1.74 ±14	-	-1.34 ±2	-1.74 ±14	-	-	2
661	5641.881	-0.001 ±0.002	4.105	-0.97 ±0.05	-1.02 ±0.05	✓	X	-1.05 ±14	-1.08 ±97	-1.00 ±2	-1.07 ±67	-	-	2, 14, 67
664	5643.078	-0.003 ±0.003	4.165	-1.20 ±0.05	-1.24 ±0.05	✓	✓	-1.10 ±14	-1.25 ±97	-1.24 ±2	-1.24 ±67	-	-	2, 67, 97
687	5669.943	-0.006 ±0.002	4.266	-0.99 ±0.05	-1.04 ±0.04	✓	X	-1.00 ±14	-	-1.06 ±2	-1.00 ±14	-	-	2, 14
691	5682.199	-0.003 ±0.003	4.105	-0.40 ±0.06	-0.43 ±0.05	✓	✓	-0.34 ±14	-0.47 ±97	-0.47 ±2	-0.47 ±67	-	-	2, 67, 97
700	5694.983	-0.003 ±0.003	4.089	-0.60 ±0.05	-0.62 ±0.05	✓	✓	-0.47 ±14	-0.61 ±97	-0.61 ±2	-0.61 ±67	-	-	2, 67, 97
737	5748.351	-0.003 ±0.003	1.676	-3.23 ±0.05	-3.27 ±0.05	✓	✓	-3.24 ±99	-3.26 ±97	-3.32 ±2	-3.24 ±99	-	-	2, 97, 99
742	5754.656	-0.005 ±0.001	1.935	-1.96 ±0.09	-2.02 ±0.07	✓	X	-2.33 ±67	-2.34 ±100	-2.28 ±2	-2.22 ±99	-	-	-
745	5760.830	-0.001 ±0.002	4.105	-0.73 ±0.04	-0.76 ±0.04	✓	✓	-0.88 ±14	-0.80 ±97	-0.77 ±2	-0.80 ±67	-	-	2, 67, 97
766	5796.079	-0.001 ±0.005	1.951	-3.57 ±0.04	-3.62 ±0.03	✓	X	-3.82 ±14	-	-3.94 ±2	-3.82 ±14	-	-	-
772	5805.217	-0.004 ±0.002	4.167	-0.57 ±0.05	-0.60 ±0.04	✓	✓	-0.58 ±14	-0.64 ±97	-0.64 ±2	-0.64 ±67	-	-	2, 14, 67, 97
785	5831.596	-0.005 ±0.001	4.167	-0.90 ±0.05	-0.95 ±0.04	✓	X	-0.94 ±14	-	-1.08 ±2	-0.94 ±14	-	-	14
791	5846.993	-0.004 ±0.002	1.676	-3.36 ±0.05	-3.40 ±0.04	✓	✓	-3.46 ±99	-3.21 ±100	-3.41 ±2	-3.46 ±99	-	-	2
846	5996.730	-0.001 ±0.002	4.236	-0.96 ±0.04	-1.01 ±0.04	✓	X	-1.04 ±14	-1.06 ±97	-1.06 ±2	-1.06 ±67	-	-	14
849	6007.310	-0.003 ±0.003	1.676	-3.33 ±0.04	-3.34 ±0.04	✓	✓	-3.40 ±99	-3.34 ±97	-3.30 ±2	-3.40 ±99	-	-	2, 97
854	6025.754	-0.004 ±0.002	4.236	-1.65 ±0.04	-1.72 ±0.04	✓	X	-1.53 ±14	-1.76 ±97	-1.78 ±2	-1.76 ±67	-	-	67, 97
859	6053.685	-0.009 ±0.002	4.236	-0.95 ±0.04	-0.99 ±0.04	✓	✓	-1.16 ±14	-1.07 ±97	-1.07 ±2	-1.07 ±67	-	-	-
870	6086.282	-0.004 ±0.002	4.266	-0.45 ±0.05	-0.47 ±0.04	✓	✓	-0.41 ±14	-0.51 ±97	-0.42 ±2	-0.53 ±67	-	-	97
881	6108.116	-0.001 ±0.002	1.676	-2.50 ±0.08	-2.58 ±0.06	✓	X	-2.60 ±99	-2.44 ±100	-2.69 ±2	-2.60 ±99	-	-	99
882	6111.070	0.000 ±0.003	4.088	-0.79 ±0.05	-0.81 ±0.04	✓	✓	-0.87 ±14	-0.87 ±97	-1.09 ±2	-0.87 ±67	-	-	-

Table F.1. $\langle g \rangle^A$) Quality-assessable (A) Analysis-independent line $a)$ Paper 1 input list $b)$ NIST $c)$ SpectroWeb $d)$ VALD3 $e)$ CHIANTI $f)$ TIPbase $g)$ TOPbase

#	Wavelength (Å) Input	E_{low} (eV) $\Delta\lambda_{grid}$	$\log(gf)$ cog grid	$\log(gf)$ this work grid	Flags QA? AI?	a)	b)	c)	d)	e)	f)	g)	h)	Recommended literature
884	6116.180	0.020 \pm 0.006	4.089	-0.19 \pm 0.08	-0.43 \pm 0.07	X	X	-0.53 \pm 14	-	-0.68 \pm 2	-0.53 \pm 14	-	-	X
888	6130.135	-0.004 \pm 0.002	4.266	-0.91 \pm 0.04	-0.93 \pm 0.04	\checkmark	X	-0.74 \pm 14	-0.96 \pm 97	-1.39 \pm 2	-0.96 \pm 67	-	-	67, 97
892	6133.963	-0.003 \pm 0.005	4.088	-1.75 \pm 0.07	-1.80 \pm 0.04	\checkmark	X	-1.92 \pm 14	-1.84 \pm 97	-2.10 \pm 2	-1.83 \pm 67	-	-	67, 97
913	6175.367	-0.004 \pm 0.002	4.089	-0.52 \pm 0.05	-0.53 \pm 0.03	\checkmark	\checkmark	-0.39 \pm 14	-0.54 \pm 97	-0.56 \pm 2	-0.53 \pm 67	-	-	2, 67, 97
914	6176.807	0.000 \pm 0.001	4.088	-0.25 \pm 0.07	-0.25 \pm 0.06	\checkmark	\checkmark	-0.26 \pm 99	-	-0.26 \pm 2	-0.26 \pm 99	-0.44 \pm 4	-	2, 99
915	6177.242	-0.003 \pm 0.003	1.826	-3.50 \pm 0.03	-3.54 \pm 0.03	\checkmark	\checkmark	-3.46 \pm 99	-3.51 \pm 97	-3.50 \pm 2	-3.46 \pm 99	-	-	97
918	6186.711	-0.004 \pm 0.002	4.105	-0.84 \pm 0.05	-0.88 \pm 0.04	\checkmark	\checkmark	-0.88 \pm 14	-0.96 \pm 97	-0.95 \pm 2	-0.96 \pm 67	-	-	14
922	6191.178	-0.003 \pm 0.003	1.676	-2.24 \pm 0.08	-2.36 \pm 0.07	\checkmark	X	-2.47 \pm 99	-	-2.35 \pm 2	-2.47 \pm 99	-	-	2
928	6204.600	-0.012 \pm 0.008	4.088	-1.07 \pm 0.04	-1.16 \pm 0.05	\checkmark	X	-1.08 \pm 99	-	-1.10 \pm 2	-1.08 \pm 99	-	-	-
937	6223.981	-0.001 \pm 0.002	4.105	-0.92 \pm 0.05	-0.96 \pm 0.04	\checkmark	\checkmark	-0.91 \pm 99	-	-0.98 \pm 2	-0.91 \pm 99	-	-	2
941	6230.089	-0.003 \pm 0.003	4.105	-1.05 \pm 0.05	-1.13 \pm 0.04	\checkmark	X	-1.26 \pm 101	-1.26 \pm 101	-1.32 \pm 2	-1.26 \pm 67	-	-	-
955	6259.595	-0.002 \pm 0.008	4.089	-1.11 \pm 0.04	-1.25 \pm 0.03	X	X	-1.24 \pm 14	-	-1.40 \pm 2	-1.24 \pm 14	-	-	X
961	6271.768	-0.003 \pm 0.005	3.306	-2.44 \pm 0.02	-2.57 \pm 0.04	X	X	-2.62 \pm 67	-2.62 \pm 97	-2.75 \pm 2	-2.62 \pm 67	-	-	X
962	6272.616	-0.004 \pm 0.017	4.266	-1.58 \pm 0.02	-1.70 \pm 0.04	X	X	-1.73 \pm 98	-	-1.98 \pm 2	-1.78 \pm 99	-	-	X
977	6316.574	-0.009 \pm 0.013	4.154	-1.71 \pm 0.13	-1.81 \pm 0.08	\checkmark	X	-1.90 \pm 67	-1.90 \pm 97	-2.75 \pm 2	-1.90 \pm 67	-	-	-
981	6322.166	-0.004 \pm 0.005	4.154	-1.11 \pm 0.04	-1.16 \pm 0.03	\checkmark	X	-1.12 \pm 14	-1.17 \pm 97	-1.31 \pm 2	-1.17 \pm 67	-	-	67, 97
983	6327.599	-0.001 \pm 0.002	1.676	-3.04 \pm 0.06	-3.06 \pm 0.05	\checkmark	\checkmark	-3.17 \pm 99	-3.15 \pm 102	-3.15 \pm 2	-3.17 \pm 99	-	-	-
988	6339.113	-0.004 \pm 0.002	4.154	-0.50 \pm 0.05	-0.61 \pm 0.05	X	X	-0.53 \pm 14	-	-0.63 \pm 2	-0.53 \pm 14	-	-	X
995	6366.480	-0.004 \pm 0.004	4.167	-0.85 \pm 0.07	-0.95 \pm 0.05	\checkmark	X	-0.87 \pm 14	-	-1.06 \pm 2	-0.87 \pm 14	-	-	-
998	6378.247	0.001 \pm 0.002	4.154	-0.79 \pm 0.04	-0.82 \pm 0.03	\checkmark	\checkmark	-0.82 \pm 99	-	-0.83 \pm 2	-0.82 \pm 99	-	-	2, 99
1005	6414.581	0.006 \pm 0.002	4.154	-1.13 \pm 0.04	-1.20 \pm 0.03	\checkmark	X	-1.16 \pm 99	-	-1.18 \pm 2	-1.16 \pm 99	-	-	2
1008	6424.851	-0.001 \pm 0.002	4.167	-1.33 \pm 0.04	-1.39 \pm 0.05	\checkmark	X	-1.36 \pm 14	-	-1.58 \pm 2	-1.35 \pm 14	-	-	14
1022	6482.798	0.001 \pm 0.007	1.935	-2.75 \pm 0.05	-2.80 \pm 0.05	\checkmark	X	-2.63 \pm 101	-2.63 \pm 102	-2.93 \pm 2	-2.63 \pm 67	-	-	-
1030	6532.873	-0.001 \pm 0.004	1.935	-3.34 \pm 0.07	-3.39 \pm 0.08	\checkmark	X	-3.35 \pm 99	-3.39 \pm 97	-3.42 \pm 2	-3.35 \pm 99	-	-	2, 97, 99
1032	6586.310	-0.004 \pm 0.002	1.951	-2.67 \pm 0.06	-2.79 \pm 0.06	\checkmark	X	-2.78 \pm 99	-2.81 \pm 97	-2.75 \pm 2	-2.78 \pm 99	-	-	2, 97, 99
1035	6598.598	-0.001 \pm 0.002	4.236	-0.86 \pm 0.04	-0.93 \pm 0.06	\checkmark	X	-0.82 \pm 14	-0.98 \pm 97	-1.10 \pm 2	-0.98 \pm 67	-	-	67, 97
1044	6635.122	-0.001 \pm 0.002	4.419	-0.70 \pm 0.04	-0.77 \pm 0.04	\checkmark	X	-0.76 \pm 14	-0.83 \pm 97	-0.82 \pm 2	-0.82 \pm 67	-	-	14
1046	6643.630	-0.004 \pm 0.002	1.676	-1.95 \pm 0.08	-2.00 \pm 0.06	\checkmark	X	-2.22 \pm 99	-2.30 \pm 102	-2.30 \pm 2	-2.22 \pm 99	-	-	-
1049	6661.324	-0.004 \pm 0.005	4.236	-1.45 \pm 0.04	-1.52 \pm 0.03	\checkmark	X	-1.49 \pm 14	-1.59 \pm 97	-1.78 \pm 2	-1.57 \pm 67	-	-	14
1086	6767.772	0.000 \pm 0.001	1.826	-2.19 \pm 0.07	-2.18 \pm 0.05	\checkmark	\checkmark	-2.14 \pm 99	-2.17 \pm 102	-2.17 \pm 2	-2.14 \pm 99	-1.69 \pm 4	-	2, 99, 102
1087	6772.315	-0.001 \pm 0.002	3.658	-0.95 \pm 0.05	-0.98 \pm 0.04	\checkmark	\checkmark	-0.80 \pm 14	-0.99 \pm 97	-0.93 \pm 2	-0.98 \pm 67	-	-	67, 97
								Zn I						
202	4680.134	-0.004 \pm 0.002	4.006	-0.74 \pm 0.14	-0.97 \pm 0.10	\checkmark	X	-0.81 \pm 103	-	-0.81 \pm 2	-0.81 \pm 103	-0.38 \pm 104	-	-
223	4722.153	0.001 \pm 0.002	4.030	-0.38 \pm 0.08	-0.48 \pm 0.08	\checkmark	X	-0.34 \pm 103	-	-0.34 \pm 2	-0.34 \pm 103	-0.38 \pm 104	-	-
161	4607.331	-0.006 \pm 0.002	0.000	0.13 \pm 0.09	0.02 \pm 0.07	\checkmark	X	0.28 \pm 105	0.28 \pm 105	0.28 \pm 2	0.28 \pm 105	-	-	-
							Sr I							
							Y II							

Table F.1. ^(a) Quality-assessable (^(A)) Analysis-independent line ^(a) Paper 1 input list ^(b) NIST ^(c) SpectroWeb ^(d) VALD3 ^(e) CHIANTI ^(f) TIPbase ^(g) TOPbase

#	Wavelength (Å) Input	E_{low} (eV) $\Delta\lambda_{grid}$	$\log(gf)$ cog grid	Flags QA? AI?	a)	b)	c)	d)	e)	f)	g)	h)	Recommended literature
298	4883.682	-0.001 ±0.002	1.084	0.07 ±0.06	-0.00 ±0.08	✓	X	0.19 ±0.06	-	0.07 ±0.07	-	-	2,107
309	4900.119	-0.001 ±0.002	1.033	-0.03 ±0.06	-0.15 ±0.05	X	X	0.03 ±0.06	-	-0.09 ±0.07	-	-	X
425	5087.416	0.004 ±0.002	1.084	-0.25 ±0.05	-0.31 ±0.04	✓	X	-0.16 ±0.06	-	-0.17 ±0.07	-	-	-
463	5200.406	0.004 ±0.002	0.992	-0.56 ±0.10	-0.64 ±0.08	✓	X	-0.47 ±0.06	-	-0.57 ±0.07	-	-	2,107
514	5289.815	0.004 ±0.002	1.033	-1.78 ±0.05	-1.83 ±0.04	✓	X	-1.68 ±0.06	-	-1.85 ±0.07	-	-	2,107
563	5402.774	-0.003 ±0.003	1.839	-0.50 ±0.07	-0.60 ±0.04	✓	X	-0.31 ±0.06	-	-0.51 ±0.08	-	-	108
588	5473.385	-0.006 ±0.003	1.738	-0.74 ±0.14	-0.89 ±0.08	✓	X	-0.78 ±0.06	-	-1.02 ±0.07	-	-	-
621	5544.611	-0.006 ±0.002	1.738	-0.81 ±0.15	-0.95 ±0.10	✓	X	-0.83 ±0.06	-	-1.09 ±0.07	-	-	-
722	5728.886	-0.001 ±0.005	1.839	-1.08 ±0.08	-1.14 ±0.06	✓	X	-1.15 ±0.06	-	-1.12 ±0.07	-	-	2,106, 107
112	4554.029	0.000 ±0.001	0.000	0.31 ±0.10	0.43 ±0.01	✓	X	0.17 ±0.09	0.14 ±0.10	0.17 ±2	-	0.46 ±4	-
95	4522.370	0.060 ±0.001	0.000	-0.82 ±0.07	-1.17 ±0.11	✓	X	-0.20 ±0.11	-	-1.70 ±2	-0.20 ±11	-	-
241	4748.730	-0.005 ±0.003	0.927	-0.36 ±0.15	-0.42 ±0.12	✓	X	-0.54 ±0.12	-	-0.86 ±2	-0.54 ±12	-	112
118	4562.359	0.006 ±0.004	0.478	0.25 ±0.09	0.12 ±0.08	✓	X	0.21 ±0.13	-	0.38 ±2	0.21 ±13	-	-
						BaII							X
						LanII							X
						CeII							

References.

- ¹ Hibbert et al. (1993); ² Lobel (2008); ³ Ralchenko et al. (2010); ⁴ Wiese & Martin (1990); ⁵ calculated in non-relativistic LS-coupling by Laverick et al. (2018) using Cunto et al. (1993) data; ⁶ Froese Fischer & Tachiev (2012); ⁷ Froese Fischer (2002); ⁸ Tachiev & Froese Fischer (2003); ⁹ Chang & Tang (1990); ¹⁰ Kurucz & Peytremann (1975); ¹¹ Butler et al. (1993); ¹² Mendoza et al. (1995); ¹³ Wiese et al. (1969); ¹⁴ Kurucz (1993); ¹⁵ Nahar & Pradhan (1993); ¹⁶ Garz (1973) rescaled using O'Brian & Lawler (1991); ¹⁷ Garz (1973); ¹⁸ Kelleher & Podobedova (2008); ¹⁹ Nahar (1993); ²⁰ Landi et al. (2013); ²¹ Zatsarinny & Bartschat (2006); ²² Biémont et al. (1993); ²³ Smith & O'Neill (1975); ²⁴ Fuhr et al. (1998); ²⁵ Smith & Raggett (1981); ²⁶ Smith (1988); ²⁷ Nicholls (1964); ²⁸ Sarah & Storey (2012); ²⁹ Lawler & Dakin (1989); ³⁰ Lawler et al. (2013); ³¹ Blackwell et al. (1982b); ³² Lorrian et al. (1988); ³³ Martin et al. (1975); ³⁴ Morton (2003); ³⁵ Blackwell et al. (1986a); ³⁶ Blackwell-Whitehead et al. (2006); ³⁷ Kosytk (1999); ³⁸ Blackwell et al. (1986a) rescaled using Grevesse et al. (1989); ³⁹ Blackwell et al. (1986a) rescaled using Holys & Führ (1977); ⁴⁰ Nitz et al. (1998); ⁴¹ Blackwell et al. (1983) rescaled using Grevesse et al. (1989); ⁴² Kuhne et al. (1978); ⁴³ Whaling et al. (1978); ⁴⁴ Holys & Führ (1980); ⁴⁵ Wood et al. (2013); ⁴⁶ Pickering et al. (2001); ⁴⁷ Roberts et al. (1973); ⁴⁸ Danzmann & Kock (1980); ⁴⁹ Kosytk & Orlova (1983); ⁵⁰ Ryabchikova et al. (1993); ⁵¹ Bizzarri et al. (1994); ⁵² Ostrovskii et al. (1958); ⁵³ Lawler et al. (2014); ⁵⁴ King (1947); ⁵⁵ Whaling et al. (1985); ⁵⁶ Bridges (priv. comm. with NIST, 1976); ⁵⁷ Sobcek et al. (2007); ⁵⁸ Tozzetti et al. (1985); ⁵⁹ Wujec & Weniger (1981); ⁶⁰ Kosytk (1981); ⁶¹ Blackwell et al. (1984); ⁶² Pinnington et al. (1993); ⁶³ Sigut (1990); ⁶⁴ Raassen & Uylings (1998a); ⁶⁵ Booth et al. (1984); ⁶⁶ Den Hartog et al. (2011); ⁶⁷ Fuhr et al. (1988); ⁶⁸ calculated in non-relativistic LS-coupling by Laverick et al. (2018) using Hummer et al. (1993) data; ⁶⁹ O'Brian et al. (1991); ⁷⁰ Blackwell et al. (1979a); ⁷¹ re-normalised values of May et al. (1974); ⁷² Ruffoni et al. (2014); ⁷³ Den Hartog et al. (1982a); ⁷⁴ Blackwell et al. (1982a); ⁷⁵ Blackwell et al. (1982a); ⁷⁶ O'Brian et al. (1991) rescaled using Ruffoni et al. (2014); ⁷⁷ Bard & Kock (1994); ⁷⁸ Blackwell et al. (1979b); ⁷⁹ Garz & Kock (1969); ⁸⁰ Bridges & Kornblith (1974); ⁸¹ Bard & Kock (1994) rescaled using O'Brian et al. (1991); ⁸² Bard et al. (1991) rescaled using Den Hartog et al. (1991); ⁸³ Blackwell et al. (1982a) rescaled using O'Brian et al. (1991); ⁸⁴ Blackwell et al. (1986b) rescaled using O'Brian et al. (1991); ⁸⁵ Blackwell et al. (1986b); ⁸⁶ Bard et al. (1991); ⁸⁷ Bard & Kock (1994) rescaled using Den Hartog et al. (1991) rescaled using O'Brian et al. (1991); ⁸⁸ Bard et al. (1991) rescaled using O'Brian et al. (1991); ⁸⁹ Blackwell et al. (1980b); ⁹⁰ Raassen & Uylings (1998b); ⁹¹ Kroll & Kock (1987); ⁹² Schnabel et al. (2004); ⁹³ Ryabchikova et al. (1999); ⁹⁴ Baschek et al. (1970); ⁹⁵ Melendez & Barbuy (2009); ⁹⁶ Moity (1983); ⁹⁷ Kosytk (1982); ⁹⁸ Wickliffe & Lawler (1997); ⁹⁹ Wood et al. (2014); ¹⁰⁰ Doerr & Kock (1985); ¹⁰¹ Lennard et al. (1975); ¹⁰² re-normalised values of Lennard et al. (1975); ¹⁰³ Warner (1968); ¹⁰⁴ Komarovskiy & Shabanova (priv. comm. with Spectr-W³, 1992); ¹⁰⁵ Parkinson et al. (1976); ¹⁰⁶ Biémont et al. (2011); ¹⁰⁷ Hannaford et al. (2001); ¹⁰⁸ Pitts & Newsom (1986); ¹⁰⁹ Miles & Newsom (1969); ¹¹⁰ Davidson et al. (1992); ¹¹¹ Corliss & Bozman (1962a); ¹¹² Lawler et al. (2001a); ¹¹³ Lawler et al. (2001b)